UNIVERSITÉ DU LUXEMBOURG

PhD-FTSM-2023-133
The Faculty of Science, Technology and Medicine

DISSERTATION

Defence held on 20/12/2023 in Luxembourg

to obtain the degree of

DOCTEUR DE L'UNIVERSITÉ DU LUXEMBOURG

EN *PHYSIQUE*

by

Alberto GARILLI
Born on 5 June 1992 in Sassari (Italy)

TOWARDS TRANSITION-BASED THERMODYNAMICS: STOPPING CRITERIA AND FLUCTUATION RELATIONS IN PARTIALLY ACCESSIBLE NETWORKS

Dissertation defence committee

Dr Matteo Polettini, dissertation supervisor
Permanent researcher, Université du Luxembourg

Dr Jean-Charles Delvenne
Professor, Université catholique de Louvain

Dr Thomas Schmidt, Chairman
Professor, Université du Luxembourg

Dr Edgar Roldán
Associate research officer, ICTP Trieste

Dr Gatien Verley, Vice Chairman
Teaching assistant, Universitè Paris-Saclay

Abstract

Discrete state space stochastic processes are typically described as successions of states and permanence times. In the markovian case the process is fully described by transition rates between pairs of states and by exponentially distributed residence times. In this case knowledge of the rates of the systems allows estimation of the thermodynamic forces driving the non-equilibrium dynamics, and we can study the statistics of extensive current-like quantities which satisfy fluctuation relations, establishing symmetries for the probability distributions. The description in terms of states, reminiscent of equilibrium thermodynamics, may not to be the best way to describe systems where only a few degrees of freedom are accessible to observation, since it requires coarse-graining procedures that break markovianity, which is only restored in certain limits. In particular, a novel approach based on the occurrence of transitions has proven to successfully generate the discrete-time sequences of few transitions that are accessible to observation. In this thesis I will review the above-mentioned transition-based coarse-graining, to which I contributed, and study the properties of the discrete-time process which generates sequences of visible transitions. The most important result is that the statistics of the currents along the observed edges satisfy a fluctuation relation when observed up to some intrinsic time (paced by the occurrence of a fixed number of visible transitions), thus recovering thermodynamic consistency that is lost in general when observing a few transitions up to the elapsing of a fixed external clock time. It will be also shown that the same coarse-graining, originally derived from first-exit time problems, can be obtained in an alternative way by working directly in the space of visible transitions with a procedure known as stochastic complementation. Finally, a discussion on some attempted research is presented, some of it offering ideas for followups on the work discussed in most of this thesis.

Contents

Publications and conferences

List of publications

1. Matteo Polettini, Alberto Garilli. Sustaining a temperature difference. *SciPost Physics*, 9, 030 (2020).

2. Pedro E. Harunari, Alberto Garilli, Matteo Polettini. Beat of a current. *Physical Review E*, 107, L042105 (2023).

3. Francesco Avanzini et al. Methods and Conversations in (Post)Modern Thermodynamics. *arXiv preprint*, arXiv:2311.01250 (2023)

4. Alberto Garilli, Pedro E. Harunari, Matteo Polettini. Fluctuation relations for a few observable currents at their own beat. *arXiv preprint*, arXiv:2312.07505 (2023)

List of contributed talks

1. Nordita 2022: Are There Fundamental Laws in Non-Equilibrium Statistical Physics?
   Title: *A fluctuation relation for single currents (The beat of a current)*, 11 May 2022, Stockholm.

2. Journées de Physique Statistique
   Title: *Flucutation Relations (FR) for marginal observers*, 27 January 2023, Paris.

List of posters

1. (Post)Modern Thermodynamics
   Title: *Fluctuation Theorems for marginal processes in transition space*, 8 December 2022, Luxembourg.

2. Smoluchowski symposium
   Title: *Fluctuation relations in the presence of hidden currents*, 26 September 2023, Krakow

Table of notation

List of common symbols in this thesis.

Spaces

Spaces are denoted by calligraphic upper-case letters.

- $\mathcal{X}$ state space;
- $\mathcal{E}$ space of edges;
- $\mathcal{T}$ transition space;
- $\mathcal{O}$ observable transition space.

Graphs

- $\mathcal{G}$ graph with nodes $x \in \mathcal{X}$ and directed edges $\boldsymbol{e}_\nu \in \mathcal{E}$, $\nu = 1, \ldots, |\mathcal{E}|$;
- ν label for directed edges or transition kind, i.e. undirected edge;
- $\mathscr{T}$ spanning tree.

Transitions

- ℓ generic observable transition $\ell \in \mathcal{O}$;
- ℓ_ν transition of kind ν;
- $\mathtt{s}(\ell)$ source state of transition ℓ;
- $\mathtt{t}(\ell)$ target state of transition ℓ.

Scalars

Scalars are usually denoted by lowercase letters.

- $q(x)$ probabilities in state space;
- p generic symbol for probabilities;

- f generic symbol for probability densities;
- $p(\ell)$, probability in transition space, $p(\ell|\ell')$ trans-transition probability;
- $r(x|y)$ transition rate from $y \in \mathcal{X}$ to $x \in \mathcal{X}$, $r(x)$ exit rate from state x;
- π probabilities of the embedded chain;
- c_ν total current of kind ν, i.e. current evaluated along the edge $\boldsymbol{e}_\nu$;
- ξ mixed currents, loop currents (from context, depending on indices);
- a edge affinities, cycle affinities, effective affinities, depending on context;
- α mixed affinities.

Vectors

Vectors are denoted by bold symbols. Greek letters are usually related to mixed quantities (example: vector of mixed current $\boldsymbol{\xi}$

- $\mathbf{1}$ unitary vector;
- $\boldsymbol{q}$ probability vectors in state space;
- $\boldsymbol{p}$ probability vectors in transition space;
- $\boldsymbol{j}$ vectors of probability currents (space of edges);
- $\boldsymbol{c}$ vector of total currents (in the context of Schnakenberg cycle decomposition it is also used to denote cycle vectors);
- $\boldsymbol{\xi}$ joint vector of total currents and mixed currents;
- $\tilde{\boldsymbol{\xi}}$ vector of a subset of the joint $\boldsymbol{\xi}$;
- $\boldsymbol{e}$ canonical basis vector or oriented edges;
- $\boldsymbol{a}$ vector of effective affinities;
- $\boldsymbol{\alpha}$ vector of mixed affinities;
- $\boldsymbol{\lambda}$ vector of counting fields;
- $\tilde{\boldsymbol{\lambda}}$ vector of a subset of counting fields;
- $\boldsymbol{\lambda}_c$ vector of counting fields for the total currents;
- $\boldsymbol{\lambda}_\xi$ vector of counting fields for the mixed currents.

Matrices

All matrices are denoted by capital letters.

- A generic matrix (or absorbing state);
- I identity matrix (of any dimension, depending on the context);
- R trans-transition matrix;
- D incidence matrix, or generic diagonal matrix;
- S survival matrix;
- Π embedded chain matrix;
- P trans-transition matrices (all transitions and observable transitions). Alternative $P_{\mathcal{O}}$ if we have to distinguish between observable trans-transition matrix and full trans-transition matrix;
- J swapping matrix;
- T taboo matrix;
- $E(\lambda_\nu)$ matrix of counting fields for the initial transition.

Trajectories

- $\mathcal{L}_n$ sequence of n transitions;
- Γ_t trajectory in state space up to time t.

Functions

- $G(\bullet)$ moment generating functions;
- $g(\bullet)$ cumulant generating functions;
- $F(\bullet)$ cumulative distribution function.

Thermodynamical quantities

- σ entropy production;
- w work;
- h heat;
- β inverse temperature.

Chapter 1

Introduction

The objective of statistical physics is to establish a connection between the microscopic description of single units, characterized by deterministic evolution equations, and the macroscopic world, where the collective behavior of all the units involved is described in terms of emergent physical quantities which allowed physicists to make predictions on very complex system with the use of just a few variables. The main application of statistical physics, developed in the first place as a theory attempting the explanation of the thermodynamics of large systems, consisted initially in thermal machines and the increasing of their efficiency [1]. More recently, it became clear that an exhaustive theory must include non-equilibrium effects to explain how useful work can be extracted from systems dominated by thermal fluctuation, as it is the case for biological processes involving the exchange of chemicals with an environment in order to sustain life at the cost of some fuel [2, 3, 4, 5], or in electronic devices of the scale of nanometers that became increasingly important with the technological development of electronic computers [6, 7, 8].

In this context, stochastic thermodynamics, a branch of physics where thermodynamical quantities, such as heat and work, are defined at the level of single realizations of a process, emerged as a promising theory to conciliate the foundational principles of thermodynamics with the effects of fluctuations, which are no more neglectable at small scales. Stochastic thermodynamics extends the laws of thermodynamics to this realm, where all quantities involved (energy, work, entropy) become fluctuating quantities [9, 10, 11].

The unpredictability given by such fluctuations, which are assumed to be generated through the interaction with large reservoirs at equilibrium, can to some extent be described with the help of the theory of stochastic processes if the degrees of freedom of the microscopic system under examination are coarse grained in a way that they can be treated as a finite set of states where the transitions between each coarse grained state can be assumed

to be memory-less. This memory-less property, known as markovianity, affects both the successions of states and the time distributions, and makes the theory of stochastic processes the perfect candidate to extrapolate a thermodynamic description out of very small systems out of equilibrium.

The most encompassing results in stochastic thermodynamics are gathered under the name of fluctuation relations [9, 12, 13, 14, 15, 16, 17], a collection of results describing how fluctuations in extensive physical quantities affect the deterministic evolution of microscopic systems, which can be recovered at the level of ensemble averages or by taking low-noise limit [18]. By comparing the statistics of such observables in forward and backward realizations of the same process, one can determine a preferred direction in time despite the fact that single realizations can lead to a negative entropy production due to fluctuations, once an entropy production is defined at the stochastic level. All fluctuations relations can be seen as a specialization of

$$\log \frac{p(\sigma_{\rm tot}(t))}{p(-\sigma_{\rm tot}(t))} = \sigma_{\rm tot}(t), \tag{1.1}$$

with $\sigma_{\rm tot}(t)$ denoting the total entropy produced by a process in a single realization at time t, containing contributions due to the heat exchanged with the environment and the work done on the system through an external driving. The relation above is valid at all times. However, the estimation of the total entropy production requires knowledge of all parameters describing the system under examination, and relies on precise measurements of fluctuating heat and work done on the system. In particular, one needs to track the evolution of the system's populations in state space which may be unfeasible in experiments. An alternative is to measure other extensive quantities such as the currents, which quantify the amount of exchanged physical quantities associated to the transitions between different states of the system, and whose average value is pushed away from equilibrium by the so called thermodynamic forces, also called affinities. Importantly, when the statistics of a set of observables satifies a fluctuation relation, it is considered a check of thermodynamic consistency since it allows to recover standard results in close-to-equilibrium frameworks, such as the fluctuation-dissipation theorem [19, 20].

Unfortunately, most of these physical quantities are often not accessible to observation. Consider for instance the case of a walking molecular motor, which is clearly out of equilibrium because of the net movement which can be appreciated over certain timescales. However, the precise chain of reactions is mostly hidden to an hypothetical observer, while the net movement can be monitored and it can be assumed to be triggered by the consumption of some metabolite, typically ATP [21, 22]. If movement of the molecular motor is the only trackable observable, the statistics of the associated current at time t will not satisfy a fluctuation relation because of the missing information about the other changes in state of the molecule during the same time.

This behavior can be explained in state space models where the dynamics on coarse-grained macroscopic states is not necessarily markovian unless specific requirements on timescales at which hidden degrees of freedom relax are satisfied [23, 24]. In particular, it is understood that markovianity is only recovered when time-scale separation exits.

Electronic circuits at the nanoscale operating in regimes where the thermal noise plays a fundamental roles are another example of physical systems which can be described by stochastic processes on networks [25]. For this kind of systems it makes sense to focus on the signal associated to some components without monitoring the full circuit. Fluctuation relations are also satisfied by non-linear components of electrical circuits, such as diodes [26], transistors [27], and quantum junctions for the counting statistics for electrons [28].

Recent developments in the context of coarse-grained models [29, 30] suggest that the emergence of non-markovianity can be circumvented if the effective dynamics is expressed in terms of sequence of visible transitions rather than successions of states and permanence times.

My work during the PhD, which is summarized in this dissertation, starts from the considerations given above. The abovementioned transition-based coarse-graining, applied to stochastic processes which can be thought as living in a graph of states and transitions, visually represented by vertices and edges respectively, offered in fact fertile ground to the development of the arguments presented in this thesis. Working initially on single observed currents in multicyclic graphs, where cycles are defined as closed circuits in state space where only the initial state is visited twice, we were able, together with my supervisor and my colleague P. Harunari, to study the statistics of currents evaluated over a single observable edge. The first result was that with a transition-based formalism, together with changing the paradigm by which currents are observed, i.e. by stopping the tracking of the observable current after a certain number n of observable transitions rather than the elapsing of a fixed external times t, their statistics satisfy a fluctuation relation without any approximation, by relying only on the assumption that the observable transition is univocally associated with a pair of states in a stochastic system. The outcome of this work [31] posed the question of how to generalize fluctuation relations for currents to the case where an arbitrary number of edges is observed. The answer proposed in this thesis, and in a forthcoming publication [82], is that one must include the information extracted from realizations of processes in transition space given by what we called mixed currents, which account for subsequent transitions over different observable edges. In this way, thermodynamic consistency can be recovered even in the case of a partial set of observable currents, which it was not the case for standard coarse-graining procedures [23, 24].

In this dissertation I provide an exhaustive treatment of the topic by introducing all it is needed to give a precise explanation to all the results

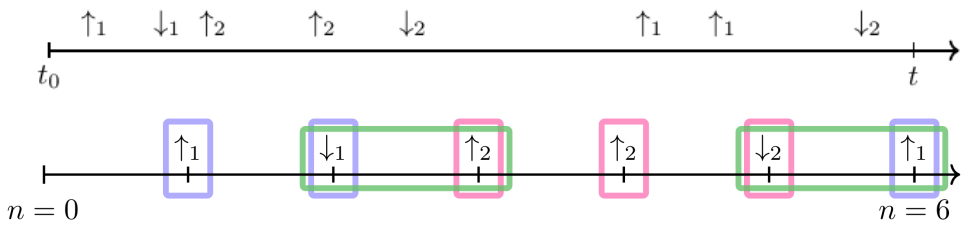

Figure 1.1: Illustration of time series of recorded events associated to observable transitions between different pairs of states, $\uparrow_1, \downarrow_1$ representing the two possible directions for the transition $x_1 \leftrightarrow y_1$ and $\uparrow_2, \downarrow_2$ the two possible directions for the transition$x_2 \leftrightarrow y_2$. (*Above*): Time-series of observable transitions up to an external time t, generated by a system obeying a markovian Master equation. (*Below*): The same sequence stopped after the occurrence of $n = 6$ observable transitions. By using first-exit time methods this process can be shown to be a Markov chain in "transition space". This grants the Fluctuation Relation (and thus thermodynamic consistency), provided not only the occurrences of the single transitions is recorded (blue and pink single-arrow boxes) but also correlations between successive transitions is (green two-arrow boxes).

achieved during the period where I worked on the topic. In particular, I start by reviewing the thermodynamics of continuous-time stochastic processes, to arrive to a discrete-time transition based description achieved by solving a class of first-exit time problems. The statistics of observables, that can be extracted from sequences of visible transitions, is studied with statistical tools with particular emphasis to moment generating functions, which are also employed to generalize fluctuation relations to the transient case. Regarding the methods, all the arguments are based on exact mathematical derivations, and all the theoretical results are supported by numerical experiment. This last point represents another central aspect of my research experience, where I gave particular importance to coding the simulations in order to reproduce the predicted results from the theory. Moreover, the support of computational methods was also useful to get some insights on what the correct theory should be and to identify the mistakes made during its formulation.

What introduced above does not represent all the work done during those years of PhD. In fact, the final Chapter of the thesis contains other projects on different topics, some of which can be related to the main study presented here, and despite being presented at the end of the dissertation it does not constitute a less important part of the research experience. Furthermore, some open questions emerged during individual work related to transition space chains and other projects I participated to are briefly treated in this Chapter.

This work is then organized as follows: Chapter 2 is dedicated to stochastic processes in continuous-time to set the basic notation and framework. From there, first-exit time procedures are used to derive the trans-transition probabilities, i.e. the probabilities of observing certain consecutive transitions among the observable ones and thus introducing the notion of discrete-time Markov chains in the space of transitions, explained in Chapter 3. In Chapter 4 the physical quantities that can be extracted from sequences of visible transitions are introduced, in particular the total currents, defined as the net amount of time a certain visible edge is crossed in a pre-defined direction, and their conjugated effective affinities, i.e. the effective thermodynamic forces that drive the observable part of the system out of equilibrium. In this context, the first novelty regards the introduction of the so-called mixed currents, accounting for consecutive transitions along different visible edges (see Fig. 1.1), and their conjugated affinities. The statistics of all quantities presented here is then studied with the tool of moment generating functions. The main results of this thesis come in Chapter 5, where the statistics of extensive observables in transition space are showed to satisfy fluctuation relations, constituting a very interesting progress in the context of coarse-gained models since such relations appear naturally for the joint probabilities of currents and mixed currents without any approximation when the total number of visible transitions is fixed, and for any number of observable mechanisms. Moreover, the same relations, first derived in the long-time limit, are specialized at all number n of observed transitions by the choice of a preferred initial probability in transition space, which cancels the effects of the boundary transitions in finite sequences of transitions. Such an approach is inspired by similar procedures which already exist for state-space processes in terms of cycle currents [32], which is explained without many details in Sec. 2.5.3. To give more consistency to the developed theory, the special case of complete sets of currents is also addressed, with the result of recovering a well known class of fluctuation relations [33] which does not require observation of mixed currents. Finally, a series of possible followups to the theory presented here and open research emerging from the PhD experience are briefly presented in Chapters 6 and 7. In particular, stochastic complementation [34] is introduced as a natural coarse-graining tool in transition space since, when applied to the full chain in this space, provides the trans-transition probabilities. This in fact is one additional result of this thesis: stochastic complementation is an exact reduction procedure if the fixed clock time is replaced by the random time of the occurrence of transitions (while for example it does not correctly reduce continuous-time Markov chains in state space as it does not respect the Poisson statistics of permanence times). Some open questions regarding a physical interpretation of preferred initial probabilities in transition space are presented here together with some studies around the convergence of statistical estimators used for numerical verification of fluctuation relations,

and the difficulties which are encountered in this framework. The outcome of a first small project about the thermodynamic cost of sustaining temperature differences [35], to which I contributed at the beginning of the PhD, is excluded from the discussion as it belongs to a different context, making use of Langevin equations and Fokker-Planck equations in the setting of thermal diffusion.

Chapter 2

Markov chains and thermodynamics

Thermodynamics, a fundamental branch of physics that studies energy and its transformations, has traditionally focused on equilibrium behavior of macroscopic systems. However, as scientific exploration delves into the microscopic and mesoscopic realms, it becomes increasingly clear that a more comprehensive framework is necessary to accurately describe their behavior.

A rapidly evolving field, called stochastic thermodynamics, extends classical thermodynamics to systems far from equilibrium, where fluctuations play a crucial role, particularly at small scales. Stochastic thermodynamics builds upon the foundational principles of thermodynamics while incorporating the effects of randomness, expanding the concepts of heat, work, and entropy production to inherently fluctuating systems. With the aid of advanced experimental techniques enabling access to the micro and mesoscopic world, stochastic thermodynamics has emerged as a good candidate for studying and understanding a diverse range of systems, including biological processes, chemical reactions, and nanoscale electronic devices [6, 7, 8].

The focus of this thesis is on systems with a finite number of states, that interact with an environment and with a short memory, in such a way that it can be effectively described using the theory of continuous-time Markov chains. This chapter provides an overview of these processes and their connection to thermodynamics, with particular emphasis on fluctuation relations, a collection of results that establish symmetries between the probabilities of forward and backward processes and characterize the irreversible nature of such systems.

2.1 Continuous-time Markov chains

The memory-less property of Markov chains grants that the evolution of the system in the future is determined only by its present-time state, and that,

provided that the system is in a certain state at initial time, the dynamics is independent of the time spent on that state before starting to observe the process. The theory of Markov chains requires that the full state space and the possible transitions are observable.

In this section we introduce the details of the theory and describe the evolution equation for the probabilities of being in a certain state at time t, known as Master Equation. The connection with physics is made through the local detailed balance assumption, that incorporates the effects of system/environment interactions is a consequence of the fact the system is viewed as interacting with several reservoirs, all competing against each other to impose their own thermodynamic equilibrium.

2.1.1 Basic assumptions

Let $\mathcal{X}$ denote the finite space of states $x \in \mathcal{X}$ of a system $\mathcal{S}$. A continuous time Markov chain is a succession of random variables $\hat{X}_i$ taking values in the set of state $\mathcal{X}$, and of permanence times $\hat{\tau}_i$, i.e. the time spent in state $\hat{X}_i$, for all $i \in [0, \hat{n}]$. By fixing the total time t, the number $\hat{n}$ of transitions occurring in a single realization of the process is itself a random variable. Then, a continuous time Markov chain can be represented as the succession

$$(\hat{X}_0, \hat{\tau}_0) \to (\hat{X}_1, \hat{\tau}_1) \to \cdots \to (\hat{X}_{\hat{n}-1}, \hat{\tau}_{\hat{n}-1}) \to (\hat{X}_{\hat{n}}, \hat{\tau}_{\hat{n}}) \tag{2.1}$$

with $\hat{\tau}_i$ indicating the time spent on state $\hat{X}_i$ before jumping to $\hat{X}_{i+1}$ and $\sum_i \hat{\tau}_i = t$. The permanence times $\hat{\tau}_i$ are exponentially distributed, that is, given parameters $r(x_i) \in \mathbb{R}_{>0}$ the probability of leaving state x_i in an interval $(\tau_i, \tau_i + dt)$ is

$$f_i(\tau_i)dt = r(x_i)e^{-r(x_i)\tau_i}dt. \tag{2.2}$$

Let us now assume that at time $t = 0$ the system is found at state $x_0 \in \mathcal{X}$. The density Eq. (2.2) tells us how the time before leaving state x_0 is distributed, according to a parameter $r(x_0)$ which is the same for every occurrence $\hat{X}_i = x_0$. Moreover, Eq. (2.2) grants the memoryless-ness property for the permanence times. In fact, given the survival probability

$$p(\tau_i > t) = 1 - \int_0^t dt'\, f_i(t') = e^{-r(x_i)t}, \tag{2.3}$$

the memoryless-ness property is expressed as

$$p(\tau_i > t + s | \tau_i > s) = p(\tau_i > t), \tag{2.4}$$

which says that the probability of an event occurring after time $t + s$ conditioned to the fact that the same event did not happen since time s, is equivalent to the survival probability at the time interval t. Eq. (2.4) is in fact easily checked to be satisfied by the exponential distribution.

At time $\hat{\tau}_0$ the system leaves state x_0 and jumps to a new state x_1 with probability $\pi(x_1|x_0)$. The parameter $r(x)$ appearing in Eq. (2.2) is then interpreted as the exit rate from state x, given by

$$r(x) = \sum_{y \in X} r(y|x) \tag{2.5}$$

with $r(y|x)$ denoting the rate (transitions per unit of time) of jumping to y from x. Then, the transition probability $\pi(y|x)$ is found to be

$$\pi(y|x) = \frac{r(y|x)}{r(x)} \tag{2.6}$$

which verifies $\sum_y \pi(y|x) = 1$. The transition probabilities Eq. (2.6) define a process, called embedded Markov chain, which is introduced in detail in Section 2.1.3.

Eqs. (2.2) and (2.6) also are the fundamental ingredients of the Gillespie algorithm, which allows to build a random trajectory by sampling two uniform random numbers between $[0, 1]$ at every step. We illustrate our own version of the algorithm in Appendix.

Now consider two states in $\mathcal{X}$, not necessarily directly connected to each other by a transition. If both states can be reached from each other through a series of transitions with a positive probability, they are said to communicate. If this is true for all pairs of states in $\mathcal{X}$ the Markov chain is said to be irreducible, and as a consequence all states are recurrent, that is, in rough words, every state can be reached arbitrarily many times in a single realization of the process. In our description we then consider the case of irreducible chains, in which every pair of states is connected by at least one path of non-vanishing probability, with the consequence of being endowed with an unique stationary distribution as explained in the next section. For now, since we are interested in describing stochastic processes from a thermodynamical point of view, we furtherly assume that all transitions between pairs of states can occur in both directions, that is, given that for a pair (x, y) if the transition rate $r(y|x) > 0$ then also $r(x|y) > 0$, a condition called micro-reversibility.

Ultimately, it is intuitive to represent the process as occurring in a graph with states represented by nodes and transitions represented by edges as represented in a simple example in Figure 2.1.

2.1.2 Master Equation

Rates and exit rates are collected in a matrix R called rate matrix. The elements of R are $R_{y,x} = r(y|x)$ for $x \neq y$ and the diagonal elements are given by the exit rates $R_{x,x} = -r(x)$. In this way it is ensured that $\sum_y R_{y,x} = 0 \ \forall x \in \mathcal{X}$, corresponding to a notion of conservation of probabilities, as

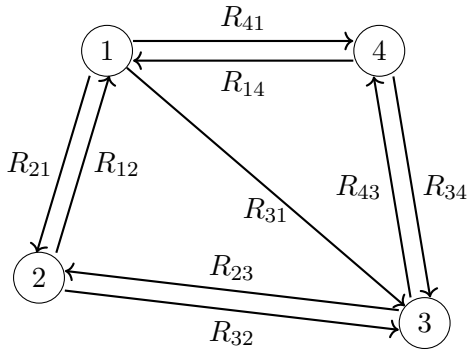

Figure 2.1: The markovian dynamics we consider can be represented as a graph with nodes denoting the states and edges denoting the allowed transitions between pairs of states (x, y), each of them endowed a transition rate $R_{xy} = r(x|y)$ from x to y. The arrows denote the possible directions each transition can occur, and notice that between states 1 and 3 we included an irreversible transition. The corresponding embedded chain is obtained by replacing the rates with the transition probabilities Eq. (2.6).

explained below. As an example, we write the rate matrix for the process in Figure 2.1(a) as

$$R = \begin{pmatrix} -r(1) & r(1|2) & 0 & r(1|4) \\ r(2|1) & -r(2) & r(2|3) & 0 \\ r(3|1) & r(3|2) & -r(3) & r(3|4) \\ r(4|1) & 0 & r(4|3) & -r(4) \end{pmatrix}. \tag{2.7}$$

The rate matrix R determines the evolution of the probability $q_t(x)$ of being in state x at time t through the Master Equation that reads

$$\frac{dq_t(x)}{dt} = \sum_y R_{x,y} q_t(y) \tag{2.8}$$

with solution

$$q_t(x) = \sum_y \left[e^{tR}\right]_{x,y} q_0(y) \tag{2.9}$$

where e^A is the matrix exponential and $q_0(y)$ denotes the initial probability of being at state y at time $t = 0$.

The Master Equation can be written in the less compact form

$$\frac{dq_t(x)}{dt} = \sum_y \left[r(x|y)q_t(y) - r(y|x)q_t(x)\right] = \sum_y j_{x,y}(t) \tag{2.10}$$

where the quantity inside the brackets $r(x|y)p_t(y) - r(y|x)p_t(x)$ is interpreted as the probability current $j_{x,y}$ from y to x. For this reason, by looking at

Eq. (2.10), we can interpret the Master Equation as a continuity equation for the probability distribution in state space.

2.1.3 Embedded Markov chain

The Master Equation expresses the evolution of the probabilities in state space at all instants of time t. In this section we introduce the notion of embedded Markov chain, which is a discrete-time chain that retains only some of the information of the continuous time process defined above.

Given a rate matrix R, we defined by Eq. (2.6) the transition probabilities that the next state after x is y. By splitting the rate matrix as a sum of a diagonal and an off-diagonal matrix, $R = -R_{\mathrm{D}} + R_{\mathrm{OD}}$, we define the matrix

$$\Pi = R_{\mathrm{OD}} R_{\mathrm{D}}^{-1} \tag{2.11}$$

with elements $\Pi_{x,y} = \pi(x|y)$ for $x \neq y$ and $\Pi_{x,x} = 0$. The matrix Eq. (2.11) is a stochastic matrix in the sense that $\sum_{x\in\mathcal{X}} \Pi_{x,y} = 1$, for all y, and all its entries are non-negative. The process generated by such a transition matrix is then a discrete-time Markov chain in state space that accounts only for the occurrence of transitions. Thus, given an initial probability $\boldsymbol{q}_0$, the vector of probabilities after n transitions is obtained as

$$\boldsymbol{q}_n = \Pi \boldsymbol{q}_{n-1} = \Pi^n \boldsymbol{q}_0. \tag{2.12}$$

For the same example represented in Figure 2.1(b), the embedded Markov chain reads

$$\Pi = \begin{pmatrix} 0 & \pi(1|2) & 0 & \pi(1|4) \\ \pi(2|1) & 0 & \pi(2|3) & 0 \\ \pi(3|1) & \pi(3|2) & 0 & \pi(3|4) \\ \pi(4|1) & 0 & \pi(4|3) & 0 \end{pmatrix}. \tag{2.13}$$

Before addressing the asymptotic properties of Markov chains, we digress on the Perron-Frobenius theorem, which is used to prove many large deviation theorems. For instance, the existence of a Perron root for a stochastic matrix grants the unicity of its stationary distribution, and the same root can be used to study the moment generating function (therefore also the scaled cumulant generating function) for the statistics of extensive observables extracted by realizations of the chain.

2.1.4 Perron-Frobenius theorem

Given a real positive square matrix M, i.e. $M_{x,y} > 0$ for all x, y, the Perron-Frobenius theorem asserts that there is a real positive eigenvalue $\mathrm{PR}(M)$ of M such that any other eigenvalue $l(M)$ of M has smaller absolute value

$$|l(M)| < PR(M), \qquad l(M) \neq PR(M). \tag{2.14}$$

The eigenvalue $\mathrm{PR}(M)$ is called *Perron-root*, and since it is the eigenvalue with the largest absolute value it is also known as *dominant eigenvalue* of M. The existence of a Perron-root has several consequences, among which

- Given $\rho(M)$ the spectral radius of M, the dominant eigenvalue is equal to $\rho(M)$
$$\rho(M) = \mathrm{PR}(M); \tag{2.15}$$
- $\mathrm{PR}(M)$ is unique, i.e. its associated left and right eigenvector are one-dimensional, and their elements can be chosen to be all positive;
- Let $\boldsymbol{v}$ the right eigenvector of M associated to the Perron-root $\mathrm{PR}(M)$ and $\boldsymbol{w}$ the correspondant left eigenvector. Thus
$$\lim_{n\to\infty} \frac{M^n}{\mathrm{PR}(M)^n} = \boldsymbol{v}\boldsymbol{w}^\top \tag{2.16}$$
if $\boldsymbol{v}$ and $\boldsymbol{w}$ are normalized such that $\boldsymbol{v}\cdot\boldsymbol{w} = 1$. The relation above states that large powers of M renormalized with the corresponding dominant eigenvalue is the spectral projection onto the eigenspace of $\mathrm{PR}(M)$, also called Perron projection;
- The Perron-root satisfy the following inequality
$$\min_y \sum_x M_{x,y} \leq \mathrm{PR}(M) \leq \max_y \sum_x M_{x,y}. \tag{2.17}$$

The theorem is here formulated for strictly positive matrices. However, it can be extended to the case of non-negative matrices M, i.e. all the entries of M are non-negative, if M is irreducible. Stochastic matrices associated to discrete-time irreducible processes, in the sense explained in Section 2.1.1, are part of this category of matrices, and thus they have a Perron-root. The properties above have some very important consequences, in particular

- A non-negative irreducible stochastic matrix Π has an unique Perron-root;
- Because of Eq. (2.17), the Perron-root of Π is $\mathrm{PR}(\Pi) = 1$, since all columns are normalized to unity. This condition and the previous one together grant that, for instance, the stochastic matrix Π has a unique stationary state, which dominates at large times, and that it is obtained from
$$\Pi\boldsymbol{q}^{\mathrm{st}} = \boldsymbol{q}^{\mathrm{st}}, \qquad \sum_x q^{\mathrm{st}}(x) = 1; \tag{2.18}$$
- For the same reason, Eq. (2.15) gives that $\rho(\Pi) = 1$. Importantly, for all square submatrices Π' of Π the spectral radius is $\rho(\Pi') < 1$, which grants that the operator-valued geometrical series converges,

i.e. $\sum_{k=0}^{\infty} [\Pi']^k = (I - \Pi')^{-1}$. This is explained by recalling that the Perron root of a non-negative irreducible matrix is a non-decreasing function of its components [36], and taking a submatrix corresponds to setting the remaining components to zero;

- Eq. (2.16) can be applied to tilted matrices $\Pi(\boldsymbol{\lambda})_{x,y} = \Pi_{x,y} e^{\lambda_{x,y}}$ (i.e. stochastic matrices dressed with counting fields, see Section. 4.4.1) to show that at large times the moment generating function for extensive currents is directly related with the Perron-root $\mathrm{PR}(\Pi(\boldsymbol{\lambda}))$.

The properties above, then, are valid for all stochastic processes, given that the state space is connected, and since Perron-Frobenius theorem applies also to non-negative matrices, it is automatically extended to the embedded chain associated to a continuous-time Markov chain. However, the rate matrix which generates continuous-time stochastic processes does not belong to any of the matrices for which Perron-Frobenius holds, since the diagonal entries $R_{x,x} = -\sum_y r_(y|x)$ of the rate matrix R are negative.

Nevertheless, it is possible to extend the theorem to rate matrices. We consider the matrix $R + \tau I$, with I the identity matrix and τ a parameter which is chosen to grant that $R + \tau I$ is non-negative. A possibility is, for instance, to choose $\tau = \max_x r(x)$, where $r(x)$ is the exit rate from state x. Thus, since $R + \tau I$ is non-negative it has an unique Perron root

$$(R + \tau I)\boldsymbol{v} = \lambda_{\mathrm{PF}} \boldsymbol{v}, \tag{2.19}$$

with $\lambda_{\mathrm{PF}} = \mathrm{PR}(R + \tau I)$ and $\boldsymbol{v}$ the corresponding eigenvector. Therefore we have also that

$$Rv = (\lambda_{\mathrm{PF}} - \tau)\boldsymbol{v} = \lambda_0 \boldsymbol{v}. \tag{2.20}$$

Given any eigenvalue λ of R, then $\lambda + \tau$ is an eigenvalue for $R + \tau I$, which satisfies Perron-Frobenius theorem. Thus

$$|\lambda + \tau| \leq \lambda_{\mathrm{PF}} = \tau + \lambda_0, \tag{2.21}$$

which means that $\Re\lambda \leq \lambda_0$, where $\Re$ denotes the real part. Specifically, for rate matrices we have that $\lambda_0 = 0$ and all the other eigenvalues have negative real part. A consequence of this is that the stationary distribution of the process defined by the rate matrix R is unique, as it is discussed in the next Section. In fact, we can consider the solution of the Master equation Eq. (2.9), and say that in the limit $t \to \infty$ the only surviving contributions to the matrix exponential is the one given by the only non-negative eigenvalue, in this case the Perron root of R.

2.1.5 Stationary state

The condition of irreducibility has consequences on the spectral properties of the rate matrix R. In fact, as a consequence of the Perron-Frobenius

theorem, the condition of irreducibility grants the uniqueness, up to a multiplicative constant, of the eigenvector $\boldsymbol{q}^{\mathrm{st}}$ associated to the eigenvalue 0. $\boldsymbol{q}^{\mathrm{st}}$ is the solution of $R\boldsymbol{q}^{\mathrm{st}} = 0$ (thus matematicians also call it invariant measure) and it is time independent because from Eq. (2.8) it also satisfies $(\exp tR)\boldsymbol{q}^{st} = \boldsymbol{q}^{st}$. If $\boldsymbol{q}^{\mathrm{st}}$ is normalized to unity it represents a probability distribution, also called stationary distribution or stationary state, and its elements $q^{\mathrm{st}}(x)$ are interpreted as the probability of being in state $x \in \mathcal{X}$ at long times $t \to \infty$.

Since the stationary state is now independent on t

$$\sum_y \left[r(x|y)q^{\mathrm{st}}(y) - r(y|x)q^{\mathrm{st}}(x)\right] = 0, \tag{2.22}$$

that can be rewritten in terms of probability currents

$$j_{x,y} = r(x|y)q^{\mathrm{st}}(y) - r(y|x)q^{\mathrm{st}}(x) \tag{2.23}$$

as

$$\sum_y j_{x,y} = 0 \tag{2.24}$$

known as Kirchhoff Current Law, a relation originally derived in the context of electrical circuits. A special case of Eq. (2.22) is obtained in the case where the rates $r^{\mathrm{d.b.}}(x|y)$ are such that each of the currents in Eq. (2.24) vanishes, that is

$$r(x|y)q^{\mathrm{eq}}(y) - r(y|x)q^{\mathrm{eq}}(x) = j_{x,y} = 0 \tag{2.25}$$

for all $x, y \in \mathcal{X}$ with $x \neq y$. The time-independent probability distribution in state space $\boldsymbol{q}^{\mathrm{eq}}$ in this special situation is then called equilibrium distribution. This means that the fluxes of probability are balanced and thus no net current is flowing between any pair of states connected by a transition.

2.2 Detailed balance

2.2.1 Global detailed balance (equilibrium)

The equilibrium condition Eq. (2.25) holds for physical systems if there exist $\{U(x), x \in \mathcal{X}\}$ such that

$$\frac{r(x|y)}{r(y|x)} = \frac{U(x)}{U(y)}, \tag{2.26}$$

also known as detailed balance. Then, parametrizing $U(x) = e^{-\beta\epsilon_x}$, with $\beta = 1/T$ the inverse temperature (we assume $k_B = 1$ throughout all the thesis) and ϵ_x an energy associated to the state x, the detailed balance condition can be expressed as

$$\frac{r^{\mathrm{d.b.}}(x|y)}{r^{\mathrm{d.b.}}(y|x)} = e^{-\beta(\epsilon_x - \epsilon_y)}, \tag{2.27}$$

and the equilibrium distribution is then expressed as

$$q^{\mathrm{eq}}(x) = \frac{e^{-\beta \epsilon_x}}{Z} \tag{2.28}$$

with Z the partition function of the canonical ensemble, since, because of probability conservation, the system can be considered as closed. Eq. (2.28) is easily proven by using Eq. (2.25) and the normalization condition for the probability distribution $\boldsymbol{q}^{\mathrm{eq}}$, $\sum_x q^{\mathrm{eq}}(x) = 1$, thus we write the equilibrium distribution as

$$q^{\mathrm{eq}}(x) = \left(1 + \sum_{y \neq x} \frac{r(y|x)}{r(x|y)} \right)^{-1} \tag{2.29}$$

that gives the probability Eq. (2.28) by use of the detailed balance condition Eq. (2.27).

The condition of detailed balance Eq. (2.27) holds for physical systems when the system is coupled to a single thermal reservoir with inverse temperature β. For such class of systems non-equilibrium appears only during the transient phase relaxation to equilibrium. For instance, one can imagine to perform an instantaneous quench of the hamiltonian of the system, thus the system will relax to the new equilibrium for the quenched hamiltonian according to some timescale.

2.2.2 Local detailed balance (non-equilibrium)

Since we are interested in non-equilibrium behavior, we look at systems where the distribution satysfying Eq. (2.22) is a non-equilibrium stationary state. This situation is obtained for instance when the system is coupled with at least two reservoirs at different temperatures or chemical potentials. In order to derive a parametrization on the rates similar to Eq. (2.27) giving non-equilibrium stationary distributions, we have to consider the dynamics of the system as the result of the competition between reservoirs, each of which tries to impose its own equilibrium.

We assume that

- the reservoirs are so large that changes in the system do not change their temperature or chemical potential;
- the relaxation time-scales of the reservoirs are assumed to be much faster than the relaxation time-scales for the open system;
- the reservoirs do not directly interact among themselves, but only through the system.

In this way, the stationary state probability satisfying Eq. (2.22) is a non-equilibrium state where each transition in the open system is associated to

a change in the entropy and/or the number of particles of the reservoirs. We can assume for simplicity that transitions between pair of states are triggered by a specific reservoir that is equilibrated with the system in the stationary state. The competition between reservoirs is then encoded in the so called Local Detailed Balance (LDB) condition. As an example, consider a graph with three states labeled as 1, 2 and 3, coupled with three thermal reservoirs with inverse temperatures $\beta_a, \beta_b, \beta_c$. For our example we do not consider chemical potentials, that can be included with some extra work [37], however this is not in the scope of our research. We have

$$\frac{r(1|2)}{r(2|1)} = e^{-\beta_a(\epsilon_1-\epsilon_2)} \qquad \frac{r(2|3)}{r(3|2)} = e^{-\beta_b(\epsilon_2-\epsilon_3)} \qquad \frac{r(3|1)}{r(1|3)} = e^{-\beta_c(\epsilon_3-\epsilon_1)}. \tag{2.30}$$

We consider now the entropy produced in the cyclic trajectory $1 \to 2 \to 3 \to 1$ (anticipating in part the discussion about trajectories and entropy production in the next session). This is given by

$$\begin{aligned}\Delta\sigma(1 \to 2 \to 3 \to 1) &= k_B \log \frac{r(1|3)r(3|2)r(2|1)}{r(3|1)r(2|3)r(1|2)} \\ &= k_B \left(\epsilon_1(\beta_c - \beta_a) + \epsilon_2(\beta_a - \beta_b) + \epsilon_3(\beta_b - \beta_c)\right).\end{aligned} \tag{2.31}$$

Thus the detailed balance condition Eq. (2.27) can be extended for non-equilibrium systems by stating that each transition (or a subset) is in equilibrium with a reservoir, and we call this condition Local Detailed Balance (LDB).

Notice that Eq. (2.31) vanishes if and only if $\beta_a = \beta_b = \beta_c$ independently on the values of the energies, which are assumed to be non-degenerate, that is equivalent to the case where the system is coupled with a single reservoir, with equilibrium distribution Eq. (2.28). The equilibrium condition can also be expressed via the Kolmogorov criterion, which states that given any cyclic path in state space $x_1 \to x_2 \to \cdots \to x_{n-1} \to x_n$ with $x_n = x_1$, then the ratio

$$\frac{r(x_n|x_{n-1})r(x_{n-1}|x_{n-2})\cdots r(x_2|x_1)}{r(x_1|x_2)r(x_2|x_3)\cdots r(x_{n-1}|x_n)} = 1. \tag{2.32}$$

In such case, it can be proven that potentials verifying Eq. (2.26) exist, and thus detailed balance holds.

2.3 Thermodynamics of Markov chains

The competition between reservoirs and the physical interpretation of rates is introduced in the context of stochastic processes through the assumption of the LDB condition, thus introducing the physics necessary to build a thermodynamic description of such processes. In fact, as we show here, by

defining the entropy production at the ensemble level we are able to prove the second law of thermodynamics

$$\langle \dot{\sigma}_{\rm tot}(t) \rangle \geq 0, \tag{2.33}$$

with $\langle \dot{\sigma}_{\rm tot}(t) \rangle$ denoting the total entropy production rate averaged on many realizations of the process with the same initial conditions. Eq. (2.33) consists of an internal and an environmental contribution, and by including LDB we get the first law

$$\langle \dot{\epsilon}(t) \rangle = \langle \dot{w}(t) \rangle + \sum_k \langle \dot{q}_k(t) \rangle, \tag{2.34}$$

where w is the work performed on the system, q_k the ingoing heat flow to the system due to the coupling with the k-th reservoir, and ϵ the internal energy.

2.3.1 Entropy production

Let us consider a system undergoing stochastic dynamics according to the Master Equation Eq. (2.8) and let $\boldsymbol{q}^{\rm st}$ denote its non equilibrium stationary solution, satisfying Eq. (2.22). Then, at long times the flows of probability inside the system are non-zero. This is accompanied by dissipation of energy leading to irreversibility, that is, the flows in the system have a preferred direction. As an example, in an electrical network dissipation is related with the loss of energy known as Joule effect. The degree of irreversibility is encoded in the so called entropy production. We first define it at the level of ensemble, thus we look at the average dissipation per unit of time, the Entropy Production Rat (EPR), the system undergoes after reaching its stationary state.

For the ensemble EPR we follow [38], where for the sake of generality we assume that transitions are triggered by different mechanisms k and that the rates are time dependent according to some protocol. First, we define the Shannon entropy of the system

$$S(t) = \langle \sigma_x(t) \rangle = -\sum_{x \in \mathcal{X}} q_x(t) \log q_x(t). \tag{2.35}$$

where $\sigma_x(t) = -\log q_x(t)$ is the self information. By taking the time derivative of Eq. (2.35) it is easy to show that it consists on two contributions

$$\dot{S}(t) = \frac{1}{2} \sum_k \sum_{\substack{x,y \in \mathcal{X} \\ y \neq x}} (r(x|y)^{(k)} q_y(t) - r(y|x)^{(k)} q_x(t)) \log \frac{r(x|y) q_y(t)}{r(y|x) q_x(t)} \tag{2.36}$$

$$+ \frac{1}{2} \sum_k \sum_{\substack{x,y \in \mathcal{X} \\ y \neq x}} (r(x|y)^{(k)} q_y(t) - r(y|x)^{(k)} q_x(t)) \log \frac{r(y|x)^{(k)}}{r(x|y)^{(k)}} \tag{2.37}$$

$$= \dot{S}_{\rm tot}(t) + \dot{S}_{\rm env}(t), \tag{2.38}$$

with $r(x|y)^{(k)}$ the transition rate from $y \in \mathcal{X}$ to $x \in \mathcal{X}$ due to the mechanism k.

The first term in the right hand side of Eq. (2.38) is interpreted as the total entropy production rate, the second one as the entropy flow to the environment. In particular, the first term is positive because

$$(a-b)\log\frac{a}{b} > 0 \qquad \text{for all positive } a,\, b, \tag{2.39}$$

and it is expressed in terms of the probability currents $j_{x,y}^{(k)}$ defined as Eq. (2.23) by use of the rates $r(x|y)^{(k)}$ and the thermodynamic force (or affinity)

$$a_{x,y}^{(k)} = \log\frac{r(x|y)^{(k)}q_y(t)}{r(y|x)^{(k)}q_x(t)}. \tag{2.40}$$

Thus the total entropy production can be written as the bilinear form

$$\dot{S}_{\text{tot}}(t) = \frac{1}{2}\sum_k \sum_{\substack{x,y\in\mathcal{X}\\ y\neq x}} j_{x,y}^{(k)} a_{x,y}^{(k)} = \sum_k \sum_{y,x<y} j_{x,y}^{(k)} a_{x,y}^{(k)}. \tag{2.41}$$

From here, it can be shown that the laws of thermodynamics are obtained at the level of ensembles of realizations of a stochastic process. In particular, the environmental contribution is shown to be related with the heat exchanged with reservoirs by use of the local detailed balance condition:

$$\dot{S}_{\text{env}}(t) = \sum_k \beta_k \langle \dot{h}_k(t)\rangle \tag{2.42}$$

with $\langle \dot{h}_k\rangle$ denoting the average flow of heat in the system due to reservoir k defined as

$$\langle \dot{h}_k(t)\rangle = \sum_{\substack{x,y\in\mathcal{X}\\ y\neq x}} j_{x,y}^{(k)}\epsilon_y \tag{2.43}$$

with $j_{x,y}^{(k)}$ denoting the flow of probability between $x \in \mathcal{X}$ and $y \in \mathcal{X}$ and Eq. (2.42) is obtained from Eq. (2.43) since the currents are anti-symmetric, i.e. $j_{x,y} = -j_{y,x}$. Moreover, from the definition of heat Eq. (2.43) we can derive the first law of thermodynamics by defining the average energy

$$\langle \epsilon(t)\rangle = \sum_{x\in\mathcal{X}} \epsilon_x q_x(t) \tag{2.44}$$

that by differentiation respect to time it can be split in a work term and a heat term Eq. (2.43). Thus we obtain the first law of thermodynamics

$$\langle \dot{\epsilon}(t)\rangle = \langle \dot{w}(t)\rangle + \sum_k \langle \dot{h}_k(t)\rangle. \tag{2.45}$$

with

$$\dot{w}(t) = \sum_{x \in \mathcal{X}} p_x(t) \dot{\epsilon}_x \tag{2.46}$$

We then safely conclude that the LDB condition on the rates, that impose that each pair of states is in equilibrium with a certain environment, provides a consistent description of thermodynamics, since the first and the second laws are recovered at the ensemble level. Also notice that, at stationarity, only the environmental entropy contributes to the total entropy. Moreover, in the case where the rates are time independent, and thus no driving protocol is applied to the system, the first law only contains the contributions from the heat exchanged with the reservoirs.

2.3.2 Stochastic entropy production

Let us consider a Markov chain as defined previously, and we consider a single realization. We indicate a trajectory in state space as $\Gamma_t = (x_0, \tau_0) \to (x_1, \tau_1) \to \cdots \to (x_n, \tau_n)$ with $\sum_i \tau_i = t$. For such realization we can define the change in the total entropy as

$$\sigma_{\text{tot}}(\Gamma_t) = \sum_{\substack{x,y \in \mathcal{X} \\ y \neq x}} \phi_{x,y}(\Gamma_t) \log \frac{r(x|y)}{r(y|x)} + \log \frac{q(x_0)}{q(x_t)}, \tag{2.47}$$

with x_0 and x_n the first and last states visited during the process. Thus the quantity Eq. (2.47) is also called stochastic entropy production. The fluxes $\phi_{x,y}$ count how many times transition $y \to x$ occur, and thus the first term can also be written in terms of total currents $c_{x,y} = \phi_{x,y} - \phi_{y,x}$ by restricting the sum according to some order relation. Since the entropy Eq. (2.47) is the total entropy produced during a realization, and the second term does not depends on extensive current-like quantities, at long times only the first term will contribute to the total entropy production. Conveniently, the total entropy can be estimated by only monitoring currents and by knowledge of the thermodynamic forces, without the need to know about the initial and final states. The main consequence is that we can find a fluctuation relation for the extensive currents.

2.3.3 Stochastic heat and work

The concepts of heat and work can also be extended to single trajectories Γ_t of a process running up to time t. For this purpose, we consider a protocol $\lambda = \lambda(t)$ according to which the rates become time-dependent.

In the following we adopt a convention where $t_k = t_{k-1} + \tau_{k-1}$, with τ_k the permanence time on the k-th visited state and t_k is evaluated respect to an initial time $t_0 = 0$, and $t_{n+1} = t$ the total time.

The total work along a trajectory is obtained as [39]

$$w(\Gamma_t) = \sum_{k=0}^{n} \int_{t_k}^{t_{k+1}} \frac{\partial \epsilon_{x_k}(\lambda)}{\partial \lambda} \dot{\lambda}\, dt + \sum_{k=1}^{n} w_{x_k, x_{k-1}}, \tag{2.48}$$

with $w_{x_k,x_{k-1}}$, $w_{x,x'} = -w_{x',x}$ an additional term which represents the energy provided by an external driving for each transition. Since in the first term in the expression above we are considering changes in energy, only due to the driving protocol, along pieces of the trajectory where no transitions are performed, the work along the trajectory Γ_t can be rewritten as

$$w(\Gamma_t) = \sum_{k=0}^{n} \left[\epsilon_{x_k}(\lambda(t_{k+1})) - \epsilon_{x_k}(\lambda(t_k))\right] + \sum_{k=1}^{n} w_{x_k, x_{k-1}}. \tag{2.49}$$

The heat exchanged with the environment accounts for the transitions occurring in Γ_t, and therefore

$$h(\Gamma_t) = \sum_{k=1}^{n} \left[\epsilon_{x_k}(\lambda(t_k)) - \epsilon_{x_{k-1}}(\lambda(t_k)) - w_{x_k, x_{k-1}}\right]. \tag{2.50}$$

It is now straightforward to see that the sum of Eqs. (2.48) and (2.50) is the change in energy along the trajectory Γ_t

$$w(\Gamma_t) + h(\Gamma_t) = \epsilon_{x_n}(\lambda(t)) - \epsilon_{x_0}(\lambda(t_0)) = \Delta\epsilon(\Gamma_t), \tag{2.51}$$

which is the stochastic version of the first law of thermodynamics. From now on we only consider cases where the rates are constant along all the dynamics. In the energy balance above, therefore, only the contribution of heat is taken into account.

2.4 Fluctuation relations

By looking at the definition Eq. (2.47) for the stochastic entropy production over a single realization of a process, we notice that there exist trajectories which provide negative entropy, thus apparently violating the second law of thermodynamics. This is surely a problem if we stick to a classical interpretation of thermodynamics that deals with large systems where fluctuations are suppressed. The great success of stochastic thermodynamics derives from the fact that such realizations with negative entropy productions are indeed allowed, and by averaging over many realizations of a process we recover the usual second law

$$\langle \sigma_{\text{tot}}(\Gamma_t) \rangle \geq 0 \tag{2.52}$$

with equality when the system's rates satisfy the global detailed balance condition Eq. (2.27). This means that realizations with positive entropy production must be more likely respect to the ones providing negative entropy.

An exact quantification of how the former are more likely than the latter is provided by the famous Fluctuation Relations (FR), which are considered the main achievement of stochastic thermodynamics.

FRs then provide a quantification of the irreversibility for a given system and are proven to hold for a very large set of out of equilibrium physical systems. To derive FRs we introduce the path probability weights, literally the probability of a single realization of the process evaluated over all the possible outcomes. Let us consider a system prepared to be in state x_0 with some probability $q(x_0)$. We indicate with Γ_t a trajectory in state space, with n transitions occurring and τ_k indicating the time spent in state x_k before jumping to x_{k+1} which is explicitly

$$\Gamma_t = \{(x_0, \tau_0), (x_1, \tau_1), \dots, (x_n, \tau_n)\}, \tag{2.53}$$

such that $\sum_{k=0}^{n} \tau_k = t$.

The probability of a trajectory Γ_t with n transitions evaluated up to time t is given by [40]

$$p(\Gamma_t) = q(x_0) \left[\prod_{i=0}^{n-1} e^{\tau_i r(x_i)} r(x_{i+1}|x_i) \right] e^{-\tau_n r(x_n)} \delta \left(\sum_{k=0}^{n} \tau_n - t \right) \tag{2.54}$$

written in terms of the permence times τ_i in state x_i and the last factor denoting the probability of not having a transition from x_n to any other state in a time τ_n, called survival probability. We want to compare the probability of a forward realization Eq. (2.54) with the probability of its time reversed trajectory $\bar{\Gamma}$

$$\bar{\Gamma}_t = \{(x_n, \tau_n), (x_{n-1}, \tau_{n-1}), \dots, (x_0, \tau_0)\}, \tag{2.55}$$

which produces the same entropy with swapped sign. The time-reversed trajectory starts from the last visited state in the forward sequence x_n and evolves up to x_0, by keeping the same permanence times in each state. Thus, by taking the log-ratio of the forward and backward path probabilities, defined as per Eq. (2.54), all the exponential contributions cancel, giving

$$\log \frac{p(\Gamma_t)}{p(\bar{\Gamma}_t)} = \log \frac{q(x_0)}{\bar{q}(x_n)} \prod_{i=0}^{n-1} \frac{r(x_{i+1}|x_i)}{r(x_i|x_{i+1})} \tag{2.56}$$

where $\bar{q}(x_n)$ is the initial probability of being in x_n in the time reversed process. If we now assume to prepare the forward process in the stationary distribution, since it remain the same during all the temporal evolution of the process, the first state in the backward trajectory is extracted from the same initial probability as in the forward process. The quantity Eq. (2.56) is then identified with the total entropy $\sigma_{\text{tot}}(\Gamma_t)$ produced by the system in the trajectory Γ_t, defined as the stochastic entropy production Eq. (2.47) by

identification of boundary terms and products of ratios of transition rates. Equation (2.56) states that the entropy production can be estimated by comparing forward and backward trajectories that provide opposite entropy production. Since there exist multiple paths Γ_t which provide the same entropy production $\sigma_{\rm tot}(t)$, we take the exponential of Eq. (2.56) and we multiply by $p(\bar{\Gamma}_t)$, and after summation over all Γ_t compatible with $\sigma_{\rm tot}(t)$ we get to

$$\frac{p(\sigma_{\rm tot}(t))}{p(-\sigma_{\rm tot}(t))} = e^{\sigma_{\rm tot}(t)}, \tag{2.57}$$

which is the detailed fluctuation relation for the total entropy production, valid at stationary state and for all times t.

The relation Eq. (2.57) can be rewritten as

$$p(-\sigma_{\rm tot}(t)) = e^{-\sigma_{\rm tot}(t)} p(\sigma_{\rm tot}(t)), \tag{2.58}$$

that when integrated over all $\sigma(t)$ provide the integral fluctuation relation

$$\langle e^{-\sigma_{\rm tot}(t)} \rangle = 1 \tag{2.59}$$

since $\int d\sigma p(\sigma) = 1$.

Now assume that an experiment is performed where the total entropy production is estimated by tracking the transitions of the system up to a time t. If at initial time the system is prepared at the stationary state, the estimated entropy production will be satisfying the FR Eq. (2.57) which describes the irreversibility of the observed system. However, this does not allow estimation of thermodynamical quantities such as the thermodynamic forces that drives the system out of equilibrium, because of the contribution given by the probabilities of the first and last visited states. Moreover, the estimation of the total entropy production $\sigma_{\rm tot}(t)$ is unfeasable since it requires knowledge of the boundary states in Γ_t and it requires sampling of the stationary probabilities $q^{\rm st}(x)$ for all $x \in \mathcal{X}$.

For a single realization Γ_t, the corresponding stochastic entropy Eq. (2.47) is decomposed in a system's term $\sigma_{\rm sys}$, which account for the probabilities of the first and last visited states in Γ_t, and a term $\sigma_{\rm env}$ which only depends on the transition rates, and it represents the exchanges with the reservoirs. For this reason, $\sigma_{\rm env}$ is also called environmental entropy produciton. This latter term accounts for occurrences of transitions, which are directly related with extensive currents which are typically associated with measurable physical quantities, such as the total electronic charge, or the total heat absorbed from the reservoir at time t. Moreover, since $\sigma_{\rm env}$ is time extensive, while $\sigma_{\rm sys}$ is not, the contribution to the total entropy production of the latter can be neglected in the limit $t \to \infty$. For this reason, we usually deal with the asymptotic version of the FR Eq. (2.57)

$$\log \frac{p(\sigma_{\rm env}(t))}{p(-\sigma_{\rm env}(t))} \asymp \sigma_{\rm env}(t), \tag{2.60}$$

In this case, it is enough to measure the total integrated currents along each edges, that are extensive quantities. The FR Eq. (2.57) is then specialized as

$$\log \frac{p_t(\{c_e\})}{p_t(\{-c_e\})} \asymp \sum_{e\in\mathcal{E}} a_e c_e(t) \tag{2.61}$$

that is now expressed in the space of edges, if each oriented $e \in \mathcal{E}$ univocally identifies a different pair of states. In fact, by denoting with $\mathtt{s}(e)$ and $\mathtt{t}(e)$ the source and target states of the transition along the edge labeled by e, the affinities and currents in this space are denoted as $a_e = a_{\mathtt{t}(e),\mathtt{s}(e)}$ and $c_e = c_{\mathtt{t}(e),\mathtt{s}(e)}$ respectively. The FR for currents Eq. (2.61) now accounts only for the fluxes in and out the reservoirs to which the system is coupled. Moreover, we don't need to provide details about the states of the system since we are only interested in the total current accumulated at time t, thus allowing estimation of the affinities, which are intensive quantities that characterize non-equilibrium.

2.5 Marginal fluctuation relation for currents

The FR Eq. (2.61) can be obtained only by monitoring all the currents flowing in the system between all pairs of states. However, this is an idealized situation that is often not achieved in practice. So we ask if there exist a minimal amount of currents to be monitored to correctly estimate the full entropy flow to the environment at some time t. The answer to that relies on a decomposition of the graph associated to the Markov chain in terms of cycles. Consider for instance a realization of a process starting from a certain state x_0, evolving to another state x_f and coming back to x_0 along the same path. In this case, the local detailed balance condition ensure that no entropy is produced in the process, thus that single realization is regarded as reversible. Conversely, if the trajectory ends in x_0 after performing a cycle, which is, no other state except the first one is visited twice, local detailed balance provides a net contribution to the entropy production, that can be positive or negative depending on the direction the cycle is closed. Thus, it is natural to associate the net production of entropy with the closure of cycles, identified by closed circuits in the graph where the dynamics takes place.

However, not all cycles are independent, and can be obtained as combinations of fundamental cycles. Also, the choice of fundamental cycles is not unique. Therefore, we need a procedure that provides a minimal set of cycles depending on which currents are monitored. In the following subsection we provide one possible way to perform such a decomposition of graphs in term of fundamental cycles.

2.5.1 Schnakenberg cycle decomposition

We summarize here a procedure reviewed by Schnakenberg in his work [41] that provides a decomposition of oriented graphs in terms of cycles through very simple steps. We are given a state space $\mathcal{X}$, a set of transitions $\mathcal{E}$ connecting pair of states in $\mathcal{X}$ and an incidence relation $D : \mathcal{E} \to \mathcal{X}$, which is associated to the matrix

$$D_{x,e} = \delta_{x,\mathtt{t}(e)} - \delta_{x,\mathtt{s}(e)} \qquad x \in \mathcal{X}, e \in \mathcal{E}, \tag{2.62}$$

with size $|\mathcal{X}| \times |\mathcal{E}|$, and with $\delta_{i,j}$ denoting the Kronecker's delta function. It is assumed that a pair of states is connected by at most one edge. We denote with $\mathscr{G}$ the directed graph that contains the states as vertices and the transitions as oriented edges $e \in \mathcal{E}$, formally defined as the triple $\mathscr{G} = (\mathcal{X}, \mathcal{E}, D)$. We then denote as $-e$ the inverse transition. Let $\mathscr{T}$ be a subgraph of $\mathscr{G}$, called spanning tree, with the following properties:

- $\mathscr{T}$ contains all the vertices of $\mathscr{G}$;
- $\mathscr{T}$ contains no cycle;
- $\mathscr{T}$ contains $|\mathcal{X}| - 1$ edges.

In fact, any two of these conditions suffice to define a tree. The edges of $\mathscr{G}$ that are not contained in $\mathscr{T}$ are called chords, and it is immediate to verify that insertion of a chord in $\mathscr{T}$ creates a cycle, which can be oriented according to the orientation of the chord. The set of all the cycles created in this way is indicated by $\mathcal{C}$. Thus for each chord we associate a cycle in $\mathscr{G}$ with the orientation given by the direction of the inserted chord. It can be proven that any other cycle in $\mathscr{G}$ can be obtained as a combination of such fundamental cycles. Given $|\mathcal{X}|$ the number of vertices in $\mathscr{G}$ and $|\mathcal{E}|$ the number of edges, provided that the graph is connected, the number of fundamental cycles denoted by $|\mathcal{C}|$, called cyclomatic number, is obtained as

$$|\mathcal{C}| = |\mathcal{E}| - |\mathcal{X}| + 1. \tag{2.63}$$

Complementarily to the $|\mathcal{C}|$ chords we can define $|\mathcal{X}| - 1$ co-chords as the edges in the spanning tree. Removal of a co-chord makes the spanning tree disconnected by creating a source island and a target island. The set of edges connecting the two islands is a cocycle, and can be oriented according to the removed co-chord. More precisely, the island containing the source state of the removed co-chord is the source island, and the island containing the target state of the removed co-chord is the target island, and the co-cycle is oriented accordingly. For each removed co-chord, then, we define the associated co-cycle by re-introducing edges to reconnect the source and

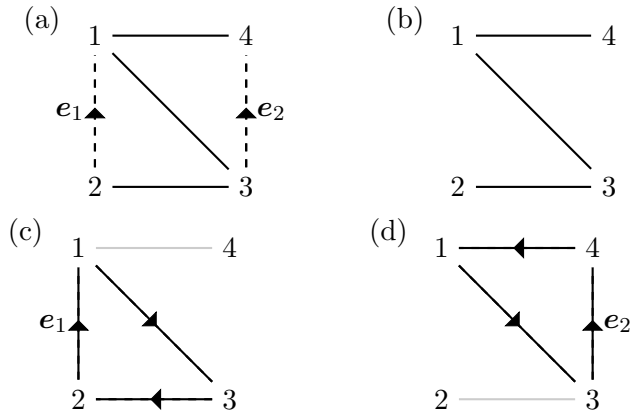

Figure 2.2: (a) A system with four states, edges $\boldsymbol{e}_1 : 2 \to 1$ and $\boldsymbol{e}_2 : 3 \to 4$ are highlighted. (b) removal of $\boldsymbol{e}_1$ and $\boldsymbol{e}_2$ makes the graph a tree $\mathscr{T}$ with no cycles. (c) Re-insertion of $\boldsymbol{e}_1$ creates the cycle $2 \to 1 \to 3 \to 2$ with the orientation parallel to $\boldsymbol{e}_1$. (d) Re-insertion of $\boldsymbol{e}_2$ creates the cycle $3 \to 4 \to 1 \to 3$ with the orientation parallel to $\boldsymbol{e}_2$.

target islands. Given that the co-chord $\boldsymbol{e}_\gamma$ was removed, the corresponding co-cycle is defined as the vector

$$\boldsymbol{c}_e^\gamma = \begin{cases} 1, & \text{if } e \text{ is parallel to the cut} \\ -1, & \text{if } e \text{ is anti-parallel to the cut} \\ 0 & \text{else.} \end{cases} \tag{2.64}$$

For convenience, the edges in the full graph are labelled such that the first $|\mathcal{X}| - 1$ are the co-chords $\boldsymbol{e}_\gamma$ and are labelled by $1 \leq \gamma \leq |\mathcal{X}| - 1$ and the remaining are the chords $\boldsymbol{e}_\alpha$ labelled by $|\mathcal{X}| \leq \alpha \leq |\mathcal{E}|$. In the following cycles and co-cycles are interpreted more in detail from an algebraical point of view.

Let us consider the Master Equation Eq. (2.10) written in terms of probability currents. The sum in the right hand side can be expressed as a sum over all edges $\sum_e D_{x,e} j_e$, with D the incidence matrix Eq. (2.62), since we assumed that states are connected by a unique mechanism and that each edge connects only two states. By defining the vector of probability currents $\boldsymbol{j}$ and the vector of probabilities in state space $\boldsymbol{q}$, the Master Equation can be rewritten in terms of D and the probability currents $\boldsymbol{j}$ as

$$\frac{d\boldsymbol{q}(t)}{dt} = D\boldsymbol{j}. \tag{2.65}$$

The $|\mathcal{C}|$ cycles $\boldsymbol{c}_\alpha$ are found to be a basis of the right null space of D, i.e. $D\boldsymbol{c}_\alpha = 0$ for all α.

The cocycles span the row space of the incidence matrix D. Cycles and cocycles, are orthogonal among each other, and form a basis that spans $\mathbb{R}^{|\mathcal{E}|}$, and minimal sets of cycles and cocycles are find by the procedure above. Given such set, it is possible to provide a decomposition for the vector of currents $\boldsymbol{j}$ and the affinities $\boldsymbol{a}$, where the elements j_e and a_e are evaluated along each edge e. As a result of such a decomposition, explained below, it is possible to provide a decomposition for the entropy production of a process in the graph $\mathscr{G}$.

Given a set of chords $\boldsymbol{e}_\alpha$ and their complementary co-chords $\boldsymbol{e}_\gamma$ and the correspondent cycle and cocycle vectors $\boldsymbol{c}_\alpha$ and $\boldsymbol{c}_\gamma$, the identity matrix over the edge space $\mathbb{R}^{|\mathcal{E}|}$ can be decomposed in two different ways as [42]

$$I = \sum_\alpha \boldsymbol{e}_\alpha \boldsymbol{c}_\alpha^\top + \sum_\gamma \boldsymbol{c}_\gamma \boldsymbol{e}_\gamma^\top \tag{2.66}$$

$$= \sum_\alpha \boldsymbol{c}_\alpha \boldsymbol{e}_\alpha^\top + \sum_\gamma \boldsymbol{e}_\gamma \boldsymbol{c}_\gamma^\top. \tag{2.67}$$

The second identity Eq. (2.67) can be used to decompose the vector of edge currents as

$$\boldsymbol{j} = \sum_\alpha \mathcal{J}_\alpha \boldsymbol{c}_\alpha + \sum_\gamma \mathcal{J}_\gamma \boldsymbol{e}_\gamma \tag{2.68}$$

where $\mathcal{J}_\alpha$ is the current along the chord $\boldsymbol{e}_\alpha$ and $\mathcal{J}_\gamma$ is called tidal current associated to co-cycle $\boldsymbol{c}_\gamma$. The first decomposition Eq. (2.66) can be used to split the vector of edge affinities $\boldsymbol{a}$ as

$$\boldsymbol{a} = \sum_\alpha \mathcal{A}_\alpha \boldsymbol{e}_\alpha + \sum_\gamma \mathcal{A}_\gamma \boldsymbol{c}_\gamma \tag{2.69}$$

where the first term is written in terms of the cycle affinities $\mathcal{A}_\alpha = \boldsymbol{a} \cdot c_\alpha$, with the property of being independent on the state space probabilities $q_x(t)$, $x \in \mathcal{X}$. In fact, by using the definition of the edge affinities Eq. (2.40) we have that

$$\begin{aligned} \mathcal{A}_\alpha &= \sum_{e \in \boldsymbol{c_\alpha}} \log \left(\frac{r(e) q_{\mathtt{s}(e)}(t)}{r(-e) q_{\mathtt{t}(e)}(t)} \right)^{c_e^\alpha} \\ &= \log \prod_{e \in \boldsymbol{c_\alpha}} \left(\frac{r(e)}{r(-e)} \right)^{c_e^\alpha}, \end{aligned} \tag{2.70}$$

where the probabilities $q_x(t)$, $x \in \mathcal{X}$ are cyclically canceled. By using the decompositions Eqs. (2.68) and (2.69) we can finally write the entropy production rate as

$$\dot{\sigma} = \boldsymbol{a} \cdot \boldsymbol{j} = \sum_\alpha \mathcal{J}_\alpha \mathcal{A}_\alpha + \sum_\gamma \mathcal{J}_\gamma \mathcal{A}_\gamma. \tag{2.71}$$

At the stationary state, the only term contributing to the entropy production rate Eq. (2.71) is the cycle term $\sum_\alpha \mathcal{A}_\alpha \mathcal{J}_\alpha$.

Notice that the vanishing of all cycle affinities Eq. (2.70) corresponds to the equilibrium condition given by the Kolmogorov's criterion Eq. (2.32).

2.5.2 Asymptotic fluctuation relation

The decomposition given in the previous section gives that at stationarity only the cycle currents contribute to the full entropy production. Thus, estimation of such currents is enough to evaluate the entropy production rate of the full system. However, if the intention is to derive fluctuation relations for such minimal set of currents we have to deal with total currents and then we evaluate the integrated entropy production at time t. Andrieux and Gaspard [33] derived a FR for cycle currents by using a technique involving the generating function of cumulants, that can be expressed in terms of a tilted matrix containing a minimal set of counting fields. We give here an euristic argument based on the decomposition Eq. (2.71).

The entropy Eq. (2.71) can be rephrased in its integrated version, where the current densities $\boldsymbol{j}$ are replaced by their integrated analogue $\boldsymbol{c}$. At long times we can assume that the integrated current typically grows linearly in time as $\boldsymbol{c} \sim \boldsymbol{j}\, t$. By now considering single realizations of a process, the total entropy production is expressed in its stochastic form Eq. (2.47) in terms of the fluctuating currents $\hat{\boldsymbol{c}}$. At long times we can approximate the total fluctuating current as $\hat{\boldsymbol{c}} \sim \hat{\boldsymbol{j}}\, t$ and by decomposing the entropy in a cycle and a tidal contribution, the cycle term dominates, thus the integrated fluctuating entropy reads

$$\hat{\sigma} = \sum_{\alpha} \mathcal{A}_\alpha \hat{c}_\alpha \tag{2.72}$$

only depending on the fluctuating currents $\hat{c}_\alpha$ evaluated on the chords, and the corresponding cycle affinities a_α. Finally, those currents satisfy the FR

$$\log \frac{p_t(\{\hat{c}_\alpha\})}{p_t(-\{\hat{c}_\alpha\})} \asymp \sum_{\alpha=1}^{|\mathcal{C}|} \mathcal{A}_\alpha \hat{c}_\alpha(t). \tag{2.73}$$

This is a great advantage, since we do not need to know about the probability distributions in state space to be able to estimate entropy production, but only about the number of fundamental cycles that constitute the full process. Moreover, each current and affinity contributing to Eq. (2.73) can be identified as macroscopic current and macroscopic affinities, being each coupled in general with a different reservoir.

The validity of the FR Eq. (2.73) is limited to the case where the set of observed currents corresponds to the chords of the underlying graph, which is said to be a complete set. When this requirement is not satisfied, it is not possible in general to find FRs unless the hidden cycles are futile, i.e. they do not contribute to the total entropy production. In the following sections we define processes in the space of visible transitions. The visible

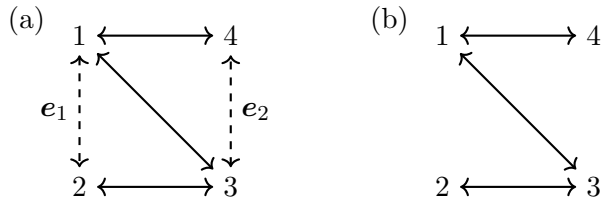

Figure 2.3: (a) The currents evaluated along the edges denoted as $\boldsymbol{e}_1$ and $\boldsymbol{e}_2$ constitute a complete set of currents since the graph contains two fundamental cycles, obtained from Schnakenberg cycle decomposition, and satisfy the asymptotic fluctuation relation Eq. (2.73). (b) The stationary state of the same process where $\boldsymbol{e}_1$ and $\boldsymbol{e}_2$ are removed is called stalling state. The currents along $\boldsymbol{e}_1$ and $\boldsymbol{e}_2$ evaluated at all times t then satisfy a transient fluctuation relation if the system is in the stalling state at initial time $t = 0$.

currents evaluated up to the occurrence of a fixed number n of transitions are proven to satisfy a FR in terms of effective affinities, thus providing a thermodynamical consistent description even in the case of partially accessible graphs.

2.5.3 Transient fluctuation relation

From now on, we replace the fluctuating stochatic currents $\hat{c}$ with the symbol c since we always refer to currents as stochastic quantities.

The asymptotic relation Eq. (2.73) for currents evaluated up to a time t, holds asymptotically at long times $t \to \infty$ since the contribution to the total entropy production given by the tidal currents can be neglected in this limit. However, this limitation can be circumvented by preparing the system according to a specific initial distribution, which makes the tidal contribution to the entropy production vanish at all times. Such a preferred distribution is called stalling distribution [32], and is the stationary state of the same process where the observable edges, along which the currents are evaluated, are removed (see Fig. 2.3).

This situation corresponds physically to switching off the observed transitions, that are switched on again at the initial time $t = 0$ after the system relaxes to the stalling distribution. Given such an initial state, then, the currents $\{c_\alpha\}$ evaluated at all times t satisfy the *transient* fluctuation relation

$$\log \frac{p_t(\{c_\alpha\})}{p_t(\{-c_\alpha\})} = \sum_{\alpha=1}^{|\mathcal{C}|} \mathcal{A}_\alpha c_\alpha(t), \tag{2.74}$$

where the symbol $\asymp$ is replaced by an equality, since the stalling distribution cancels the contribution to the total entropy production given by the state of the system at initial and final times.

Chapter 3

Markov chains in transition space

The Markov chains in state space introduced in the previous Chapter induce a dynamics on transitions that is the central object of study in this thesis. In particular we are interested in the dynamics of few observable transitions, in fewer number than the cycle currents introduced in Sec. 2.5.1. We obtain such dynamics by coarse-graining procedures involving first-exit time problems, which consist in determining the distribution of the time elapsed before a predefined threshold or boundary is crossed for the first time. In this case, we are interested in the probability of observing certain sequences of transitions at any time, by integrating out the inter-transition times. The process so obtained is a discrete-time Markov chain, where, importantly, the time is ticked by the occurrence of the transitions themselves, and whose evolution is generated by a transition matrix in the space of observable transitions. Importantly, the coarse-graining procedure reproduces the dynamics of the partial currents exactly, without need of time-scale separation or of weak coupling.

An alternative derivation of the dynamics relies on the not very well-known method of stochastic complementation, introduced in Chapter 6.

In this Chapter we first consider the simple case where a single transition in both directions can be observed, with explicit calculations. For this special case the notion of inter-transition time probability density is introduced by use of a first-exit time approach, with the derivation of the so-called survival matrix, the generator of a stochastic dynamics where probability is not conserved. We then extend the treatiment to the case where an arbitrary number of transitions is observable. At the end of the Chapter another limit case is addressed, where all transitions are observable. The latter provides a process that is equivalent to the original embedded chain, but lifted to the space of transitions.

Before addressing the main points of this Chapter, we introduce tradi-

tional first-exit time problems, which are then generalized to where only few observable transitions are considered.

3.1 First-exit time problems

First-exit time problems, also called first hitting time, or only hitting time, appear in many fields such as physics, engineering, biology, ecology and finance. A typical example of first-exit time problem is known as the gambler's ruin, where a gambler, given an initial budget, gains and loses money with some probability. One can for instance evaluate the probability to lose all the money in a finite time and calculate the average time this event occurs. First-exit time problems can be used in many context to evaluate the life expectancy of patients [43, 44], the lifetime and relaxation time of unfolded proteins [45], lifetime of engineering systems [46] and to measure ecological resilience [47].

Given a Markov chain, the first-exit time is defined as the time in which a certain event, belonging to some set, occur. If the threshold consists in a set of states A, then the first-exit time is defined formally as

$$\tau_A = \inf\{t|\hat{X}(t) \in A\}, \tag{3.1}$$

and is itself a random variable. We are then interested in the probability distribution of the first-exit time τ_A. In the case where the threshold is a subset of states, the probability density that the subset A is first reached at time t, indicated as $f_A(t)$, is obtained from the original full process by setting all the rates $r(y|x)$ with $x \in A$ equal to zero, and thus all the corresponding exit rates. The new rate matrix, now indicated with $\tilde{R}$, generates a Markov jump process where the dynamics is stucked in A for all times $t \geq \tau_A$. For this reason, the states in A are also called absorbing states.

As an example, we consider the usual example in Figure. 2.1, and we assume that the process is stopped when the state $x = 1$ is reached for the first time. Thus, the modified rate matrix $\tilde{R}$ now reads

$$\tilde{R} = \begin{pmatrix} 0 & r(1|2) & 0 & r(1|4) \\ 0 & -r(2) & r(2|3) & 0 \\ 0 & r(3|2) & -r(3) & r(3|4) \\ 0 & 0 & r(4|3) & -r(4) \end{pmatrix}, \tag{3.2}$$

and it is still a well defined Markov chain since $\sum_y \tilde{R}_{y,1} = 0$. The probability of reaching $x = 1$ for the first time is then determined by the so called survival probability, namely the probability of not being in $x = 1$ at time t, thus it is obtained from the solution of the corresponding Master equation by summing over all the non-absorbing states $x \neq 1$. Being the Master equation

$$\frac{d\tilde{q}_t(x)}{dt} = \sum_y \tilde{R}_{x,y}\tilde{q}_t(y), \tag{3.3}$$

we see that the dynamics on the non-absorbing states $x \neq 1$ is uncoupled from the evolution of $\tilde{q}(1)$, because the column of $\tilde{R}$ associated to $x = 1$ has all zero entries. Thus, for $x \neq 1$, the formal solution is

$$\tilde{q}_t(x) = \sum_y \left[e^{tS}\right]_{x,y} q_0(y) \qquad\qquad x, y \neq 1, \tag{3.4}$$

with $q_0(y)$ an initial probability in state space. The evolution of $\tilde{q}_t(x)$ is expressed in terms of a matrix S, called survival matrix obtained as the sub-matrix of the original rate matrix R which is obtained by eliminating the rows and columns associated to absorbing states. Thus, the survival probability is obtained by summing the probabilities Eq. (3.4) over all $x \neq 1$

$$\sigma_\varnothing(t) = \sum_{x \neq 1} \tilde{q}_t(x). \tag{3.5}$$

Let $f_{x=1}(t)$ denote the probability density of being absorbed in $x = 1$ in a time interval $[t, t + dt)$ and let $F(t) = P(\tau \leq t) = \int_{\tau \leq t} f_{x=1}(\tau) d\tau$ the cumulative distribution function, interpreted as the probability of being absorbed in $x = 1$ before time t. The cumulative distribution is then complementary with $\sigma_\varnothing(t)$, which is the probability of not being absorbed in $x = 1$ at time t. Thus, $F(t)$ and $\sigma_\varnothing(t)$ are related as $F(t) = 1 - \sigma_\varnothing(t)$, and the first-exit time density can be obtained as

$$f_{x=1}(t) = -\frac{d\sigma_\varnothing(t)}{dt}. \tag{3.6}$$

The same first -exit problem can be conditioned to any state $z \neq 1$ by setting $\tilde{q}_0(y) = \delta_{z,y}$.

The first-exit problems treated here are defined for continuous time Markov chains generated by rate matrices R. For the same example above, where the state $x = 1$ is absorbing, a first-exit time problem can be established for the embedded chain associated to the process. Given the embedded transition matrix Π derived from R, the problem now consists in determining the probability that the process is absorbed after n transitions. In such case, the modified transition matrix becomes, if $x = 1$ is absorbing

$$\tilde{\Pi} = \begin{pmatrix} 1 & \pi(1|2) & 0 & \pi(1|4) \\ 0 & 0 & \pi(2|3) & 0 \\ 0 & \pi(3|2) & 0 & \pi(3|4) \\ 0 & 0 & \pi(4|3) & 0 \end{pmatrix}, \tag{3.7}$$

since the process now stays in the absorbing state $x = 1$ with probability one after the first time it is reached. Also in this case it is possible to derive a survival probability and thus the probability of absorbtion at a certain n, with n the total number of transitions occurring in the original

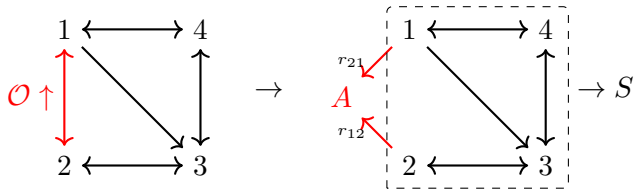

Figure 3.1: The probability for the system to perform a visible transition after another visible one can be obtained from the continuous time dynamics by re-directing observable edges to fictitious states that act as absorbing states. In this way, first-exit time problems provide the so called survival probability, the probability of not performing any observable transition at time t. Such probability is related with the inter transition times distribution.

process, via similar methods as in the continuous time case, except that the time derivative has to be replaced with its discrete-time analogue. We do not give the details here. However, a first-exit time problem is used in this work in Chapter 6, since first-exit time problems in the space of transitions (see Chapter 4) are equivalent to the stochastic complementation of the process respect to a partial set of observable transitions. In particular, the elements of the complemented matrix are exactly the same as the trans-transition probabilities, i.e. the probabilities of subsequent transitions, that are introduced in the next section.

In fact, here we only considered the case where the absorbing set A is extracted from the original set of states in the full Markov chain with rate matrix R. One may ask what is the time of first performing a certain transition, or a set of transitions, between pairs of states. In such case, the problem can be solved in an analogous way by introducing a new absorbing state to the dynamics, that is connected to the source and target states of the considered transitions. This is the situation we consider in this thesis, since it allows to derive the probabilities of performing certain sequences of transitions, by conditioning over the target state of the previous transition, as explained in the next section.

3.2 Trans-transition probabilities

In the following we employ the first-exit time approach used in Refs. [29, 31, 48] to derive inter-transition time distributions between observable transitions, starting from the simplest case of a single observable edge.

3.2.1 Single observable transition

Consider the 4-states graph illustrated in Fig. 3.1 as an example. We consider for the moment the case of forward and backward transitions between two states 1 and 2, denoted as $\uparrow$ when $2 \to 1$ and with $\downarrow$ when $1 \to 2$. We are interested in the probability $p(\ell|x)$ of performing the visible transition $\ell \in \{\uparrow, \downarrow\}$ for the first time conditioned to state $x \in \mathcal{X}$, after preparing the system with probability $\boldsymbol{q}_0 = (q_0(x))$, $x \in \mathcal{X}$ in state space. We use a first-exit time approach to calculate such probability.

The full system is subject to a markovian dynamics, with generator the rate matrix

$$R = \begin{pmatrix} -r(1) & r(1|2) & r(1|3) & r(1|4) \\ r(2|1) & -r(2) & r(2|3) & 0 \\ r(3|1) & r(3|2) & -r(3) & r(3|4) \\ r(4|1) & 0 & r(4|3) & -r(4) \end{pmatrix}, \tag{3.8}$$

thus the vector of state space probabilities $\boldsymbol{q}_t$ at time t satisfy the Master Equation Eq. (2.8). After introduction of a fictitious absorbing state A, the transitions denoted by $\uparrow$ and $\downarrow$ are deviated to A. Then, the evolution of this new system is rephrased as a Master Equation that accounts for the fact that the dynamics is stucked in A after the first time it is reached, thus involving modified state probabilities $\tilde{\boldsymbol{q}}(t)$ and the probability $q_A(t)$ of being in A at time t as

$$\frac{d}{dt}\begin{pmatrix} q_A(t) \\ \tilde{\boldsymbol{q}}(t) \end{pmatrix} = \tilde{R}\begin{pmatrix} q_A(t) \\ \tilde{\boldsymbol{q}}(t) \end{pmatrix} \tag{3.9}$$

with now $\tilde{R}$ being a modified rate matrix, that for our specific example reads

$$\tilde{R} = \left(\begin{array}{c|cccc} 0 & r_{21} & r_{12} & 0 & 0 \\ \hline 0 & -r_1 & 0 & r_{13} & r_{14} \\ 0 & 0 & -r_2 & r_{23} & 0 \\ 0 & r_{31} & r_{32} & -r_3 & r_{34} \\ 0 & r_{41} & 0 & r_{43} & -r_4 \end{array}\right) = \left(\begin{array}{c|cccc} 0 & r_{21} & r_{12} & 0 & 0 \\ \hline \mathbf{0} & \multicolumn{4}{c}{S} \end{array}\right). \tag{3.10}$$

The survival matrix S introduced in the previous equation is obtained from the original rate matrix R by setting to zero the rates corresponding to the observable transitions, differently from the traditional first-exit time processes explained in Sec. 3.1. This difference is explained by the fact that in traditional first-exit time problems we consider a subset of the full state space as absorbing, while in the case of first-exit time problems based on the occurrence of some transitions we are adding fictitious states which are considered as absorbing.

This procedure can be generalized to an arbitrary number of observable edges. Remarkably, despite the introduction of the absorbing state A, the evolution of the probability of the original state space remains uncoupled from the evolution of the probability $\tilde{\boldsymbol{q}}(t)$ in the absorbing state, since it

does not depend on the probability $q_A(t)$. In fact, if the latter only depends on the original rates and the probability in the source states in the observed transition, the modified probability vector of the non-fictitious states evolves as

$$\frac{d}{dt}\tilde{\boldsymbol{q}}(t) = S\tilde{\boldsymbol{q}}(t) \tag{3.11}$$

with formal solution $\tilde{\boldsymbol{q}}(t) = e^{S\,t}\boldsymbol{q}(0)$, with $\boldsymbol{q}_0$ the initial probability at time $t = 0$. Differently from a standard Markov chain, the probability $\tilde{\boldsymbol{q}}(t)$ is not normalized because of probability leaks to the absorbing state. Then, the probability of not having performed an observable transition up to time t starting from an initial probability $\boldsymbol{q}(0)$ is found by summing the elements of the vector in the left hand side of Eq. (3.9) on state space $\mathcal{X}$

$$\sigma_{\varnothing}(t) = \sum_{y\in\mathcal{X}} \tilde{q}_y(t) = \sum_{y,z\in\mathcal{X}} \left[e^{S\,t}\right]_{y,z} q_z(0). \tag{3.12}$$

The quantity above is also called unconditional survival probability, with $\sigma_{\varnothing}(t) = 1 - F(t)$, $F(t)$ denoting the cumulative probability function of performing the observable transition before time t. As in the example in Sec. 3.1, it is possible to calculate the probability density that an observable transition occurs in the time interval $[t, t+dt)$ from the survival probability Eq. (3.12) as

$$\begin{aligned} f_{\text{jump}}(t) &= -\frac{d}{dt}\sigma_{\varnothing}(t) \\ &= r(\uparrow)\sum_x \left[e^{tS}\right]_{\mathtt{s}(\uparrow),x} q_x(0) + r(\downarrow)\sum_x \left[e^{tS}\right]_{\mathtt{s}(\downarrow),x} q_x(0) \end{aligned} \tag{3.13}$$

for the case of a single observable edge, where $r(\ell) = r(\mathtt{t}(\ell)|\mathtt{s}(\ell))$ denotes the transition rate associated to transition ℓ.

Let us now assume that the system is in state x at initial time with certainty, such that $p_z(0) = \delta_{x,z}$. Thus the conditional survival probability now reads

$$\sigma_t(\varnothing|x) = \sum_{y\in\mathcal{X}} \left[e^{S\,t}\right]_{y,x}. \tag{3.14}$$

By repeating the procedure adopted to derive Eq. (3.13) the probability density of observing a transition in the interval $[t, t+dt)$ is

$$f_{\text{jump}}(t|x) = r(\uparrow)\left[e^{tS}\right]_{\mathtt{s}(\uparrow),x} + r(\downarrow)\left[e^{tS}\right]_{\mathtt{s}(\downarrow),x}. \tag{3.15}$$

Equation (3.15) consists in two contributions, representing the probability density that the transitions $\uparrow$ or $\downarrow$ occur first respectively. Notice that in the derivation of Eq. (3.15) we used a single absorbing state A and we distinguished each contribution to Eq. (3.15) by associating each of them to different observable transitions, whereas we could have used distinct absorbing states each of which is associated to a transition in an unique direction,

which lead to an equivalent result, as explained in Appendix A of Ref. [29]. This point is made more clear in Section 3.2.2 where we prove that the inverse of the survival matrix can be interpreted in terms of path probabilities along the hidden part of the system.

So far, the derived probabilities are not accounting for previous observable transitions. However, by considering the case where x is the target state of an observable transitions, the density Eq. (3.15) can be conditioned to the previous transition being the one with target state x. In our simple example, $x = 1$ is the target state of transition $\uparrow$, while $x = 2$ is the target of transition $\downarrow$. Finally we write

$$f_t(\text{jump}|\uparrow) = f_t(\uparrow|\uparrow) + f_t(\downarrow|\uparrow) \tag{3.16}$$

where $f_t(\ell|\ell') = r(\ell)\left[e^{tS}\right]_{\mathtt{s}(\ell),\mathtt{t}(\ell')}$ is the probability density of performing the observable transition ℓ at time t, given that at $t = 0$ the transition ℓ' was observed. To obtain the probabilities we are looking for, i.e. the probabilities of observing ℓ after ℓ' at any time, we integrate the equation above over time. The left-hand side is 1, since it is the probability of ever observing any observable transition. On the right-hand side, each term is integrated as follows

$$\begin{aligned} p(\ell|\ell') &= \int_0^\infty dt\, f_t(\ell|\ell') \\ &= r(\ell)\int_0^\infty dt\, \left[e^{tS}\right]_{\mathtt{s}(\uparrow),\mathtt{t}(\ell')} \\ &= -r(\ell)S^{-1}_{\mathtt{s}(\ell),\mathtt{t}(\ell')} \end{aligned} \tag{3.17}$$

where convergence is granted since S has an unique dominant eigenvalue according to the Perron-Frobenius theorem (see Sec. 2.1.4). The equation above defines the trans-transition probabilities $p(\ell|\ell') = -r(\ell)S^{-1}_{\mathtt{s}(\ell),\mathtt{t}(\ell')} > 0$, the probabilities of observing ℓ after ℓ' at any time. At fixed ℓ' we have $\sum_\ell p(\ell|\ell') = 1$ and thus trans-transition probabilities are normalized. The trans-transition probabilities can then be arranged in a stochastic matrix P, called trans-transition matrix, with normalized columns. In the single transition case it reads

$$P = \begin{pmatrix} p(\uparrow|\uparrow) & p(\uparrow|\downarrow) \\ p(\downarrow|\uparrow) & p(\downarrow|\downarrow) \end{pmatrix}. \tag{3.18}$$

The so-defined trans-transition matrix is then a transition matrix generating a discrete-time Markov chain in the space of transitions, with the probability vector associated to each observed transition evolving as

$$\boldsymbol{p}_{n+1} = P\boldsymbol{p}_n = P^n\boldsymbol{p}_1 \tag{3.19}$$

if the system is prepared in a way such that the first occurrence is ℓ with probability given by $p_1(\ell)$. These can be related to the initial state in $\mathcal{X}$ by

$$p_1(\ell) = -r(\ell) \sum_x \left[S^{-1}\right]_{s(\ell),x} q_0(x), \tag{3.20}$$

which is obtained from the unconditional survival probability Eq. (3.14).

3.2.2 Hidden paths

Above, we have expressed the trans-transition probabilties in terms of the survival matrix S through its inverse. Here we show that the matrix elements $S^{-1}_{x,y}$ have an interpretation in terms of path probabilities along the hidden transitions that complement the observable ones.

Let T the matrix with entries $T_{x,y} = 1 - \sum_\ell \delta_{\mathtt{s}(\ell),x}\delta_{\mathtt{t}(\ell),y}$, with all unitary elements except for the pair of states (x, y) that are connected by an observable transition. Then, given a rate matrix R, the correspondent survival matrix is defined via the element-wise (Hadamard) matrix product $S = R \circ T$ with components $S_{x,y} = R_{x,y}T_{x,y}$. The matrix T is also referred as *taboo* matrix, to underline that the evolution for the first-exit time process is arrested when a visible transition occurs.

Now consider the trans-transition probabilities defined by Eq. (3.17). The survival matrix can be splitted into a diagonal and an off-diagonal part $S = -S_{\mathrm{D}} + S_{\mathrm{OD}}$, with $S_{\mathrm{D}} = R_{\mathrm{D}}$ collecting the exit rates. Then

$$S = (S_{\mathrm{OD}}S_{\mathrm{D}}^{-1} - I)S_{\mathrm{D}} \tag{3.21}$$

with I the identity matrix. By recalling that the rate matrix R is expressed in a similar way in terms of the transition matrix for the embedded Markov chain, then Eq. (3.21) can be written in terms of the survival transition matrix $\Sigma = \Pi \circ T$, thus giving $S = (\Sigma - I)S_{\mathrm{D}}$. The trans-transition probabilities can then be written as

$$p(\ell|\ell') = r(\ell)\left[S_{\mathrm{D}}^{-1}(I-\Sigma)^{-1}\right]_{\mathtt{s}(\ell),\mathtt{t}(\ell')} = \pi(\ell)\sum_{m\in\mathbb{N}}\left[\Sigma^m\right]_{\mathtt{s}(\ell),\mathtt{t}(\ell')}, \tag{3.22}$$

with $\pi(\ell) = \pi(\mathtt{s}(\ell)|\mathtt{t}(\ell))$ being the transition probability associated with the observed transition ℓ, and where the second equality follows from the fact that Σ has spectral radius $\rho(\Sigma) < 1$ [31] (see also Sec. 2.1.4). The m-th power of Σ then weights all path probabilities of lenght m occurring along hidden transitions. In fact, if $x_0 = \mathtt{t}(\ell')$

$$\Sigma^m_{\mathtt{s}(\ell),\mathtt{t}(\ell')} = \sum_{x_1\cdots x_m} \delta_{x_m,\mathtt{s}(\ell)} \prod_{k=0}^{m-1} \pi(x_{k+1}|x_k)T_{x_{k+1},x_k}. \tag{3.23}$$

Thus, the trans-transition probabilities account for all the possible trajectories along hidden transitions connecting the target states $\mathtt{t}(\ell')$ of the conditioned transition ℓ' and the source $\mathtt{s}(\ell)$ of transition ℓ.

3.2.3 Average time of performing n transitions

Consider a system prepared with state space probability $\boldsymbol{q}_0$ at initial time $t = 0$. The probability density of performing the first observable transition in the time interval $[t, t + dt)$ is expressed by Eq. (3.13). We are interested in the average time it takes to perform n transitions in the case of a single observable edge. This kind of analysis, while not entering directly the main results, is crucial to compare stopping criteria, in particular stopping-t and stopping-n, in a meaningful way when running simulations. In fact we discuss in Sec. 5.4.3 a possible attempt of comparing fairly different stopping criteria on the same process which affects the statistics of current-like observables, where Eq. (3.29) may play a role.

The average time to perform the first transition is given by

$$\langle t_1 \rangle = \int_0^\infty dt\, t\, f_{\text{jump}}(t) = \sum_\ell \sum_{x \in \mathcal{X}} q_x(0) \int_0^\infty dt\, t\, \left[e^{tS}\right]_{\mathtt{s}(\ell),x} r(\ell). \tag{3.24}$$

The integral in the right-hand side is solved by expanding the matrix exponential in power series

$$\begin{aligned}
\int_0^\infty dt\, t\, e^{tS} &= \int_0^\infty dt \sum_{k=0}^\infty \frac{t^{k+1} S^k}{k!} \\
&= S^{-2} \left(\sum_{k=0}^\infty \frac{t^{k+2} S^{k+2}}{(k+2)!} (k+1) \right) \Bigg|_0^\infty \\
&= S^{-2} \left(\sum_{k=2}^\infty \frac{t^k S^k}{k!} (k-1) \right) \Bigg|_0^\infty \\
&= S^{-2} \left(tS \sum_{k=1}^\infty \frac{t^k S^k}{k!} - \sum_{k=2}^\infty \frac{t^k S^k}{k!} \right) \Bigg|_0^\infty \\
&= S^{-2} \left(tS \left(e^{tS} - I \right) - e^{tS} + I + tS \right) \Big|_0^\infty \\
&= S^{-2} \left(tS e^{tS} - e^{tS} + I \right) \Big|_0^\infty = S^{-2},
\end{aligned} \tag{3.25}$$

Then finally

$$\langle t_1 \rangle = \sum_\ell \sum_x r(\ell) \left(S^{-2}\right)_{s(\ell),x} q_0(x) \tag{3.26}$$

which is related with the squared inverse of the survival matrix S. For the successive transitions we invoke the evolutions of probabilities in the space of transitions defined by Eq. (3.19) in terms of the trans-transition matrix P. In fact, when transition ℓ is observed, the system is in state $\mathtt{t}(\ell)$ in the instant right after the occurrence of ℓ with probability 1. In fact, the average time at which n observable transitions occur is given by

$$\langle t_n \rangle = \langle t_1 \rangle + \sum_{k=2}^n \sum_\ell \sum_x r(\ell) \left(S^{-2}\right)_{s(\ell),x} q_{k-1}(x). \tag{3.27}$$

Consider the state state space probability $\boldsymbol{q}_1$ right after the first transition. With reference to the graph represented in Fig. 3.1 the target state of $\uparrow$ is $x = 1$ and the target of $\downarrow$ is $x = 2$. Then, in the case of a single observable transition

$$\boldsymbol{q}_1^\top = (p_1(\uparrow), p_1(\downarrow), 0, 0) \tag{3.28}$$

and $p_1(\ell)$ are obtained by use of Eq. (3.20). This is extended at each step since $\boldsymbol{q}_k^\top = (p_k(\uparrow), p_k(\downarrow), 0, 0)$ with $\boldsymbol{p}_k = P\boldsymbol{p}_{k-1}$. Finally Eq. (3.27) becomes

$$\langle t_n \rangle = \langle t_1 \rangle + \sum_{k=2}^{n} \sum_{\ell} \sum_{x=1,2} r(\ell) \left(S^{-2}\right)_{s(\ell),x} \left(P^{k-2}\boldsymbol{p}_1\right)(x). \tag{3.29}$$

3.2.4 Average time for multiple observable transitions

The average time of observing n observable transitions can be extended to the case of an arbitrary number of visible transitions occurring in the system. In fact, the same arguments can be reproduced up to Eq. (3.27). The only difference with the single-transition case is that in the case of multiple observable transitions the same state can be the tip of two or more visible transitions, thus after the first transition

$$q_1(x) = \sum_{\ell} p_1(\ell)\delta_{\mathtt{t}(\ell),x}, \tag{3.30}$$

which is, the probability of being in state x after the first visible transition is determined by the probability of the first transition being any transition with target state x. The expression above can be generalized as

$$q_k(x) = \sum_{\ell} p_k(\ell)\delta_{\mathtt{t}(\ell),x} = \sum_{\ell,\ell'} \left[P^{k-1}\right]_{\ell,\ell'} p_1(\ell')\delta_{\mathtt{t}(\ell),x}, \tag{3.31}$$

which can be plugged inside Eq. (3.27). Thus, for multiple observable transitions

$$\langle t_n \rangle = \langle t_1 \rangle + \sum_{k=2}^{n} \sum_{\ell,\ell',\ell''} \sum_{x} r(\ell) \left(S^{-2}\right)_{s(\ell),x} \left[P^{k-1}\right]_{\ell',\ell''} p_1(\ell'')\delta_{\mathtt{t}(\ell'),x}, \tag{3.32}$$

where we give up on a compact representation as in Eq. (3.29) where the initial vector in transition space is multiplied with the $(k-2)$-th power of the trans-transition matrix P. However, this is still possible in the case where states are reached by no more than one visible transition and for some choices of their orientations.

In the next subsection we consider the case where all transitions are observable. The Markov chain so obtained in the space of transitions is nothing more than the original embedded chain of the full process in state space, from which it automatically inherits its irreducibility. This construction will be used explicitly in Chapter 6.

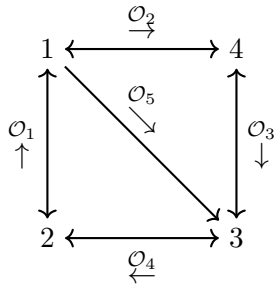

Figure 3.2: A graph where all transitions are visible. The transitions are denoted as $\mathcal{O}_\nu$ and the arrows next to the edges denote the conventional positive direction of the observable transitions.

3.2.5 All edges are observable

In the case where all edges can be observed, the survival matrix reduces to a diagonal matrix with entries the original exit rates. With reference to Fig. 3.2 the observable transitions are labeled by $\mathcal{O}_\nu$ with $\nu = 1, \cdots, 5$, and the arrows next to the edges denote the conventional positive direction for the transition (symbol $\uparrow_\nu$). Also notice that one of the transitions (labeled by $\nu = 5$) only occurs in one direction. For this example, the survival matrix reads

$$S_{\text{full}} = \begin{pmatrix} -r(1) & 0 & 0 & 0 \\ 0 & -r(2) & 0 & 0 \\ 0 & 0 & -r(3) & 0 \\ 0 & 0 & 0 & -r(4) \end{pmatrix}, \tag{3.33}$$

with $r(x)$ the exit rate from state x. The trans-transition probabilities are then

$$p_{\text{full}}(\ell|\ell') = \begin{cases} \pi(\ell) & \text{if} \quad \mathtt{t}(\ell') = \mathtt{s}(\ell) \\ 0, & \text{otherwise,} \end{cases} \tag{3.34}$$

not depending on the conditioned transition ℓ'. In fact, since all transitions are observed, it is possible to reconstruct the full graph, and no hidden cycles are performed. Consequently, the diagonal elements in the trans-transition matrix P_{full} vanish, and it is never possible to observe two subsequent transitions along the same edge in the same direction. Another consequence is that if a transition ℓ can occur after a transition ℓ' or ℓ'' then the source $\mathtt{s}(\ell)$ is the target $\mathtt{t}(\ell') = \mathtt{t}(\ell'')$ for both ℓ' and ℓ''.

For the example in Fig. 3.2 the trans-transition matrix obtained in the

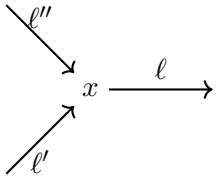

Figure 3.3: When all transitions are observable, the trans-transition probability for a transition ℓ is not conditioned to the previous one and $p(\ell|\ell') = p(\ell|\ell'')$ for all ℓ', ℓ'' whose target $\mathtt{t}(\ell') = \mathtt{t}(\ell'') = x$ is the source $\mathtt{s}(\ell) = x$ of ℓ.

case where all transitions are visible reads

$$P_{\text{full}} = \begin{array}{c} \\ \uparrow_1 \\ \downarrow_1 \\ \uparrow_2 \\ \downarrow_2 \\ \uparrow_3 \\ \downarrow_3 \\ \uparrow_4 \\ \downarrow_4 \\ \uparrow_5 \end{array} \begin{array}{c} \begin{array}{ccccccccc} \uparrow_1 & \downarrow_1 & \uparrow_2 & \downarrow_2 & \uparrow_3 & \downarrow_3 & \uparrow_4 & \downarrow_4 & \uparrow_5 \end{array} \\ \begin{pmatrix} 0 & \pi_{12} & 0 & 0 & 0 & 0 & \pi_{12} & 0 & 0 \\ \pi_{21} & 0 & 0 & \pi_{21} & 0 & 0 & 0 & 0 & 0 \\ \pi_{41} & 0 & 0 & \pi_{41} & 0 & 0 & 0 & 0 & 0 \\ 0 & 0 & \pi_{14} & 0 & 0 & \pi_{14} & 0 & 0 & 0 \\ 0 & 0 & \pi_{34} & 0 & 0 & \pi_{34} & 0 & 0 & 0 \\ 0 & 0 & 0 & 0 & \pi_{43} & 0 & 0 & \pi_{43} & \pi_{43} \\ 0 & 0 & 0 & 0 & \pi_{23} & 0 & 0 & \pi_{23} & \pi_{23} \\ 0 & \pi_{32} & 0 & 0 & 0 & 0 & \pi_{32} & 0 & 0 \\ \pi_{31} & 0 & 0 & \pi_{31} & 0 & 0 & 0 & 0 & 0 \end{pmatrix} \end{array}, \tag{3.35}$$

where $\pi_{ij} = \pi(i|j)$. The trans-transition matrix above is sparse because not all transition can occur one after another. Also, from the property explained in Fig. 3.3, all the trans-transition probabilities on the same line have the same value, and the number of independent rows and columns equals the number of states. Such a process is in all equivalent to the original state space, from which it inherits irreducibility.

Later in Chapter 6 we will use full transition space processes to prove that the trans-transition matrix for a reduced number of observable transitions can be obtained from the full one by using stochastic complementation, a not-so-well known state-space reduction procedure, here applied to transition matrices in the space of transitions.

3.3 Trajectories in transition space

Let us consider a discrete-time Markov chain in the space of observable transitions with trans-transition matrix given by Eq. (3.17). A trajectory $\mathcal{L}_n$ of lenght n in transition space is a sequence $\ell^{(1)} \to \ell^{(2)} \to \cdots \to \ell^{(n)}$ of observable transitions regardless the inter-transition time between each of them.

For a single realization $\mathcal{L}_n$, the probability of observing such a sequence given that the first transition occurs with probability $p_1(\ell^{(1)})$ is given by

$$p(\mathcal{L}_n) = p_1(\ell^{(1)}) \prod_{k=1}^{n-1} p(\ell^{(k+1)}|\ell^{(k)}). \tag{3.36}$$

3.4 Time reversal

Under the requirement that each observable transition can be observed in both directions, it is possible to define the time-reversed sequence $\bar{\mathcal{L}}_n$ as the sequence where both the order of the occurrencies and the direction of each transition in $\mathcal{L}_n$ is reversed

$$\bar{\mathcal{L}}_n = \bar{\ell}^{(n)} \to \bar{\ell}^{(n-1)} \to \cdots \to \bar{\ell}^{(1)} \tag{3.37}$$

with $\bar{\ell}$ the inverse transition of ℓ. In fact, when a succession $\ell \to \ell'$ can be observed, there exist at least one state space path connecting the target state $\mathtt{t}(\ell)$ of ℓ and the source state $\mathtt{s}(\ell')$ of ℓ'. Therefore, if both $\bar{\ell}'$ and $\bar{\ell}$ are observable there also exist at least one state space path connecting $\mathtt{s}(\ell')$ and $\mathtt{t}(\ell)$, and the succession $\bar{\ell}' \to \bar{\ell}$ can be observed with positive probability. The probability of the time-reversed sequence $\mathcal{L}_n$ is then expressed as

$$p(\bar{\mathcal{L}}_n) = \bar{p}_1(\bar{\ell}^{(n)}) \prod_{k=1}^{n-1} p(\bar{\ell}^{(k)}|\bar{\ell}^{(k+1)}), \tag{3.38}$$

where $\bar{p}_1$ specifies that the probability of the first transition in $\bar{\mathcal{L}}_n$ does not necessarily have to be sampled from the same distribution as the forward trajectory.

As an example, consider the forward sequence with $n = 6$

$$\mathcal{L}_6 : \uparrow_1 \to \downarrow_1 \to \downarrow_2 \to \uparrow_2 \to \downarrow_1 \to \downarrow_1 \ . \tag{3.39}$$

Its probability reads

$$p(\mathcal{L}_6) = p_1(\uparrow_1)p(\downarrow_1 \mid \uparrow_1)p(\downarrow_2 \mid \downarrow_1)p(\uparrow_2 \mid \downarrow_2)p(\downarrow_1 \mid \uparrow_2)p(\downarrow_1 \mid \downarrow_1), \tag{3.40}$$

for some initial probability $\boldsymbol{p}_1$. The time-reversed sequence of $\mathcal{L}_6$ is then

$$\bar{\mathcal{L}}_6 = \uparrow_1 \to \uparrow_1 \to \downarrow_2 \to \uparrow_2 \to \uparrow_1 \to \downarrow_1, \tag{3.41}$$

with probability

$$p(\bar{\mathcal{L}}_6) = \bar{p}_1(\uparrow_1)p(\uparrow_1 \mid \uparrow_1)p(\downarrow_2 \mid \uparrow_1)p(\uparrow_2 \mid \downarrow_2)p(\uparrow_1 \mid \uparrow_2)p(\downarrow_1 \mid \uparrow_1), \tag{3.42}$$

assuming that the first transition in the time-reversed sequence occurs with probability $\bar{\boldsymbol{p}}_1$.

In the following we derive the stochastic matrix that generates sequences of observable transitions such that the currents evaluated along those sequences are time-reversed. Before proceeding we recall that in state space the generator of the continuous time reversed dyamics can be obtained directly from the original rate matrix R by applying a similarity transformation on its transposal $R^\top$ as

$$\bar{R} = P_{\rm st}^{-1} R^\top P_{\rm st} \tag{3.43}$$

with $P_{\rm st}$ the diagonal matrix with elements proportional to the stationary distribution of the process generated by R [49]. It can be easily checked that $\bar{R}$ is indeed the generator of a continuous time Markov chain. This is possible because the permanence times in each state are not affected by the time-reversal operation, and only the sequence of visited states is inverted. For processes in the visible transition space the transposal is replaced by another operation, that we call block anti-transposition. The reason is that the time reversed sequences of transitions are obtained by both inverting their order and orientations. Without invoking the stationary distribution in transition space, the time reversed stochastic matrix $\bar{P}$ can be obtained directly by combining block-antitransposition and transposition at least in the case where only the total currents are considered.

3.4.1 Block anti-transposition

By anti-transposition we intend a transposition over the anti-diagonal, differently than the usual transposition which is made with respect to the diagonal of a matrix. For a 2×2 matrix A with elements

$$A = \begin{pmatrix} a & b \\ c & d \end{pmatrix}, \tag{3.44}$$

its anti-transposal is obtained as

$$A^\perp = \begin{pmatrix} d & b \\ c & a \end{pmatrix}. \tag{3.45}$$

In a process generated by a trans-transition matrix, the probability of two subsequent transitions $\bar{\ell}^{(k)} \to \bar{\ell}^{(k-1)}$ in the time-reversed sequence $\bar{\mathcal{L}}_n$ is evaluated by considering the trans-transition probability $p(\bar{\ell}^{(k-1)}|\bar{\ell}^{(k)})$, whereas in the forward sequence $\ell^{(k-1)} \to \ell^{(k)}$ the probability of such a succession is given by the probability $p(\ell^{(k)}|\ell^{(k-1)})$. Thus we seek a process with generator $\bar{P}$ whose forward outcomes have the same probability as time-reversed sequences.

We start from the simple case of a single observable transition. The anti-transposal of the trans-transition matrix reads in this case

$$P^\perp = \begin{pmatrix} p(\downarrow | \downarrow) & p(\uparrow | \downarrow) \\ p(\downarrow | \uparrow) & p(\uparrow | \uparrow) \end{pmatrix}. \tag{3.46}$$

The matrix above is not a stochastic matrix since the sum of its elements over the columns is not normalized. However, its rows are, and therefore its transposal reads

$$\left(P^{\perp}\right)^{\top} = \begin{pmatrix} p(\downarrow \mid \downarrow) & p(\downarrow \mid \uparrow) \\ p(\uparrow \mid \downarrow) & p(\uparrow \mid \uparrow) \end{pmatrix} \tag{3.47}$$

whose columns are normalized to unity. More specifically, given a forward sequence of observable transitions, the matrix Eq. (3.47) can generate the same sequence but with each element $\ell^{(k)}$, $k = 1, \ldots, n$ flipped in direction. Thus this is the generator of time-reversed sequences $\bar{\mathcal{L}}_n$ since, as it will be proven later in Sec. 4.4.1, it also generates the statistics of currents with flipped sign.

However, anti-transposition combined with transposition does not provide the time reversal matrix $\bar{P}$ in the case where more than one edge is accessible to observation, due to the mixed trans-transition contributions $p(\ell_\nu|\ell_\mu)$, $\mu \neq \nu$. To solve the issue, it is necessary to generalize the anti-transposition operation in the case of several observable transitions. In order to do that we define the matrix

$$J = \bigoplus_{\nu=1}^{N} \begin{pmatrix} 0 & 1 \\ 1 & 0 \end{pmatrix} \tag{3.48}$$

where N indicates the number of observed edges. The direct sum symbol $\bigoplus$ means here that the matrix J is composed by N 2×2 square blocks arranged in the diagonal and each representing the first Pauli matrix, and all other entries are zero. Given a generic $2N \times 2N$ matrix A, the block anti-transposition is then defined as

$$A^{\perp} = JA^{\top}J. \tag{3.49}$$

For instance, consider the 4×4 matrix

$$A = \begin{pmatrix} A_{11} & A_{12} \\ A_{21} & A_{22} \end{pmatrix}, \tag{3.50}$$

with A_{ij} being 2×2 matrices. Then, the block anti-transposition of A is obtained as

$$A^{\perp} = \begin{pmatrix} A_{11}^{\perp} & A_{21}^{\perp} \\ A_{12}^{\perp} & A_{22}^{\perp} \end{pmatrix}. \tag{3.51}$$

Notice that we used the same symbol to identify standard anti-transposition and the block anti-transposition, where the ambiguity is solved since for 2×2 matrices they represent exactly the same operation. Finally, by applying block anti-transposition to a trans-transition matrix P of size $2N \times 2N$, with $N > 1$, the time-reversed trans-transition matrix reads

$$\bar{P} = (P^{\perp})^{\top} = JPJ, \tag{3.52}$$

whose columns are easily proven to be normalized. The sequences generated with $\bar{P}$ reproduce the statistics of time-reversed total currents as proven in Sec. 4.4.1.

Chapter 4

Observables in transition space

The aim of this thesis is to show that a transition based formalism becomes the most natural way to describe the thermodynamics of open systems. In fact, this approach provides fluctuation relations for currents even in the case where a single or a few transitions can be monitored by the observer, as it will be ultimately proven in the next Chapter, at least in the simplest case where a single mechanism contributes to each observable transition.

In this Chapter we introduce the relevant measurable quantities that can be extracted from realizations of processes living in the space of visible transition, which are generated by the trans-transition matrices derived previously. In particular we consider total currents, the net amount of times observable edges are crossed in a specified direction, and mixed currents, estimated by counting the amount of times transitions along an observable edge are followed by transitions along a different edge. In parallel to that, also the effective forces driving the system out of equilibrium can be defined consistently and can be estimated empirically from experiments performed at stationarity.

The statistics of the considered observables is studied mainly from the point of view of generating functions, whose symmetries are employed to derive fluctuation relations for the observable currents.

4.1 What is an observable transition?

Transitions between states in a physical system are typically associated with the transport of an extensive quantity. In atomic models, for instance, transitions between atomic configurations can be accompanied with the emission (when the atom is relaxing to an energetically more stable state) or the absorbtion of a photon carrying an energy equal to the difference in energy between the two states involved. In fluorescence spectroscopy, the same

phenomena is exploited, where for each electronic state several vibrational states are also present. In this case, the frequency of the light emitted (and absorbed) by a molecule corresponds to the difference in energies between vibrational states on the same electronic level or between vibrational states on different electronic states.

Other examples can be found in biology when monitoring the flow of chemicals that allow the motion of a molecular motor. In this case, the motion of the motor can be measured by use of precise imaging techniques, and each step can be associated with the consumption of ATP despite the fact that the internal metabolic cycles converting ATP in ADP and viceversa are hidden to the observer [21, 22, 50].

In chemical reaction networks, the idea of chemostatting corresponds on some chemical species being controlled by an external entity, via the coupling with a particle reservoir or because they are nearly constant over certain timescales [51]. One can for instance measure the flow of chemicals in and out the chemostatted reservoirs, while the remaining part of the reaction chain can not be tracked.

As last example we can consider an electronic circuit where several conductors are connected with each other to form an electrical network, where the state of the system corresponds to the electronic population on each conductor [25]. In this case, the transition of electrons between pairs of conductors can be measured by two-terminal devices such as tunnel junctions, diodes or MOS transistors.

For an open system, kept out of equilibrium by coupling to multiple thermal, particle, or even information reservoirs [52, 53], monitoring such quantities is important to estimate the entropy flow to the environment, that constitute a signature of non-equilibrium. However, it is a well known fact that a consistent estimation can be done in the case where the set of observed currents constitute a complete set, since their statistics satisfy in this case the fluctuation relation Eq. (2.73) while in most cases only a minimal set of observables is experimentally accessible.

4.2 Transition space

In this section we formalize the notion of transition space and the subspace of observable transitions, given a process on a graph.

Consider a Markov chain on a graph $\mathscr{G} = (\mathcal{X}, \mathcal{E}, D)$ with $|\mathcal{X}|$ vertices and $|\mathcal{E}|$ edges and let $\nu = 1, \cdots, |\mathcal{E}|$ label each edge, and D an incidence relation $D : \mathcal{E} \to \mathcal{X}$. Each edge $\boldsymbol{e}_\nu$ is oriented arbitrarily, and the transition parallel to $\boldsymbol{e}_\nu$ is denoted by $\uparrow_\nu$. Along the same edge the inverse transition can be defined and is denoted with $\downarrow_\nu$. Then, for each edge, two possible transitions in the opposite direction can occur, and $\mathcal{T}_\nu = \{\uparrow_\nu, \downarrow_\nu\}$ denotes the set of possible transitions along one edge. By now considering all edges

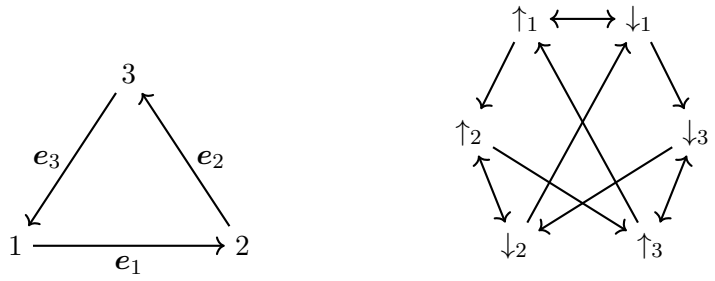

Figure 4.1: *Left:* An unicyclic process in state space where all possible transitions are observable in both directions, with arrows denoting the positive orientation for the directed edges $\boldsymbol{e}_\nu$, with $\nu = 1, 2, 3$ labelling the edge where the transition occur, also referred as the *kind* or *type* of transition. The transition parallel to $\boldsymbol{e}_\nu$ is indicated with $\uparrow_\nu$, and its reversed transition is $\downarrow_\nu$. *Right:* The process in the space of transitions where the nodes denote the transitions along observed edges and the arrows denote the trans-transitions with non-zero probabilities.

ν, the space of all transitions is denoted as $\mathcal{T} = \bigcup_\nu \mathcal{T}_\nu$ and its elements $\ell \in \mathcal{T}$ span all the set of possible transitions within the system. The set $\mathcal{T}$ is then referred as full transition space, and in the case where all transitions are accessible to observation a dynamics on transitions is equivalent to the dynamics in state space, as anticipated in the previous Chapter, if only the embedded markov chain is considered.

4.2.1 Reduced transition space

In the case where a reduced number of transitions is observable, the effective process becomes a semi-Markov process because of the inter-transition times being not generally exponentially distributed, apart when the process is unicyclic. However, in this case the trans-transition probabilities are still defined, and thus it is possible to build the effective process in the space of transitions at discrete time, where the internal time ticks whenever an observable transition occurs.

The reduced space of transitions is denoted as $\mathcal{O} = \bigcup_{\nu'} \mathcal{T}_{\nu'}$ with ν' running on the set of observable edges. From now on the symbol ℓ is referred to a generic transition in this space and ℓ_ν to a transition along edge $\boldsymbol{e}_\nu$ since we assumed that each pair of states is connected by at most one edge. All observable transitions in $\mathcal{O}$ are required to be bi-directional. Thus, for each ℓ_ν the inverse transition, i.e. the transition along the same edge ν in the opposite direction, is indicated as $\bar{\ell}_\nu$ and also occurs with non-vanishing probability. Let us denote by $p_n(\ell)$ the probability that the n-th observable

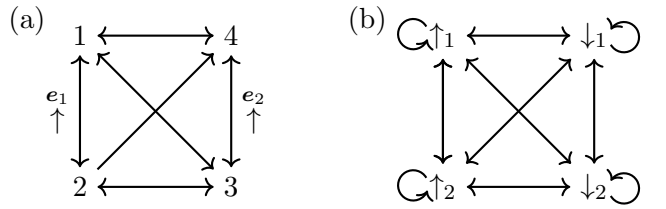

Figure 4.2: (a) A graph with two visible transitions along edges denoted with $\boldsymbol{e}_1$ and $\boldsymbol{e}_2$. The arrows denote the conventional positive sign for the currents, which is denoted, for each edge, as $\uparrow_\nu$, with $\nu = 1, 2$. (b) Since the number N of observable edges satisfies $N \leq |\mathcal{C}|$, with $|\mathcal{C}|$ the number of fundamental cycles, and the graph where $\boldsymbol{e}_1$ and $\boldsymbol{e}_2$ are removed is irredicible, the corresponding graph in the space of observable transitions is completely connected under the assumption that the visible transitions are bi-directional. For this reason the loops connecting observable transitions in one direction to themselves appear.

transition in a sequence of visible transitions is ℓ. This quantity evolves by

$$p_n(\ell) = \sum_{\ell'} P_{\ell,\ell'} p_{n-1}(\ell') = \sum_{\ell'} P^{n-1}_{\ell,\ell'} p_1(\ell'), \tag{4.1}$$

as introduced previously, with $p_1(\ell)$ the probability that the first observed transition is ℓ, connected with the initial condition in state space by Eq. (3.20). For N observable edges, the trans-transition matrix P obtained by the coarse-graining procedure explained in the previous chapter is a $2N \times 2N$ squared matrix if transitions in each visible edge can be observed in both directions, a condition that is required to grant the existence of time-reversed sequences of visible transitions since it grants hidden irreducibility (for details, see Sec. 5.5.2 in the next Chapter).

With the above condition, the matrix P can be divided in N^2 blocks of dimension 2×2. The blocks on the diagonal of P

$$P_\nu = \begin{pmatrix} p(\uparrow_\nu \mid \uparrow_\nu) & p(\uparrow_\nu \mid \downarrow_\nu) \\ p(\downarrow_\nu \mid \uparrow_\nu) & p(\downarrow_\nu \mid \downarrow_\nu) \end{pmatrix} \tag{4.2}$$

account for subsequent transitions along the same edge, and the off-diagonal blocks

$$P_{\nu,\mu} = \begin{pmatrix} p(\uparrow_\nu \mid \uparrow_\mu) & p(\uparrow_\nu \mid \downarrow_\mu) \\ p(\downarrow_\nu \mid \uparrow_\mu) & p(\downarrow_\nu \mid \downarrow_\mu) \end{pmatrix} \tag{4.3}$$

for subsequent transitions along different edges, in particular the transitions over edges ν that are conditioned on transitions over another edge $\mu \neq \nu$. We will see later that this distinction is crucial as we will need to define not only edge currents at stopping n but also mixed currents, playing an important role in the derivation of fluctuation relations for marginally observable systems.

4.3 Currents and affinities

In this section we introduce the physical observables that we can extract from realizations of processes evolving by Eq. (4.1) in transition space, in particular current-like observables. Each observable is conjugated with effective affinities, or effective thermodynamic forces, which maintain the system out of equilibrium.

Currents

Let us consider a Markov chain on the graph $\mathscr{G} = (\mathcal{X}, \mathcal{E}, D)$, where $1 \leq N \leq |\mathcal{E}|$ edges are accessible to observation. For an edge to be observable we require that the amount of times $n_{\uparrow_\nu}$ and $n_{\downarrow_\nu}$ the edge is crossed can be monitored in both directions. By considering a single sequence of transitions $\mathcal{L}_n$ of lenght n, for each edge $\boldsymbol{e}_\nu$, $\nu = 1, \dots, N$, the total current is defined as the net amount of times the edge is crossed as

$$c_\nu(\mathcal{L}_n) = n_{\uparrow_\nu}(\mathcal{L}_n) - n_{\downarrow_\nu}(\mathcal{L}_n) = \sum_{\ell \in \mathcal{L}_n} (\delta_{\uparrow_\nu,\ell} - \delta_{\downarrow_\nu,\ell}) \,. \tag{4.4}$$

The elementary contribution of a single transition ℓ_ν to the total current of kind ν is then defined as

$$j(\ell_\nu) = \begin{cases} +1, & \text{if} \quad \ell_\nu = \uparrow_\nu \\ -1, & \text{if} \quad \ell_\nu = \downarrow_\nu \,. \end{cases} \tag{4.5}$$

The current Eq. (4.4) is the main observable in our discussion. However, those currents are not the only observables that can be extracted from single realizations $\mathcal{L}_n$. In fact, we can define in general the quantity

$$\xi_{\ell_\nu \ell'_\mu}(\mathcal{L}_n) = n_{\ell_\nu \ell'_\mu}(\mathcal{L}_n) - n_{\bar{\ell}'_\mu \bar{\ell}_\nu}(\mathcal{L}_n), \tag{4.6}$$

with $n_{\ell\ell'}(\mathcal{L}_n)$ the number of times transition ℓ occurs right after ℓ' in a sequence $\mathcal{L}_n$. For $\nu = \mu$ and $\ell_\nu = \ell'_\mu = \uparrow_\nu$, the quantity Eq. (4.6) is called *loop current* along edge ν

$$\xi_\nu(\mathcal{L}_n) = n_{\uparrow_\nu \uparrow_\nu}(\mathcal{L}_n) - n_{\downarrow_\nu \downarrow_\nu}(\mathcal{L}_n) \tag{4.7}$$

and it is defined if an observable transition can be observed subsequently in the same direction in $\mathcal{L}_n$. This is the case when only a partial set of edges is accessible to observation. More specifically, indicating with $|\mathcal{C}|$ the number of fundamental cycles in the process, which can be determined by use of Schnakenberg graph decomposition (see Section 2.5.1), the number N of observable transitions is $N \leq |\mathcal{C}|$, and the graph where the corresponding edges are removed is irreducible. The coarse grained trans-transition matrix have then strictly positive diagonal elements in correspondance to the observable edge ν. If it's the case, then the name *loop current* derives from the

fact that in the graph representation in transition space, diagonal elements in the trans-transition matrix are represented by self loops around $\uparrow_\nu$ and $\downarrow_\nu$ (as in the example represented in Figure 4.2). When $\mu \neq \nu$ the quantities Eq. (4.6) are called *mixed currents*, and represent currents associated with subequent occurrences in $\mathcal{L}_\nu$ along different edges.

Together with the total currents Eq. (4.4), the mixed currents Eq. (4.6) play a central role in the discussion about fluctuation relations. The loop currents Eq. (4.7) instead represent roughly (up to boundary terms) the number of times a cycle is closed around an observed edge. Their introduction in this treatment is limited to the fact that they can be connected to the total current c_ν along the same edge via a linear transformation, a crucial step in the derivation of the most general fluctuation relation for a reduced set of observable currents.

Affinities

Analogously to the currents we can define the thermodynamic forces that drive the system out of equilibrium, also called affinities. Given the trans-transition probabilities $p(\ell|\ell')$, we define the quantities

$$\alpha_{\ell_\nu \ell'_\mu} = \log \frac{p(\ell_\nu|\ell'_\mu)}{p(\bar{\ell}'_\mu|\bar{\ell}_\nu)}. \tag{4.8}$$

When $\nu = \mu$ and $\ell_\nu = \ell'_\mu = \uparrow_\nu$, the quantity Eq. (4.8) takes the name of effective affinity, and it is interpreted as the effective force that drives the transitions along edge ν

$$a_\nu = \log \frac{p(\uparrow_\nu \mid \uparrow_\nu)}{p(\downarrow_\nu \mid \downarrow_\nu)}. \tag{4.9}$$

Notice that the greek symbol α used in Eq. (4.8) is replaced with the latin character a: by convention we will use from now on latin letters to define conjugated quantities related to the total currents and greek letters for quantities related to mixed currents. Importantly, the effective affinity a_ν is conjugated to both the total current c_ν and the loop current ξ_ν along the same edge $\boldsymbol{e}_\nu$, as will become more clear in Section 5.5.2 when deriving the general FR for currents.

When $\mu \neq \nu$ we call the quantity Eq. (4.8) mixed affinities

$$\alpha_{\ell_\nu \ell_\mu} = \log \frac{p(\ell_\nu|\ell_\mu)}{p(\bar{\ell}_\mu|\bar{\ell}_\nu)}. \tag{4.10}$$

The quantity Eq. (4.10) is conjugated to the respective mixed current $\xi_{\ell_\nu \ell_\mu}$ only in the case where the loop currents ξ_ν are tracked instead of total currents c_ν. This will be more clear later when discussing fluctuation relations.

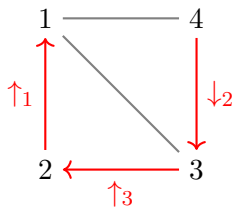

Figure 4.3: An example of graph with two fundamental cycles but three observable currents (along the red arrows). A transition $\uparrow_1$ can be followed by the same transition $\uparrow_1$ only after performing $\uparrow_3$, because the number of observable currents is greater than the number of fundamental cycles in the graph. Thus, since $p(\uparrow_1 \mid \uparrow_1) = 0$, it is not possible to define an effective affinity conjugated with the current along $\boldsymbol{e}_1$.

We anticipate that when total currents c_ν are taken as reference observables, the mixed currents $\xi_{\ell_\nu \ell_\mu}$ are conjugated with the so-called *shifted* mixed affinities

$$\tilde{\alpha}_{\ell_\nu \ell_\mu} = \alpha_{\ell_\nu \ell_\mu} - \frac{1}{2}(a_\nu j(\ell_\nu) + a_\mu j(\ell_\mu)), \tag{4.11}$$

where we recall that $j(\ell_\nu)$ is the elementary current carried by transition ℓ_ν, as defined by Eq. (4.5).

As a final remark, when the set of observable currents form a complete set, that is, one current per cycle is observed, then the effective affinity a_ν conjugated to the current c_ν or ξ_ν along the edge $\boldsymbol{e}_\nu$ becomes the cycle affinity conjugated with the current along the chord $\boldsymbol{e}_\nu$, defined by Eq. (2.70). When a larger number of currents is observed, an affinity of the type Eq. (4.9) might not be defined (see Fig. 4.3 for an example where this happens), and certainly it is not when all edges in $\mathscr{G}$ are visible.

4.4 Generating functions for currents's moments

Given a Markov chain, the currents statistics at stopping n is encoded in their joint probability distribution that we denote here with $p_n(\boldsymbol{\xi})$ where $\boldsymbol{\xi}$ is a vector of currents containing both the total currents and the mixed currents defined in the previous section. For instance, for two observable transitions we consider

$$\boldsymbol{\xi}^\top = (c_1\,,\, c_2\,,\, \xi_{\uparrow_1\uparrow_2}\,,\, \xi_{\uparrow_1\downarrow_2}\,,\, \xi_{\downarrow_1\uparrow_2}\,,\, \xi_{\downarrow_1\downarrow_2}). \tag{4.12}$$

4.4.1 Moment Generating Function

The statistics of fluctuating observables can be described in terms of the so called Moment Generating Functions (MGF), analogous to the Laplace

transform for probability distributions. In the most general case we can choose an arbitrary subset of $\boldsymbol{\xi}$. Given a process stopped after the occurrence of n observable transitions over N edges, we consider a subset $\tilde{\boldsymbol{\xi}}$ of the currents along the visible edges. The outcome space of all the considered currents is discrete, and thus their MGF is defined as

$$G_n(\tilde{\boldsymbol{\lambda}}) = \langle e^{\tilde{\boldsymbol{\lambda}}\cdot\tilde{\boldsymbol{\xi}}} \rangle = \sum_{\tilde{\boldsymbol{\xi}}\in\mathcal{F}_n} e^{\tilde{\boldsymbol{\lambda}}\cdot\tilde{\boldsymbol{\xi}}} p_n(\tilde{\boldsymbol{\xi}}) \tag{4.13}$$

with $\mathcal{F}_n$ denoting the filtration for the currents $\tilde{\boldsymbol{\xi}}$ after n observable transitions, i.e., the set of possible observable outcomes of a measurement of the current. The conjugate variables $\tilde{\boldsymbol{\lambda}}$, called counting fields, have the same number of elements as the considered subset of currents. If an element of $\tilde{\boldsymbol{\xi}}$ is a total current c_ν along edge ν then its conjugated counting field is denoted as λ_ν, and mixed currents in $\tilde{\boldsymbol{\xi}}$ are conjugated to the counting fields $\lambda_{\ell_\nu\ell_\mu}$, $\mu \neq \nu$. The counting fields $\lambda_{\ell_\nu\ell_\mu}$ are assumed to have the same antisymmetry properties as the mixed currents with respect to the notion of time reversal introduced in Section 3.4, i.e. $\lambda_{\ell_\nu\ell_\mu} = -\lambda_{\bar{\ell}_\mu\bar{\ell}_\nu}$.

Given an element of $\tilde{\boldsymbol{\xi}}$ its k-th statistical moment is obtained as

$$\mu_k(c_\nu) = \left.\frac{\partial^k G_n(\tilde{\boldsymbol{\lambda}})}{\partial\lambda_\nu^k}\right|_{\lambda_\nu=0} \tag{4.14}$$

$$\mu_k(\xi_{\ell_\nu\ell_\mu}) = \left.\frac{\partial^k G_n(\tilde{\boldsymbol{\lambda}})}{\partial\lambda_{\ell_\nu\ell_\mu}^k}\right|_{\lambda_{\ell_\nu\ell_\mu}=0} \tag{4.15}$$

where the first line is for total currents c_ν and the second line for the mixed currents $\xi_{\ell_\nu\ell_\mu}$. The first moment μ_1 denotes the average, the second moment μ_2 is related to its variance and so on, accordingly to the properties of moment generating functions. Later on we provide an alternative writing for the MGF Eq. (4.13) in terms of a tilted trans-transition matrix $P(\tilde{\boldsymbol{\lambda}})$ containing the counting fields conjugated to the currents of interest.

4.4.2 Tilted matrices

The elements $p(\ell_\nu|\ell'_\mu)$ of the trans-transition matrix P are modified as follows. Given that the observable transition ℓ'_μ occurred, we consider a trans-transition $\ell'_\mu \to \ell_\nu$. To this sequence of observable transitions is associated a current $\xi_{\ell_\nu\ell'_\mu}$, which can be increased or decreased. The total current associated with ℓ_ν is also increased or decreased accordingly. We now provide an explicit expression for the modified matrix, called tilted matrix, depending on which of the currents associated with occurrences $\ell'_\mu \to \ell_\nu$ are included in the joint statistics $p_n(\tilde{\boldsymbol{\xi}})$ under consideration, remembering that for now we choose an arbitrary subset $\tilde{\boldsymbol{\xi}}$ of $\boldsymbol{\xi}$, for the sake of generality.

Consider for instance the diagonal blocks P_ν Eq. (4.2) of the trans-transition matrix P, defined by Eq. (3.17). If the current c_ν of kind ν is measured (and thus is contained in $\tilde{\boldsymbol{\xi}}$), then its elements are tilted as

$$P(\tilde{\boldsymbol{\lambda}})_{\ell_\nu \ell'_\nu} = P_{\ell_\nu \ell'_\nu} e^{\lambda_\nu j(\ell_\nu)}, \tag{4.16}$$

otherwise it remains the same as the original elements of the trans-transition matrix $P(\tilde{\boldsymbol{\lambda}})_{\ell_\nu \ell'_\nu} = P_{\ell_\nu \ell'_\nu}$. The quantity λ_ν above is the counting field conjugated with the current c_ν.

The off-diagonal blocks Eq. (4.3) are tilted by considering the mixed currents. For an explanation, consider a succession $\ell_\mu \to \ell_\nu$ with $\mu \neq \nu$, that both contributes to the total current c_ν and the mixed current $\xi_{\ell_\nu \ell_\mu}$. If c_ν is included in $\tilde{\boldsymbol{\xi}}$, then we introduce the counting field λ_ν as it is done previously for the diagonal blocks P_ν. If the mixed current $\xi_{\ell_\nu \ell_\mu}$ is also included in the joint statistics of $\tilde{\boldsymbol{\xi}}$, then we also introduce the mixed counting field $\lambda_{\ell_\nu \ell_\mu} = -\lambda_{\bar{\ell}_\mu \bar{\ell}_\nu}$ so that the elements in the off-diagonal blocks are tilted as

$$P(\tilde{\boldsymbol{\lambda}})_{\ell_\nu \ell_\mu} = P_{\ell_\nu \ell_\mu} e^{\lambda_\nu j(\ell_\nu) + \lambda_{\ell_\nu \ell_\mu}}, \tag{4.17}$$

which is the case where both the current c_ν and $\xi_{\ell_\nu \ell_\mu}$ are included in the joint statistics. Given ν and $\mu \neq \nu$, we consider the following subcases

- $c_\nu, \xi_{\ell_\nu \ell_\mu} \notin \tilde{\boldsymbol{\xi}}$ then $P(\tilde{\boldsymbol{\lambda}})_{\ell_\nu \ell_\mu} = P_{\ell_\nu \ell_\mu}$;
- $c_\nu \notin \tilde{\boldsymbol{\xi}}$ and $\xi_{\ell_\nu \ell_\mu} \in \tilde{\boldsymbol{\xi}}$, then $P(\tilde{\boldsymbol{\lambda}})_{\ell_\nu \ell_\mu} = P_{\ell_\nu \ell_\mu} e^{\lambda_{\ell_\nu \ell_\mu}}$;
- if $c_\nu \in \tilde{\boldsymbol{\xi}}$ and $\xi_{\ell_\nu \ell_\mu} \notin \tilde{\boldsymbol{\xi}}$, then $P(\tilde{\boldsymbol{\lambda}})_{\ell_\nu \ell_\mu} = P_{\ell_\nu \ell_\mu} e^{\lambda_\nu j(\ell_\nu)}$.

This construction may seem complicated and it will be explained with a specific example later in this section, as it provides a general recipe to construct tilted matrices which provide the MGF for sets of currents evaluated from sequences of visible transitions. Also, so far there is apparently no reason to consider a subset of all the currents which can be extracted from sequences of observable transitions. However, as in the case of cycle currents in state space, not all the currents in $\boldsymbol{\xi}$ are independent, as it is found by employing the analogue of Kirchhoff current law. Moreover, in the case of complete sets of currents (Sec. 5.6) we will only consider the joint statistics of total currents, by setting $\tilde{\boldsymbol{\xi}} = \boldsymbol{c}$, with $[\boldsymbol{c}]_\nu = c_\nu$.

4.4.3 Evolution equation for the MGF at stopping-n

Having defined the tilted trans-transition matrix we can now provide an alternative re-writing for the MGF Eq. (4.13). Let us split the reduced vector of counting fields in two parts, one containing the counting fields conjugated to the total currents and one containing the ones conjugated to the mixed currents as follows:

$$\tilde{\boldsymbol{\lambda}} = (\tilde{\boldsymbol{\lambda}}_c \,,\, \tilde{\boldsymbol{\lambda}}_\xi), \tag{4.18}$$

and define the matrix

$$E(\tilde{\boldsymbol{\lambda}}_c) = \bigoplus_{\nu=1}^{N} \tilde{E}(\lambda_\nu) \tag{4.19}$$

with

$$\tilde{E}(\lambda_\nu) = \begin{cases} I & \text{if} \quad c_\nu \text{ is not contained in } \tilde{\boldsymbol{\xi}} \\ \begin{pmatrix} e^{\lambda_\nu} & 0 \\ 0 & e^{-\lambda_\nu} \end{pmatrix} & \text{else} \end{cases} . \tag{4.20}$$

For simplicity of notation, we define the unitary vector $\mathbf{1}$ with elements $[\mathbf{1}]_{\ell_\nu} = 1$ for all ℓ_ν and for all ν. Given the probability for the first transition $\boldsymbol{p}_1$, the MGF Eq. (4.13) is rewritten as

$$G_n(\tilde{\boldsymbol{\lambda}}) = \mathbf{1} \cdot [P(\boldsymbol{\lambda})]^{n-1} E(\tilde{\boldsymbol{\lambda}}_c) \boldsymbol{p}_1 . \tag{4.21}$$

The expression above is a readaptation of analogous writings for the MGF in terms of tilted matrices in the case of discrete-time Markov chains in state space [54]. The main difference is that the matrix $E(\tilde{\boldsymbol{\lambda}}_c)$ is included to take into account the contribution to the total currents in $\tilde{\boldsymbol{\lambda}}$ carried by the first occurring transition in a sequence $\mathcal{L}_n$, whereas in state space there is no charge associated to the first visited state.

Before giving some explicit examples we prove, as anticipated in Section 3.4.1, that the MGF of the process with trans-transition matrix $\bar{P}$ defined by Eq. (3.52) is indeed the generating function of the time reversed currents when $\tilde{\boldsymbol{\xi}} = \boldsymbol{c}$. In fact

$$\begin{aligned} \bar{G}_n(\boldsymbol{\lambda}) &= \mathbf{1} \cdot \left[\bar{P}(\boldsymbol{\lambda}_c)\right]^{n-1} E(\boldsymbol{\lambda}_c) \boldsymbol{p}_1 \\ &= \mathbf{1} \cdot J \left[P(-\boldsymbol{\lambda}_c)\right]^{n-1} J E(\boldsymbol{\lambda}_c) \boldsymbol{p}_1 \\ &= \mathbf{1} \cdot J \left[P(-\boldsymbol{\lambda}_c)\right]^{n-1} E(-\boldsymbol{\lambda}_c) J \boldsymbol{p}_1 = G(-\boldsymbol{\lambda}_c) \end{aligned} , \tag{4.22}$$

where we used that $\bar{P}(\boldsymbol{\lambda}_c) = JP(-\boldsymbol{\lambda}_c)J$, that $JE(\boldsymbol{\lambda}_c) = E(-\boldsymbol{\lambda}_c)J$ and that $\mathbf{1} \cdot J = \mathbf{1}$. The MGF Eq. (4.22) is then equal to $G(-\boldsymbol{\lambda}_c)$, thus generating the statistics of the time-reversed currents $\{-c_\nu\}$ when the system is prepared with initial probability $\bar{\boldsymbol{p}}_1 = J\boldsymbol{p}_1$, that swaps the probability of the first transition with its time reversed along the same edge.

In the following we provide explicit expressions in the following cases:

- a single observable transition in both directions;
- two distinguishable observable transitions in both directions.

4.4.4 Example: single observable transitions

Consider the case where only the transitions $\uparrow$ and $\downarrow$ are observable. The set of observable currents is then composed by the single current c along one of

the edges of the graph $\mathscr{G}$ describing the system, and we are interested in its MGF. Since there is a single observable current, the only possible choice is $\tilde{c} = c$ conjugated to the counting field λ. Since there are no mixed currents, the tilted trans-transition matrix $P(\lambda)$ is constructed as

$$P(\lambda) = \begin{pmatrix} p(\uparrow \mid \uparrow)e^{\lambda} & p(\uparrow \mid \downarrow)e^{\lambda} \\ p(\downarrow \mid \uparrow)e^{-\lambda} & p(\downarrow \mid \downarrow)e^{-\lambda} \end{pmatrix}. \tag{4.23}$$

Analogously, the matrix $E(\lambda)$ reads

$$E(\lambda) = \begin{pmatrix} e^{\lambda} & 0 \\ 0 & e^{-\lambda} \end{pmatrix}, \tag{4.24}$$

accounting for the contributions of the first transition. Being the system prepared such that the first transitions occurs with probability $\boldsymbol{p}_1$ and that the process runs up to the occurrence of n transitions, the MGF for the statistics of c is found accordingly to Eq. (4.21). In this simple example we can compute explicitly the MGF for small values of n. For $n = 2$ for instance

$$\begin{aligned} G_2(\lambda) &= \mathbf{1} \cdot P(\lambda)E(\lambda)\boldsymbol{p}_1 \\ &= e^{2\lambda}p(\uparrow \mid \uparrow)p_1(\uparrow) + p(\uparrow \mid \downarrow)p_1(\downarrow) + p(\downarrow \mid \uparrow)p_1(\uparrow) + e^{-2\lambda}p(\downarrow \mid \downarrow)p_1(\downarrow) \\ &= \sum_{c \in \mathcal{F}_2} e^{c\lambda} p_2(c), \end{aligned} \tag{4.25}$$

since the filtration for the single current c at time $n = 2$ is $\mathcal{F}_2 = \{-2, 0, 2\}$, thus confirming that Eqs. (4.13) and (4.21) are equivalent.

4.4.5 Example: two observable transitions

The case of two observable transitions in both directions presents a larger set of subcases. We start from the case where $\tilde{\boldsymbol{\xi}} = \boldsymbol{\xi}$, thus all currents are included in the joint statistics, being $\boldsymbol{\xi}^{\top} = (c_1\,,\, c_2\,,\, \xi_{\uparrow_1\uparrow_2}\,,\, \xi_{\uparrow_1\downarrow_2}\,,\, \xi_{\downarrow_1\uparrow_2}\,,\, \xi_{\downarrow_1\downarrow_2})$. Thus also $\tilde{\boldsymbol{\lambda}} = \boldsymbol{\lambda}$ with $\boldsymbol{\lambda} = (\lambda_1\,,\, \lambda_2\,,\, \lambda_{\uparrow_1\uparrow_2}\,,\, \lambda_{\uparrow_1\downarrow_2}\,,\, \lambda_{\downarrow_1\uparrow_2}\,,\, \lambda_{\downarrow_1\downarrow_2})$. Here, by indicating for brevity $p_{\ell_\nu\ell_\mu} = p(\ell_\nu|\ell_\mu)$ the tilted trans-transition matrix reads

$$P(\boldsymbol{\lambda}) = \begin{pmatrix} p_{\uparrow_1\uparrow_1}e^{\lambda_1} & p_{\uparrow_1\downarrow_1}e^{\lambda_1} & p_{\uparrow_1\uparrow_2}e^{\lambda_1+\lambda_{\uparrow_1\uparrow_2}} & p_{\uparrow_1\downarrow_2}e^{\lambda_1+\lambda_{\uparrow_1\downarrow_2}} \\ p_{\downarrow_1\uparrow_1}e^{-\lambda_1} & p_{\downarrow_1\downarrow_1}e^{-\lambda_1} & p_{\downarrow_1\uparrow_2}e^{-\lambda_1+\lambda_{\downarrow_1\uparrow_2}} & p_{\downarrow_1\downarrow_2}e^{-\lambda_1+\lambda_{\downarrow_1\downarrow_2}} \\ p_{\uparrow_2\uparrow_1}e^{\lambda_2-\lambda_{\downarrow_1\downarrow_2}} & p_{\uparrow_2\downarrow_1}e^{\lambda_2-\lambda_{\uparrow_1\downarrow_2}} & p_{\uparrow_2\uparrow_2}e^{\lambda_2} & p_{\uparrow_2\downarrow_2}e^{\lambda_2} \\ p_{\downarrow_2\uparrow_1}e^{-\lambda_2-\lambda_{\downarrow_1\uparrow_2}} & p_{\downarrow_2\downarrow_1}e^{-\lambda_2-\lambda_{\uparrow_1\uparrow_2}} & p_{\downarrow_2\uparrow_2}e^{-\lambda_2} & p_{\downarrow_2\downarrow_2}e^{-\lambda_2} \end{pmatrix}, \tag{4.26}$$

where for all the mixed currents we imposed the positive verse being from transitions along edge 2 towards edge 1. Thus, Eq. (4.21) provides the MGF for the joint distribution $p_n(\boldsymbol{\xi})$ for all total and mixed currents after n observable transitions.

In the case where, for instance, we are interested in the statistics of only the total currents currents $\tilde{\boldsymbol{\xi}} = (c_1\,,\,c_2)$ with conjugated fields $\tilde{\boldsymbol{\lambda}} = (\lambda_1\,,\,\lambda_2)$ the tilted trans-transition matrix reads

$$P(\tilde{\boldsymbol{\lambda}}) = \begin{pmatrix} p_{\uparrow_1\uparrow_1}e^{\lambda_1} & p_{\uparrow_1\downarrow_1}e^{\lambda_1} & p_{\uparrow_1\uparrow_2}e^{\lambda_1} & p_{\uparrow_1\downarrow_2}e^{\lambda_1} \\ p_{\downarrow_1\uparrow_1}e^{-\lambda_1} & p_{\downarrow_1\downarrow_1}e^{-\lambda_1} & p_{\downarrow_1\uparrow_2}e^{-\lambda_1} & p_{\downarrow_1\downarrow_2}e^{-\lambda_1} \\ p_{\uparrow_2\uparrow_1}e^{\lambda_2} & p_{\uparrow_2\downarrow_1}e^{\lambda_2} & p_{\uparrow_2\uparrow_2}e^{\lambda_2} & p_{\uparrow_2\downarrow_2}e^{\lambda_2} \\ p_{\downarrow_2\uparrow_1}e^{-\lambda_2} & p_{\downarrow_2\downarrow_1}e^{-\lambda_2} & p_{\downarrow_2\uparrow_2}e^{-\lambda_2} & p_{\downarrow_2\downarrow_2}e^{-\lambda_2} \end{pmatrix}, \tag{4.27}$$

providing the MGF for the joint distribution $p_n(c_1, c_2)$, since the mixed currents are not taken into account.

As a last example, consider $\tilde{\boldsymbol{\xi}} = (c_1\,,\,\xi_{\uparrow_1\uparrow_2})$ with conjugated fields $\tilde{\boldsymbol{\xi}} = (\lambda_1\,,\,\lambda_{\uparrow_1\uparrow_2})$. Then

$$P(\tilde{\boldsymbol{\lambda}}) = \begin{pmatrix} p_{\uparrow_1\uparrow_1}e^{\lambda_1} & p_{\uparrow_1\downarrow_1}e^{\lambda_1} & p_{\uparrow_1\uparrow_2}e^{\lambda_1+\lambda_{\uparrow_1\uparrow_2}} & p_{\uparrow_1\downarrow_2}e^{\lambda_1} \\ p_{\downarrow_1\uparrow_1}e^{-\lambda_1} & p_{\downarrow_1\downarrow_1}e^{-\lambda_1} & p_{\downarrow_1\uparrow_2}e^{-\lambda_1} & p_{\downarrow_1\downarrow_2}e^{-\lambda_1} \\ p_{\uparrow_2\uparrow_1} & p_{\uparrow_2\downarrow_1} & p_{\uparrow_2\uparrow_2} & p_{\uparrow_2\downarrow_2} \\ p_{\downarrow_2\uparrow_1} & p_{\downarrow_2\downarrow_1}e^{-\lambda_{\uparrow_1\uparrow_2}} & p_{\downarrow_2\uparrow_2} & p_{\downarrow_2\downarrow_2} \end{pmatrix}, \tag{4.28}$$

which provides the MGF for the joint distribution $p_n(c_1, \xi_{\uparrow_1\uparrow_2})$ by use of Eq. (4.21).

4.4.6 Tilted matrix for loop currents

So far we explained how to construct the tilted matrix appearing in the MGF written in the form Eq. (4.21) to obtain the statistics of a subset of observable currents. However, one might be interested in finding the MGF in the case where the total currents c_ν are replaced by the loop currents ξ_ν, defined by Eq. (4.7). This can be easily done by giving just a couple of observations: in fact, since the loop currents only account for subsequent occurrences $\ell_\nu \to \ell_\nu$, the first transition in a sequence $\mathcal{L}_n$ does not contribute to the total loop current. Moreover, this also holds for occurrences $\ell_\nu \to \bar{\ell}_\nu$ and $\ell_\nu \to \ell_\mu$ with $\mu \neq \nu$ that instead were contributing to the total current c_ν. Thus, by going back to the example of two observable transitions, and in the case where we are interested in the statistics of all the observable loop currents and mixed currents, we consider the vector

$$\boldsymbol{\xi}^\top = (\xi_1\,,\,\xi_2\,,\,\xi_{\uparrow_1\uparrow_2}\,,\,\xi_{\uparrow_1\downarrow_2}\,,\,\xi_{\downarrow_1\uparrow_2}\,,\,\xi_{\downarrow_1\downarrow_2}) \tag{4.29}$$

conjugated with the counting fields

$$\boldsymbol{\lambda}^\top = (\lambda_1\,,\,\lambda_2\,,\,\lambda_{\uparrow_1\uparrow_2}\,,\,\lambda_{\uparrow_1\downarrow_2}\,,\,\lambda_{\downarrow_1\uparrow_2}\,,\,\lambda_{\downarrow_1\downarrow_2}). \tag{4.30}$$

In this case the tilted trans-transition matrix would read

$$P(\boldsymbol{\lambda}) = \begin{pmatrix} p_{\uparrow_1\uparrow_1}e^{\lambda_1} & p_{\uparrow_1\downarrow_1} & p_{\uparrow_1\uparrow_2}e^{\lambda_{\uparrow_1\uparrow_2}} & p_{\uparrow_1\downarrow_2}e^{\lambda_{\uparrow_1\downarrow_2}} \\ p_{\downarrow_1\uparrow_1} & p_{\downarrow_1\downarrow_1}e^{-\lambda_1} & p_{\downarrow_1\uparrow_2}e^{\lambda_{\downarrow_1\uparrow_2}} & p_{\downarrow_1\downarrow_2}e^{\lambda_{\downarrow_1\downarrow_2}} \\ p_{\uparrow_2\uparrow_1}e^{\lambda_{\downarrow_1\downarrow_2}} & p_{\uparrow_2\downarrow_1}e^{\lambda_{\uparrow_1\downarrow_2}} & p_{\uparrow_2\uparrow_2}e^{\lambda_2} & p_{\uparrow_2\downarrow_2} \\ p_{\downarrow_2\uparrow_1}e^{\lambda_{\downarrow_1\uparrow_2}} & p_{\downarrow_2\downarrow_1}e^{\lambda_{\uparrow_1\uparrow_2}} & p_{\downarrow_2\uparrow_2} & p_{\downarrow_2\downarrow_2}e^{-\lambda_2} \end{pmatrix}, \tag{4.31}$$

giving the MGF for the joint distribution $p_n(\boldsymbol{\xi})$

$$G_n(\boldsymbol{\lambda}) = \mathbf{1} \cdot [P(\boldsymbol{\lambda})]^{n-1} \boldsymbol{p}_1, \tag{4.32}$$

for a loop and mixed currents evaluated after n transitions in a system prepared with initial probability $\boldsymbol{p}_1$. The matrix $E(\boldsymbol{\lambda}_c)$ does not appear since the first occurring transition does not contribute to the loop currents.

As suggested by Eq. (4.31), the tilted matrix in the case where loop currents are considered takes a much simpler form, and it affects the expression of the MFG Eq. (4.32). An additional advantage of shifting the attention to loop currents, rather than total currents, is that FRs are derived straightforwardly for the joint set of loop currents and mixed currents. As it will be explained in Sec. 5.2, in fact, FRs can be rephrased as symmetries for the MGFs, by including the conjugated affinities. In the case where the attention is on loop currents, conjugated with the effective affinities $\{a_\nu\}$, the mixed currents are conjugated with the mixed affinities $\{\alpha_{\ell_\nu\ell_\mu}\}$ defined by Eq. (4.10). Moreover, as it will be explained in Section. 5.7, preferred initial probabilities such that FRs are satisfied at all n, are always uniform when the joint statistics of all loop currents and all mixed currents is considered, regardless of the number of observable edges. These facts will be used in the next Chapter as the starting points to derive the FR for the joint set of total currents $\{c_\nu\}$ and mixed currents $\{\xi_{\ell_\nu\ell_\mu}\}$.

Chapter 5

Fluctuation relations at stopping n

The description of stochastic processes in terms of discrete-time Markov chains in the space of transitions presented so far is not just a sterile alternative to the common treatment in terms of successions of states and permanence times, as will emerge from the results obtained in this Chapter, which represents the center of this thesis.

The latter approach is limited to very special situations where a sufficient number of degrees of freedom have to be accessible in order to provide coherent estimation of thermodynamic quantities such as the entropy production.

In fact, as explained in Chapter 2, the best we can do to estimate the entropy production of the full system is to observe a minimal number of currents that form a complete set, relying on the cycle decomposition reviewed by Schnakenberg [41]. However, this is an idealized situation often not achievable in practice, due mainly to technological limitations in accessing microscopic degrees of freedom. As mentioned in the Introduction of this work, this is a very well known issue, partially solved by means of physically motivated assumptions that restrict the sight to just a few real world circumstances.

This Chapter wraps up of the previously discussed transition based techniques, to address the problem of marginally accessible graphs from a new point of view, and constitute the most important section of this thesis. The main result presented here states briefly that even in the case of just few observed currents, it is possible to prove fluctuation relations under a few assumptions:

- the full system is markovian;
- each observable transition is associated to a unique pair of states;
- the statistics of the currents are evaluated up to the occurrence of

a fixed number of observed transitions that are accessible, whereas traditionally they are evaluated up to the elapsing of an external clock time;

- correlations between successive events (mixed currents) are considered.

The second point states that we want to avoid situations where transitions between different pairs of states are not distinguishable. For instance, if $\ell : x_1 \to y_1$ and $\ell' : x_2 \to y_2$ but ℓ and ℓ' are associated with the same observable quantity (for instance, the differences in energies $\epsilon_{x_1} - \epsilon_{y_1}$ and $\epsilon_{x_2} - \epsilon_{y_2}$ are the same), then we lose the renewal property since we can not identify an unique source and target state for each transition.

Regarding the third point, the two stopping criteria, that represent different observational paradigms, are referred respectively as stopping-n and stopping-t. In this Chapter we first focus on a single observable current, in which case, in fact, no data about mixed currents needs to be collected. We then generalize to the case of an arbitrary number of observed edges, where we have to include contributions from the mixed currents introduced in the previous Chapter, up to a limit case where a complete set of currents is observable. In this limit case, we measure one current per cycle with no need to monitor mixed currents, and we recover a well-known result [33], but at fixed n rather than fixed t.

As a final note, all the fluctuation relations derived here holds asymptotically at large n. Interestingly, they all can be specialized to any finite number of occurrences n if the system is prepared in a special initial probability, referred as preferential or preferred probability, whose physical interpretation is still lacking in this work. The results here are mainly achieved by considering the MGF for currents at stopping-N defined in Section 4.4.1. In fact, fluctuation relations can be interpreted as a symmetry of the MGF as explained in Sec. 5.2.

5.1 FRs for joint probabilities

Let N denote the number of observable edges in a graph $\mathscr{G}$ where a markovian dynamics takes place. For simplicity of notation we consider the entire set of total currents and mixed currents which can be extracted from sequences $\mathcal{L}_n$ of observable transitions, collected in the vector $\boldsymbol{\xi}$ (see Sec. 4.4.1) and the arguments here and in the next section are extended for any subset of currents $\tilde{\boldsymbol{\xi}}$ that satisfy a FR.

Let $p_n(\boldsymbol{\xi})$ denote the joint probability for $\boldsymbol{\xi}$ evaluated at the occurrence of n observable transitions and let $\boldsymbol{f}$ (the symbol f meaning "force") the vector of the conjugated affinities. Saying that the joint probability $p_n(\boldsymbol{\xi})$

satisfy a FR means that

$$\log \frac{p_n(\boldsymbol{\xi})}{p_n(-\boldsymbol{\xi})} = \boldsymbol{f} \cdot \boldsymbol{\xi}, \tag{5.1}$$

which is achievable asymptotically at large n or exactly under

- the choice of a preferred probability in transition space $\boldsymbol{p}_1^*$;
- by some post-selection of realizations $\mathcal{L}_n$.

The expression above represents the detailed FR, a symmetry for the probability distributions. This chapter is dedicated to proving that such a relation is satisfied by transition space processes. In the following Section, we give another expression for FRs in terms of MGFs.

5.2 FRs as symmetries of the MGF

The joint probability for the total currents and mixed current can be expressed in terms of the MGF Eq. (4.13)

$$G_n(\boldsymbol{\lambda}) = \sum_{\boldsymbol{\xi} \in \mathcal{F}_n} e^{\boldsymbol{\lambda} \cdot \boldsymbol{\xi}} p_n(\boldsymbol{\xi}), \tag{5.2}$$

with $\boldsymbol{\lambda}$ the vector of the conjugated counting fields and $\mathcal{F}_n$ the filtration of $\boldsymbol{\xi}$ after n observable transitions. If the statistics of the currents $\boldsymbol{\xi}$ satisfy an FR like Eq. (5.1), then

$$\begin{aligned} G_n(\boldsymbol{\lambda}) &= \sum_{\boldsymbol{\xi} \in \mathcal{F}_n} e^{\boldsymbol{\lambda} \cdot \boldsymbol{\xi}} p_n(-\boldsymbol{\xi}) e^{\boldsymbol{f} \cdot \boldsymbol{\xi}} \\ &= \sum_{\boldsymbol{\xi} \in \mathcal{F}_n} p_n(\boldsymbol{\xi}) e^{-\boldsymbol{\lambda} \cdot \boldsymbol{\xi} - \boldsymbol{f} \cdot \boldsymbol{\xi}} = G_n(-\boldsymbol{f} - \boldsymbol{\lambda}), \end{aligned} \tag{5.3}$$

The FR can then be written as the symmetry Eq. (5.3) for the MGF, that was already showed can be expressed in terms of tilted matrices containing the counting fields in Sec. 4.4.3. The rightmost hand side of Eq. (5.3) is then written as

$$G_n(-\boldsymbol{f} - \boldsymbol{\lambda}) = \mathbf{1} \cdot [P(-\boldsymbol{f} - \boldsymbol{\lambda})]^{n-1} E(-\boldsymbol{a} - \boldsymbol{\lambda_c}) \boldsymbol{p}_1 \tag{5.4}$$

with $\boldsymbol{a}$ denoting the vector of the effective affinities associated to the total currents only, and $\boldsymbol{\lambda}_c$ the vector of the respective counting fields. The symmetry Eq. (5.3) is verified if there exist the following transformation for the tilted matrix

$$E(-\boldsymbol{\lambda}_c) P(\boldsymbol{\lambda}) E(\boldsymbol{\lambda}_c) = D^{-1} P(-\boldsymbol{f} - \boldsymbol{\lambda})^{\perp} D, \tag{5.5}$$

with D denoting a real diagonal matrix and $\perp$ denoting block anti-transposition as defined in Section 3.4.1 by Eq. (3.49). The relation above is justified since Eq. (5.3) states that the the tilted matrices $P(\boldsymbol{\lambda})$ and $P(-\boldsymbol{f}-\boldsymbol{\lambda})$ are related by a similarity transformation $P(\boldsymbol{\lambda}) = \Theta^{-1}P(-\boldsymbol{f}-\boldsymbol{\lambda})\Theta$ for some matrix Θ. The two matrices share the same eigenvalues and in particular their Perron root, which determines the asymptotic statistics of currents. The relation Eq. (5.5) is obtained with the choice $\Theta = JDE(-\boldsymbol{\lambda_c})$, since $J^{-1} = J$, $E(\boldsymbol{\lambda}_c)^{-1} = E(-\boldsymbol{\lambda}_c)$, and $A^{\perp} = JA^{\top}J$. In fact, a square matrix preserves its eigenvalues under transposition.

Therefore, Eq. (5.3) for the observable currents holds if it is possible to find a matrix D such that Eq. (5.5) is satisfied. However, for the joint set of total currents and mixed currents, it results to be impossible to find such matrix in the case where the affinities in $\boldsymbol{f}$ conjugated with the mixed currents are chosen to be the mixed affinities $\{\alpha_{\ell_\nu \ell_\mu}\}$ defined by Eq. (4.10). With this choice, fortunately, Eq. (5.3) is valid if the total currents are replaced by the loop currents Eq. (4.7), and in such case Eq. (5.5) reduces to

$$P(\boldsymbol{\lambda}) = P(-\boldsymbol{f}-\boldsymbol{\lambda})^{\perp}, \tag{5.6}$$

Therefore, the joint probability of loop and mixed currents also satisfy the FR in the detailed form Eq. (5.1), as we verify explicitly in terms of path probabilities in the next section. We exploit this fact to find an expression for the affinities conjugated to the mixed currents in the case where the focus is on the total currents $\{c_\nu\}$, replacing the loop currents, such that Eq. (5.5) holds. As a result, the choice falls on the tilted mixed affinities, which were anticipated in Sec. 4.3 by Eq. (4.11).

Thus, we proceed as following: first we write explicitly the ratios of probabilities for forward and backward realizations $\mathcal{L}_n$ and $\bar{\mathcal{L}}_n$ to see that a detailed FR for the loop currents and mixed currents is readily obtained. From here, a rewriting of the total current in terms of loop currents and mixed currents allow the extension of such FR to the case of total currents, by also defining the correct mixed affinities, conjugated with the mixed currents, to be used to verify Eq. (5.5). Note in fact that the formulations in terms of path probabilities and in terms of moment generating functions are equivalent. While the second approach is characterized by an outstanding simplicity it needs an explicit expression for some quantities, as the effective affinities and the mixed affinities, the first one consent to extract the abovementioned quantities, unlocking a treatment in terms of moment generating functions.

Before addressing this, we start from considerations on the single current FR [31] which is also recovered as a special case from the generalized FR provided in Sec. 5.5.2. At the end of this Chapter, we study the limit case where the set of observed currents form a complete set, thus satisfying a FR where no mixed current appears, and we extend fluctuation relations to

hold at all n by the choice of a preferred initial distribution, also derived by exploiting the symmetry Eq. (5.3).

5.3 Path probability ratios

In Section 3.3 we provided the expression for the probability of a single realization of the process in transition space, generated by the transition matrix P with elements the trans-transition probabilities the we recall to be expressed as

$$P_{\ell_\nu \ell'_\mu} = p(\ell_\nu|\ell'_\mu) = -r(\ell_\nu) S^{-1}_{\mathtt{s}(\ell_\nu),\mathtt{t}(\ell'_\mu)}, \tag{5.7}$$

where $r(\ell) = r(\mathtt{t}(\ell)|\mathtt{s}(\ell))$ denotes the transition rate from the source state $\mathtt{s}(\ell)$ to the target state $\mathtt{t}(\ell)$ of the observable transition ℓ, and S the survival matrix. Eq. (5.7) is written here by highlighting, with the use of greek indices ν and μ, that trans-transition probabilities in the off-diagonal blocks of P have elements associated to subsequent transitions over different edges. For N observable transitions in both directions, by using Eq. (3.36) and the probability of the correspondant backward realization Eq. (3.38) we can immediately write the ratio of forward-to-backward probabilities as

$$\frac{p(\mathcal{L}_n)}{p(\bar{\mathcal{L}}_n)} = \frac{p_1(\ell^{(1)})}{p_1(\bar{\ell}^{(n)})} \prod_{\nu=1}^{N} \left(\frac{p(\uparrow_\nu \mid \uparrow_\nu)}{p(\downarrow_\nu \mid \downarrow_\nu)} \right)^{\xi_\nu(\mathcal{L}_n)} \prod_{\substack{(\ell_\nu,\ell_\mu) \\ \mu>\nu}} \left(\frac{p(\ell_\nu|\ell_\mu)}{p(\bar{\ell}_\nu|\bar{\ell}_\mu)} \right)^{\xi_{\ell_\nu\ell_\mu}(\mathcal{L}_n)}, \tag{5.8}$$

straightforwardly expressed in terms of the loop currents $\xi_\nu(\mathcal{L}_n)$ and the mixed currents $\xi_{\ell_\nu\ell_\mu}(\mathcal{L}_n)$ evaluated along a single realization $\mathcal{L}_n$ in the observable transition space, and where the second product is made over all possible pairs (ℓ_ν, ℓ_μ) with the restriction $\mu > \nu$ to avoid double counting, since we are free to choose the positive direction for the mixed currents, that satisfy $\xi_{\ell_\nu\ell_\mu} = -\xi_{\bar{\ell}_\mu\bar{\ell}_\nu}$ according to the notion of time-reversal introduced in Section 3.4. In Eq. (5.8) we can recognize the effective affinities a_ν and the mixed affinities $\alpha_{\ell_\nu\ell_\mu}$ that were defined in the previous Chapter by Eqs.(4.9) and (4.10) respectively. Then, the logarithm of Eq. (5.8) is expressed as

$$\log \frac{p(\mathcal{L}_n)}{p(\bar{\mathcal{L}}_n)} = \sum_{\nu=1}^{N} a_\nu \xi_\nu(\mathcal{L}_n) + \sum_{\substack{(\ell_\nu,\ell_\mu) \\ \mu>\nu}} \alpha_{\ell_\nu\ell_\mu} \xi_{\ell_\nu\ell_\mu}(\mathcal{L}_n) + \log p_1(\ell^{(1)}) - \log p_1(\ell^{(n)}). \tag{5.9}$$

The equation above is already in the form of a FR for the loop currents ξ_ν and the mixed currents $\xi_{\ell_\nu\ell_\mu}$ in a single realization $\mathcal{L}_n$. The expression above, together with the relation Eq. (5.6), thus suggests that summing over all possible realizations $\mathcal{L}_n$ which provide a certain outcome for the loop currents and the mixed currents, one obtains a FR involving the joint prob-

ability of such currents and their time reversed outcomes

$$\log \frac{p_n(\{\xi_\nu\},\{\xi_{\ell_\nu\ell_\mu}\},\ell^{(1)},\ell^{(n)})}{p_n(\{-\xi_\nu\},\{-\xi_{\ell_\nu\ell_\mu}\},\bar{\ell}^{(1)},\bar{\ell}^{(n)})} = \sum_{\nu=1}^{N} a_\nu \xi_\nu(\mathcal{L}_n) + \sum_{\substack{(\ell_\nu,\ell_\mu)\\ \mu>\nu}} \alpha_{\ell_\nu\ell_\mu}\xi_{\ell_\nu\ell_\mu}(\mathcal{L}_n) + u(\ell^{(n)}) - u(\ell^{(1)}). \tag{5.10}$$

The expression above is exact at all n and still relying on the knowledge of the first and last transitions in the sequence $\mathcal{L}_n$. The boundary transitions are encoded in potential terms $u(\ell) = -\log p_1(\ell)$ evaluated at the boundaries of $\mathcal{L}_n$. To make the boundary term vanish one may choose the first and the last transition to be the time reversal of each other, or prepare the sytem in a way such that the probability distribution on the first transition is uniform. In any case, the relation Eq. (5.10) holds asymptotically with no boundary term since it is bounded and thus it can be neglected in this limit.

The FR above is used as a starting point to derive the FR for the integrated currents c_ν, relying on a rewriting of $c_\nu(\mathcal{L}_n)$ in terms of the loop currents $\xi_\nu(\mathcal{L}_n)$ in single realizations $\mathcal{L}_n$. Indeed, $c_\nu(\mathcal{L}_n)$, $\xi_\nu(\mathcal{L}_n)$ and the mixed currents $\xi_{\ell_\nu\ell_\mu}(\mathcal{L}_n)$ are related by a linear expression. The result is a FR for the total currents where both the mixed affinities and the boundary terms are shifted.

The reason why we proceed in this way, as anticipated in Section 5.2, is because the mixed affinities defined as Eq. (4.10) makes the expression Eq. (5.5) not achievable when the focus is on the total currents $\{c_\nu\}$, unless they are replaced by the shifted mixed affinities Eq. (4.11) anticipated in Chapter 4. The shifted mixed affinities are then used to verify the FR for currents and mixed currents at the level of their MGF Eq. (4.13), thus unlocking this approach that now can be used to derive FRs for complete sets of currents and transient FRs.

Before describing the general case of an arbitrary number of observable transitions we discuss the FR for a single observable current. In fact it provides elementary arguments that can be extended to more general cases.

5.4 Fluctuation relation for one observable current

In this section we study the simple case of a single observable current at stopping-n for which a FR is achieved [31]. Consider for instance the graph illustrated in Fig. 5.1(a) where only transitions $\uparrow$: $2 \to 1$ and $\downarrow$: $1 \to 2$ are observable, to be seen here as an example to help visualize the problem. By solution of a first-exit time problem, as explained in Chapter 3, it is possible

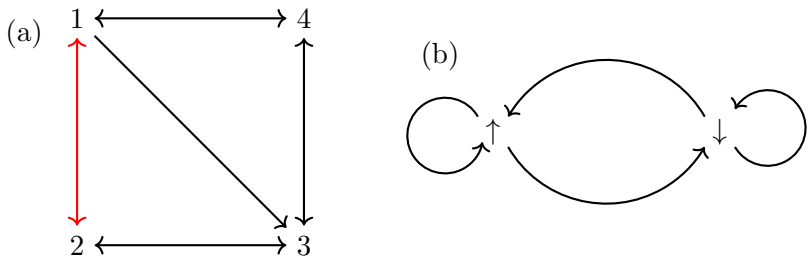

Figure 5.1: (a) A graph where only the transitions between states 1 and 2 are observable. (b) The corresponding graph in the single observable transition space where only ↑: $2 \to 1$ and ↓: $1 \to 2$ are observable

to construct a discrete time process in transition space with transition matrix P containing the trans-transition probabilities $p(\ell|\ell')$ with $\ell = \uparrow, \downarrow$. The corresponding graph in transition space is illustrated in Fig. 5.1(b). By now considering paths in this space we write the ratio of forward to backward realizations of the process by use of Eq. (5.8) now adapted to the single transitions' case. Since we are considering a single observable kind, no mixed current can be extracted from the reduced process in the observable transition space, so that Eq. (5.8) reads

$$\frac{p(\mathcal{L}_n)}{p(\bar{\mathcal{L}}_n)} = \frac{p_1(\ell^{(1)})}{p_1(\ell^{(\bar{n})})} \left(\frac{p(\uparrow \mid \uparrow)}{p(\downarrow \mid \downarrow)}\right)^{\xi(\mathcal{L}_n)}, \tag{5.11}$$

with $\xi(\mathcal{L}_n) = n_{\uparrow\uparrow}(\mathcal{L}_n) - n_{\downarrow\downarrow}(\mathcal{L}_n)$ the loop current. As already explained, the equation above is already in the form of a FR for the loop current ξ, holding asymptotically or by choice of an uniform $\boldsymbol{p}_1$ under the assumption that the forward and backward processes are sampled from the same initial probabilities. In fact, Eq. (5.6) is verified by using the effective affinity $a = \log p(\uparrow \mid \uparrow)/p(\downarrow \mid \downarrow)$. Explicitly, if only loop currents are observed

$$P(\lambda) = \begin{pmatrix} p(\uparrow \mid \uparrow)e^{\lambda} & p(\uparrow \mid \downarrow) \\ p(\downarrow \mid \uparrow) & p(\downarrow \mid \downarrow)e^{-\lambda} \end{pmatrix} \tag{5.12}$$

according to the tilting explained in Section 4.4.6, and

$$\begin{aligned} P(-a-\lambda)^{\perp} &= \begin{pmatrix} p(\downarrow \mid \downarrow)e^{a+\lambda} & p(\uparrow \mid \downarrow) \\ p(\downarrow \mid \uparrow) & p(\uparrow \mid \uparrow)e^{-a-\lambda} \end{pmatrix} \\ &= \begin{pmatrix} p(\uparrow \mid \uparrow)e^{\lambda} & p(\uparrow \mid \downarrow) \\ p(\downarrow \mid \uparrow) & p(\downarrow \mid \downarrow)e^{-\lambda} \end{pmatrix} = P(\lambda). \end{aligned} \tag{5.13}$$

However, we are interested in a FR for the total current c, defined for single realizations $\mathcal{L}_n$ by $c(\mathcal{L}_n) = n_{\uparrow}(\mathcal{L}_n) - n_{\downarrow}(\mathcal{L}_n)$ that tracks the net amount of times the observable edge is crossed. Thus, a rewriting of the probability ratio Eq. (5.11) in terms of the total current requires a linear expression connecting $\xi(\mathcal{L}_n)$ and $c(\mathcal{L}_n)$.

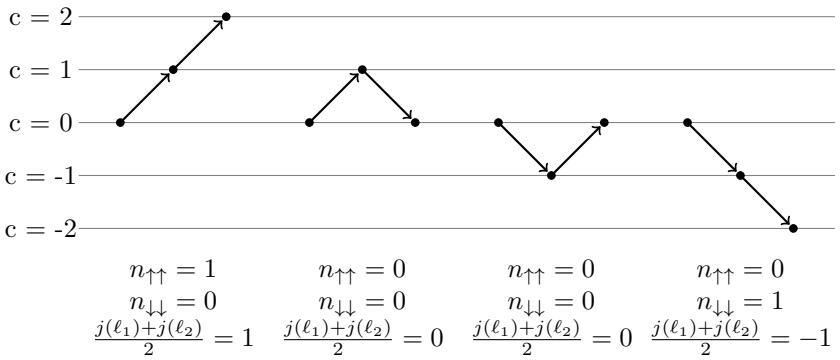

Figure 5.2: For the simple example $n = 2$ it is immediate to verify Eq. (5.14) where the current c is related with the loop current ξ and a boundary term involving the first and the last contributions to the total current.

5.4.1 Rewriting the loop current

As explained in [31] it is very easy to check that (see Fig. 5.2, taken from Ref. [31])

$$c(\mathcal{L}_n) = \xi(\mathcal{L}_n) + \frac{1}{2}(j(\ell^{(1)}) + j(\ell^{(n)})), \tag{5.14}$$

where the total current along the observable edge is expressed as a linear expression involving the loop current and half the sum of the first and last contributions to the total current in $\mathcal{L}_n$, denoted by $j(\ell^{(1)})$ and $j(\ell^{(n)})$. Thus the expression Eq. (5.14) can be plugged in the ratio Eq. (5.11) to obtain

$$\frac{p(\mathcal{L}_n)}{p(\bar{\mathcal{L}}_n)} = \frac{p_1(\ell^{(1)})}{p_1(\ell^{\bar{(n)}})} \left(\frac{p(\uparrow \mid \uparrow)}{p(\downarrow \mid \downarrow)}\right)^{c(\mathcal{L}_n) - \frac{1}{2}(j(\ell^{(1)}) - j(\bar{\ell}^{(n)}))}, \tag{5.15}$$

where we also used that $j(\ell) = -j(\bar{\ell})$. By also recognizing the quantity in the parentheses as the effective affinity $a = \log p(\uparrow \mid \uparrow)/p(\downarrow \mid \downarrow)$, summing the expression above over all realizations $\mathcal{L}_n$ such that $c(\mathcal{L}_n) = c$ and taking the logarithm we get [31]

$$\log \frac{p_n(c, \ell^{(1)}, \ell^{(n)})}{p_n(-c, \bar{\ell}^{(1)}, \bar{\ell}^{(n)})} = a\, c + \tilde{u}(\ell^{(n)}) - \tilde{u}(\ell^{(1)}) \tag{5.16}$$

that is a fluctuation relation for the joint probabilities of outcomes c of the current and the first and last transitions being $\ell^{(1)}$ and $\ell^{(n)}$ respectively. The contributions from the transitions at the boundaries are absorbed in a term $\tilde{u}(\ell) = u(\ell) + j(\ell)a/2$, shifted respect to $u(\ell) = -\log p_1(\ell)$ by a quantity depending on its carried current and the effective affinity a. Since $j(\ell) = \pm 1$, the boundary, or *potential*, term is bounded and thus in the limit $n \to \infty$ the FR reads

$$\log \frac{p_n(c)}{p_n(-c)} \asymp a\, c \tag{5.17}$$

now unconditioned on the first and last transitions since they can be marginalized out. This can also be done at all n in the case where trajectories are post selected such that $\ell^{(1)} = \ell^{(n)}$ or by selecting as initial state the *preferred* distribution

$$p_1(\ell) = \frac{p(\ell|\ell)}{p(\uparrow \mid \uparrow) + p(\downarrow \mid \downarrow)}, \tag{5.18}$$

that is verified to make the boundary term $\tilde{u}(\ell^{(n)}) - \tilde{u}(\ell^{(1)})$ vanish at all n. The preferred distribution Eq. (5.18) in the case of single observable currents is very important to make the FR Eq. (5.16) transient at all n especially when trying to verify by numerical experiments. In fact, a numerical verification of FRs relies on occurrencies of rare events in the tails of the distribution of c and in particular the ones that contribute negatively to the total entropy production. Those outcomes become even more rare when increasing n thus is hard to conclude that a FR for such currents at stopping-n is verified by an experiment. Being able to make shorter simulations, constitute a great advantage since the amount of data needed for the convergence of the estimated probabilities can now be handled. In Section 5.4.3 we give such a numerical verification of Eq. (5.16) in the case of vanishing potential by use of the initial probability Eq. (5.18).

5.4.2 Jarzynski equality

The detailed FR for a single current with vanishing potential Eq. (5.16) can be written in an integral form by summation over all possible outcomes for the current c. In this case, we can rewrite Eq. (5.16) as

$$p_n(c)e^{-a\,c} = p_n(-c). \tag{5.19}$$

The current c takes values in $\{-n,\, -n{+}2,\, \ldots,\, n{-}2,\, n\}$ because the stopping-n criterion grants that the outcome space of c is bounded. Thus, by summing both sides over all such outcomes we get

$$\langle e^{-a\,c} \rangle = 1, \tag{5.20}$$

also known as Jarzynski's equality. The outcome space of c being bounded constitute a statistical advantage when verifying Eq. (5.20). In fact it is well known that the statistical estimator $\exp -x$, with x a random variable, has convergence issues due to the unboundedness of the outcome space of x when evaluated after the elapsing of a fixed external time t. In fact, rare negative outcomes of x might kick the average of $\exp -x$ much above 1, thus forcing an experimenter to increase the size of the sample with no warranty that another even rarer outcome will not occur. If the spectrum of the random variable is bounded, with extremal negative value $-x^*$, occurrences of such extreme value contribute to the average at most by e^{-x^*}/m with m the size of the sample. Working at stopping n then consent the Jarzynski's equality

to be experimentally more accessible. In Chapter 7 we indagate further the problem of the bad convergence of such estimators.

5.4.3 Numerical Simulations

In this section we provide a numerical verification of the FR Eq. (5.16) at stopping-n by also comparing the result with outcomes of the same process at stopping-t.

The examined system is the one represented in Fig. 5.1 where the rates chosen are summarized in the caption in Fig. 5.3. The numerical experiment was performed in two different ways by also proving the equivalence in the statistics of outcomes c for the integrated current along the observed edge in the case of continuous time Markov chain stopped after n observable transitions and processes at stopping-n generated directly via the discrete time chain with trans-transition matrix P obtained from the rate matrix R of the full system.

The first experiment makes use of the Gillespie algorithm (see Appendix) to generate trajectories in state space, with waiting times sampled from the exponential densities with parameter the exit rates, and transition probabilities obeying the embedded chain with transition matrix Π obtained from R. Given the transition rates, the system is found at time $t = 0$ in one of the states according to an initial probability in state space $\boldsymbol{q}(0)$. Then, once the state x_0 is chosen, an exponential time with parameter the exit rate $r(x_0)$ is sampled and the system jumps to x_1 with probability $r(x_1|x_0)/r(x_0)$. At this point the procedure is repeated until:

1. an external clock time t is elapsed (blue crosses);

2. n observable transitions in either direction are performed (black dots).

The experiment at stopping-t is prepared at initial time in the so called stalling state [32], the stationary state of the process where the observed edge is removed. In the case of complete currents, in fact, it provides a transient FR at all t [32, 33, 55], thus if the system would satisfy a marginal FR at stopping-t this would be the best candidate initial distribution. In fact, for this initial distribution, a single current satisfy an exact FR-like relation according to some auxiliary dynamics [55, 56]. However, as it can be seen in Fig. 5.3 (imported from Ref. [31]) a FR is not satisfied by currents at stopping-t. At stopping-n, i.e. when the same process is stopped after the occurrence of n observable transitions, the statistics of currents show a different behavior. When the system is prepared in a way such that the probability of the first observbale transition is distributed as the preferred probability $\boldsymbol{p}_1^*$ in the observable transition space, which is related to some initial state in state space via Eq. (3.20), the currents satisfy a FR as it can be seen by looking at the black dots in Fig. 5.3 which lie on the line with slope the effective affinity $a = \log p(\uparrow \mid \uparrow)/p(\downarrow \mid \downarrow)$.

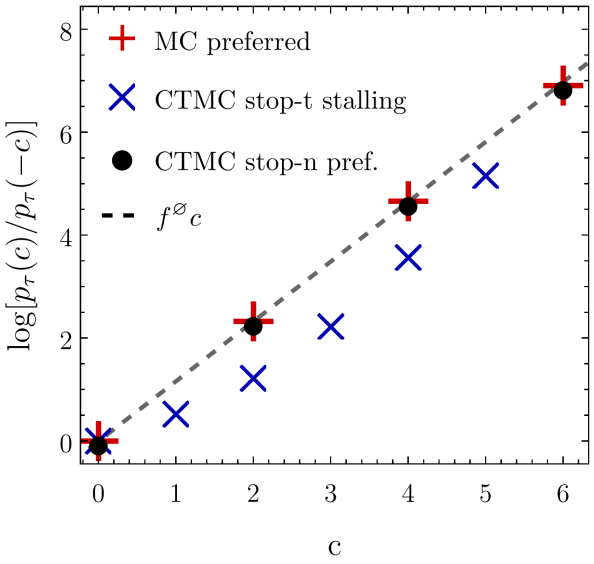

Figure 5.3: Plot of the log-ratios between probabilities of forward outcomes c and the correspondent backward outcome $-c$. The chosen transition rates are $r(2|1) = 5$, $r(1|2) = 4$, $r(4|1) = 2$, $r(1|4) = r(2|3) = r(3|1) = r(3|2) = r(3|4) = r(4|3) = 1$ where an irreversible transition is included by chosing $r(1|3) = 0$. The calculated effective affinity is then $a \sim 1.163$. The experiments are performed in different ways: *blue crosses:* Continuous time markov chain (CTMC) at stopping t prepared at the stalling state at $t = 0$; *black dots:* CTMC at stopping $n = 6$, prepared in the initial state giving the preferred probability in transition space; *red crosses:* Discrete chain with generator the trans-transition matrix for the observable transitions, calculated from the rate matrix R, prepared in the preferred probability. All the experiments consist in samples of 10^8 trajectories. With this plot we prove that the FR for single currents is satisfied by the process at stopping n, with n the number of observable transitions performed by the system.

The second experiment is carried directly in the space of transitions after calculations of the trans-transition probabilities through Eq. (3.17) thus by calculating the inverse of the survival matrix S. The trans-transition probabilities are then arranged in a stochastic matrix P and after choosing the preferred initial probability the system is updated at each step according to the trans-transitoion proabilities $p(\ell|\ell')$. The outcome of this experiment, represented by red crosses in Fig. 5.3, also satisfies the same FR thus proving the equivalence between the process in state space and the process in the observable transition space at stopping-n.

Before concluding this section, we discuss more precisely the criterion we used to determine the time t at which the experiment at stopping-t is

performed to be as fair as possible with respect to the same experiment performed at stopping-n. In the numerical experiment shown in Fig. 5.3, in fact, we first choose $n = 6$ and then $t = \langle \tau_n \rangle$, with τ_n the time at which the system performs n observable jumps in a single realization of the process at stopping-n, and its average can be calculated via Eq. (3.29). However, if we consider the converse, i.e. the average number of observable transitions observed at stopping-t with $t = \langle \tau_n \rangle$, it does not correspond to n, which is $\langle n_t \rangle = \langle n_{\langle \tau_n \rangle} \rangle \neq n$. The same happens for instance in the case of Poisson distributions, for which there is no correspondence between the average number of events at a certain time and number of events occurring in a certain average time. Therefore, our comparison turns out not to be completely fair, thus remains valid since we are more interested in the qualitative behavior of the statistics of currents evaluated at different stopping criteria.

To try to solve this issue we can employ for instance the expression for the average time for the system to perform n transition that we calculated in Section. 3.2.3 with Eq. (3.29). This should be compared with the average number of transitions performed at the same average time. By letting $f(t) = f_{\text{jump}}(t)$ for brevity of notation, the average number of observable transitions during a generic time t is given by

$$\langle n_t \rangle = \int_0^t \int_{t_1}^t \cdots \int_{t_{n-1}}^t dt_1 \cdots dt_n \, f(t_1) f(t_2 - t_1) \cdots f(t_n - t_{n-1}) \sigma_\varnothing(t - t_n), \tag{5.21}$$

with $f(\tau)$ the unconditional probability density of performing a observable transition at time τ Eq. (3.13) and $\sigma_\varnothing(\tau)$ the unconditional survival probability Eq. (3.12). This last calculation however can be done up to a certain point, thus our discussion around it stops here. The main idea is to find a statistical estimator, say $\phi(\bullet)$, such that $\phi(n_{\phi(\tau_n)}) = n$, so that the comparison of the statistics of currents at stopping-t and stopping-n can be done as fairly as possible.

More details about the simulations and the code can be found in Appendix A.

5.5 Multiple currents

Extending the FR Eq. (5.16) to multiple observable currents along different edges requires, as introduced in Chapter 4, the introduction of cross information encoded in the so-called mixed currents. Previously, in Section 5.3, we already derived a FR for the loop currents and the mixed currents that is used here as a starting point to derive FRs for total currents. As done for the case of a single observable current, the extension to an arbitrary number of observable transitions in both directions must employ some linear relation

involving loop currents and total integrated currents. This is done by properly cutting the sequences $\mathcal{L}_n$ of observable transitions in subsequences of transitions along the same edge. As a result, explained in the next section, the total current c_ν along edge $\boldsymbol{e}_\nu$ is a linear combination of the loop current ξ_ν along the same edge and the mixed currents involving edge $\boldsymbol{e}_\nu$ and all other edges $\boldsymbol{e}_\mu$ with $\mu \neq \nu$.

5.5.1 Rewriting loop currents

Consider an outcome $\mathcal{L}_n$ generated by a process with trans-transition matrix P, and consider a subsequence $\mathcal{L}^{(i)}_{\nu_i}$ of $\mathcal{L}_n$ that contains only transitions along the same edge $\boldsymbol{e}_{\nu_i}$. From now on, a transition of *kind* ν is referred as a transition along the observable edge $\boldsymbol{e}_\nu$ in either direction.

Such a subsequence is referred as *snippet* of kind ν_i. For one such snippet $\mathcal{L}^{(i)}_{\nu_i}$, with the subscript (i) denoting its position respect to other snippets in the full sequence $\mathcal{L}_n$, ν_i indicating its kind, the relation between loop current and total currents Eq. (5.14) is

$$c_\nu(\mathcal{L}^{(i)}_{\nu_i}) = \xi_\nu(\mathcal{L}^{(i)}_{\nu_i}) + \frac{1}{2}(j(\ell^{(1_i)}) + j(\ell^{(n_i)})) \tag{5.22}$$

where, if $\mathcal{L}^{(i)}_{\nu_i}$ has lenght n_i, $\ell^{(1_i)}$ and $\ell^{(n_i)}$ denote the first and last transitions in the considered snippet. We are interested in finding a relation between the total integrated current $c_\nu(\mathcal{L}_n)$ of kind ν in the full sequence $\mathcal{L}_n$ with the loop current $\xi_\nu(\mathcal{L}_n)$ of the same kind. Intuitively, the total current evaluated in the full trajectory is given by the sum of the currents carried by each snippets in $\mathcal{L}_n$ of the same kind. Thus, we have to perform the sum over all snippets i' such that $\nu_{i'} = \nu$

$$c_\nu(\mathcal{L}_n) = \sum_{i'} c_\nu(\mathcal{L}^{(i')}_\nu) = \sum_{i'} \xi_\nu(\mathcal{L}^{(i')}_\nu) + \frac{1}{2}\sum_{i'}(j(\ell^{(1_{i'})}_\nu) + j(\ell^{(n_{i'})}_\nu)). \tag{5.23}$$

The first term $\sum_{i'} \xi_\nu(\mathcal{L}^{(i')}_\nu)$ is obviously the loop current ξ_ν of kind ν evaluated in the full trajectory $\mathcal{L}_n$. For the remaining terms we need some extra work. The sum $\sum_{i'} j(\ell^{(1_{i'})}_\nu)$ represents the sum over all current's contributions given by the first occurrence in each snippet of the same kind considered above, and precisely, some snippets will begin with a transition $\uparrow_\nu$ and the others with $\downarrow_\nu$. In the former case, the first transition carries a current $j(\uparrow_\nu) = +1$, and in the latter $j(\downarrow_\nu) = -1$. Snippets beginning with $\uparrow_\nu$ preceded by snippets of a different kind μ will then contribute to the total current as $\sum_{\mu\neq\nu}\sum_{\ell_\mu} n_{\uparrow_\nu \ell_\mu}$, while snippets beginning with $\downarrow_\nu$ preceded by other snippets of kind $\mu \neq \nu$ contribute as $-\sum_{\mu\neq\nu}\sum_{\ell_\mu} n_{\downarrow_\nu \ell_\mu}$. Along those cases, we have to consider the fact that if the first transition in the full trajectory $\mathcal{L}_n$ is $\uparrow_\nu$ or $\downarrow_\nu$ it must be taken into account separately.

Consequently

$$\sum_{i'} j(\ell_\nu^{(1_{i'})}) = \sum_{i'} (\delta_{\uparrow_\nu,\ell_\nu^{(1_{i'})}} - \delta_{\downarrow_\nu,\ell_\nu^{(1_{i'})}}) = \sum_{\mu\neq\nu}\sum_{\ell_\mu} (n_{\uparrow_\nu\ell_\mu}(\mathcal{L}_n) - n_{\downarrow_\nu\ell_\mu}(\mathcal{L}_n)) + (\delta_{\uparrow_\nu,\ell^{(1)}} - \delta_{\downarrow_\nu,\ell^{(1)}}), \quad (5.24)$$

where the last term in the right hand side considers the possibility that the first transition in the full sequence $\mathcal{L}_n$ is of kind ν. Analogous arguments can be given for the sum $\sum_{i'} j(\ell_\nu^{(n_{i'})})$, accounting for the last transition in each snippet of kind ν. In this case, the total current carried by these transitions is related with the number of times $\uparrow_\nu$ or $\downarrow_\nu$ preceed any other transition of kind $\mu \neq \nu$, where the possibility that the last transition in $\mathcal{L}_n$ is $\uparrow_\nu$ or $\downarrow_\nu$ must also be considered, thus obtaining

$$\sum_{i'} j(\ell_\nu^{(n_{i'})}) = \sum_{i'} (\delta_{\uparrow_\nu,\ell_\nu^{(n_{i'})}} - \delta_{\downarrow_\nu,\ell_\nu^{(n_{i'})}}) = \sum_{\mu\neq\nu}\sum_{\ell_\mu} (n_{\ell_\mu\uparrow_\nu}(\mathcal{L}_n) - n_{\ell_\mu\downarrow_\nu}(\mathcal{L}_n)) + (\delta_{\uparrow_\nu,\ell^{(n)}} - \delta_{\downarrow_\nu,\ell^{(n)}}). \quad (5.25)$$

Now Eqs. (5.24) and (5.25) are plugged inside Eq. (5.23)

$$c_\nu(\mathcal{L}_n) = \xi_\nu(\mathcal{L}_n) + \partial_\nu(\ell^{(1)},\ell^{(n)}) + \frac{1}{2}\sum_{\mu\neq\nu}\sum_{\ell_\mu}(n_{\uparrow_\nu\ell_\mu} - n_{\downarrow_\nu\ell_\mu} + n_{\ell_\mu\uparrow_\nu} - n_{\ell_\mu\downarrow_\nu}), \quad (5.26)$$

where $\partial_\nu(\ell^{(1)},\ell^{(n)}) = \frac{1}{2}(\delta_{\ell_\nu^{(1)}\uparrow_\nu} - \delta_{\ell_\nu^{(1)}\downarrow_\nu} + \delta_{\ell_\nu^{(n)}\uparrow_\nu} - \delta_{\ell_\nu^{(n)}\downarrow_\nu})$ defines a boundary term accounting for the first and last transitions in the full sequence $\mathcal{L}_n$. To interpret the last term in the expression above we consider a specific $\mu \neq \nu$ and expand the quantity inside the parentheses by summing over the outcomes $\ell_\mu = \uparrow_\nu, \downarrow_\nu$ that is

$$\begin{aligned}\sum_{\ell_\mu}&(n_{\uparrow_\nu\ell_\mu} - n_{\downarrow_\nu\ell_\mu} + n_{\ell_\mu\uparrow_\nu} - n_{\ell_\mu\downarrow_\nu}) \\ &= (n_{\uparrow_\nu\uparrow_\mu} - n_{\downarrow_\nu\uparrow_\mu} + n_{\uparrow_\nu\downarrow_\mu} - n_{\downarrow_\nu\downarrow_\mu} + n_{\uparrow_\mu\uparrow_\nu} - n_{\uparrow_\nu\downarrow_\nu} + n_{\downarrow_\mu\uparrow_\nu} - n_{\downarrow_\mu\downarrow_\nu}) \\ &= (\xi_{\uparrow_\nu\uparrow_\mu} - \xi_{\downarrow_\nu\uparrow_\mu} + \xi_{\uparrow_\nu\downarrow_\mu} - \xi_{\downarrow_\nu\downarrow_\mu}) \end{aligned} \quad (5.27)$$

where we recognized the four mixed currents from transitions of kind μ to transitions of kind ν. By noticing that the sign of the mixed currents in the expression above depends on the elementary contribution $j(\ell_\nu)$ to the total current of the transitions $\ell_\nu \in \{\uparrow_\nu, \downarrow_\nu\}$ we finally obtain

$$\begin{aligned} c_\nu(\mathcal{L}_n) &= \xi_\nu(\mathcal{L}_n) + \partial_\nu(\ell^{(1)},\ell^{(n)}) + \frac{1}{2}\sum_{\ell_\nu}\sum_{\mu\neq\nu}\sum_{\ell_\mu}\xi_{\ell_\nu\ell_\mu}(\mathcal{L}_n) j(\ell_\nu) \\ &= \xi_\nu(\mathcal{L}_n) + \partial_\nu(\ell^{(1)},\ell^{(n)}) + \frac{1}{2}\sum_{\substack{\sigma,\mu \\ \sigma>\mu}}\sum_{(\ell_\mu,\ell_\sigma)}\xi_{\ell_\mu\ell_\sigma}(\mathcal{L}_n)(\delta_{\mu,\nu} j(\ell_\mu) + \delta_{\sigma\nu} j(\ell_\sigma)), \end{aligned} \quad (5.28)$$

where in the second line the last sum was changed into a sum over all mixed currents by taking into account that we choose orientations for the mixed currents such that $\mu > \nu$. The relation above is then an extension of Eq. (5.14) to the case of multiple observable currents and can be used to derive the FR for total currents c_ν.

5.5.2 Generalized FR for currents

The decomposition Eq. (5.28) given above can be inverted to express the loop currents in terms of total currents, mixed currents and a boundary term. This can now be inserted into Eq. (5.9) which now reads

$$\begin{aligned}\frac{p(\mathcal{L}_n)}{p(\bar{\mathcal{L}}_n)} &= \sum_{\nu=1}^{N} a_\nu c_\nu(\mathcal{L}_n) - \sum_{\nu=1}^{N} a_\nu \partial_\nu(\ell^{(1)}, \ell^{(n)}) \\ &\quad - \frac{1}{2}\sum_{\nu}\sum_{\substack{\sigma,\mu \\ \sigma>\mu}}\sum_{(\ell_\mu,\ell_\sigma)} a_\nu \xi_{\ell_\mu\ell_\sigma}(\mathcal{L}_n)(\delta_{\mu,\nu} j(\ell_\mu) + \delta_{\sigma\nu} j(\ell_\sigma)) \\ &\quad + \sum_{\substack{\sigma,\mu \\ \sigma>\mu}}\sum_{(\ell_\mu,\ell_\sigma)} \alpha_{\ell_\mu\ell_\sigma}\xi_{\ell_\mu\ell_\sigma}(\mathcal{L}_n) + u(\ell^{(n)}) - u(\ell^{(1)}), \end{aligned} \tag{5.29}$$

with $u(\ell) = -\log p_1(\ell)$. The relation above is then re-written in the form of an FR for currents by applying the Kronecker's deltas and by renaming indices, this allowing regrouping of similar terms as

$$\log\frac{p(\mathcal{L}_n)}{p(\bar{\mathcal{L}}_n)} = \sum_{\nu=1}^{N} a_\nu c_\nu(\mathcal{L}_n) + \sum_{\substack{(\ell_\nu,\ell_\mu) \\ \mu>\nu}} \tilde{\alpha}_{\ell_\nu\ell_\mu}\xi_{\ell_\nu\ell_\mu}(\mathcal{L}_n) + \tilde{u}(\ell^{(n)})) - \tilde{u}(\ell^{(1)})) \tag{5.30}$$

with

$$\tilde{\alpha}_{\ell_\nu\ell_\mu} = a_{\ell_\nu\ell_\mu} - \frac{1}{2}(a_\nu j(\ell_\nu) + a_\mu j(\ell_\mu)), \tag{5.31}$$

$$\tilde{u}(\ell) = u(\ell) + \frac{1}{2}\left(\sum_\nu a_\nu j(\ell_\nu)\delta_{\ell,\ell_\nu}\right) + \tilde{v}, \tag{5.32}$$

that denote respectively the shifted mixed affinities, already anticipated by Eq. (4.11) and a shifted potential accounting for boundary terms, with a constant $\tilde{v}$ that is fixed by normalization of initial probabilities.

At this point, we can use the shifted mixed affinities Eq. (5.31) to verify the relation Eq. (5.5) and thus the FR Eq. (5.3). In fact, a FR is verified if there exist a matrix D such that the similarity relation

$$[E(-\boldsymbol{\lambda}_c)P(\boldsymbol{\lambda})E(-\boldsymbol{\lambda}_c)]_{\ell_\nu\ell'_\mu} = \left[D^{-1}P(-\boldsymbol{f}-\boldsymbol{\lambda})^\perp D\right]_{\ell_\nu\ell'_\mu} \tag{5.33}$$

is established for all ℓ_ν, ℓ'_μ. There exists indeed such matrix, that is proved to also be diagonal. Thus we consider its elements $D_{\ell_\nu,\ell'_\mu} = d(\ell_\nu)\delta_{\ell_\nu,\ell'_\mu}$ so that Eq. (5.5) is by components

$$p(\ell_\nu|\ell'_\nu) = p(\bar{\ell}'_\nu|\bar{\ell}_\nu)\frac{d(\ell_\nu)}{d(\ell_\nu)}e^{a_\nu j(\ell'_\nu)} \qquad \mu = \nu \tag{5.34}$$

$$p(\ell_\nu|\ell_\mu) = p(\bar{\ell}_\mu|\bar{\ell}_\nu)\frac{d(\ell_\nu)}{d(\ell_\nu)}e^{a_\mu j(\ell_\mu)+\tilde{\alpha}_{\ell_\nu\ell_\mu}} \qquad \mu \neq \nu. \tag{5.35}$$

after cancelation of the counting fields, with $\tilde{\alpha}_{\ell_\nu\ell_\mu}$ the shifted mixed affinities Eq. (5.31). The first expression provides that

$$\frac{d(\ell_\nu)}{d(\bar{\ell}_\nu)} = e^{-a_\nu j(\ell_\nu)}, \tag{5.36}$$

and because of definition Eq. (4.9), the elements $d(\ell_\nu) \propto p(\bar{\ell}_\nu|\bar{\ell}_\nu)$. Moreover, when inserted into Eq. (5.54) and using the definition Eq. (5.31), it gives

$$\frac{d(\ell_\nu)}{d(\ell_\mu)} = e^{\frac{1}{2}(a_\mu j(\ell_\mu)-a_\nu j(\ell_\nu))} = \frac{p(\bar{\ell}_\nu|\bar{\ell}_\nu)b_\nu}{p(\bar{\ell}_\mu|\bar{\ell}_\mu)b_\mu}, \tag{5.37}$$

where proportionality constants b_ν for kind ν are introduced. This gives

$$\frac{b_\nu}{b_\mu} = \left(\frac{p(\uparrow_\mu \mid \uparrow_\mu)p(\downarrow_\mu \mid \downarrow_\mu)}{p(\uparrow_\nu \mid \uparrow_\nu)p(\downarrow_\nu \mid \downarrow_\nu)}\right)^{\frac{1}{2}}, \tag{5.38}$$

and since it has to hold for all pairs of kinds ν and μ, it gives

$$b_\nu \propto \prod_{\mu\neq\nu} \left(p(\uparrow_\mu \mid \uparrow_\mu)p(\downarrow_\mu \mid \downarrow_\mu)\right)^{\frac{1}{2}} \tag{5.39}$$

and finally

$$d(\ell_\nu) = p(\bar{\ell}_\nu|\bar{\ell}_\nu) \prod_{\mu\neq\nu} \left(p(\uparrow_\mu \mid \uparrow_\mu)p(\downarrow_\mu \mid \downarrow_\mu)\right)^{\frac{1}{2}} \propto e^{-\frac{1}{2}a_\nu j(\ell_\nu)}. \tag{5.40}$$

It is immediate to check that the elements above satisfy Eq. (5.5), thus a FR holds for the joint set of total currents $\{c_\nu\}$ and the mixed currents $\{\xi_{\ell_\nu\ell_\mu}\}$ at the level of their MGF, and we see that the crucial point is to use the shifted mixed affinities Eq. (5.31) conjugated with the mixed currents.

Since the symmetry Eq. (5.3) holds, then Eq. (5.30) can be ultimately summed over all possible outcomes $\ell_2, \cdots, \ell_{n-1}$ compatible with outcomes $c_\nu(\mathcal{L}_n) = c_\nu$ and $\xi_{\ell_\nu\ell_\mu}(\mathcal{L}_n) = \xi_{\ell_\nu\ell_\mu}$, to obtain the detailed FR for the joint set of total currents, the mixed currents, and the boundary transitions

$$\begin{aligned}\log \frac{p_n(\{c_\nu\}, \{\xi_{\ell_\nu\ell_\mu}\}, \ell^{(1)}, \ell^{(n)})}{p_n(\{-c_\nu\}, \{-\xi_{\ell_\nu\ell_\mu}\}, \bar{\ell}^{(1)}, \bar{\ell}^{(n)})} &= \sum_{\nu=1}^{N} a_\nu c_\nu \\ &+ \sum_{\substack{(\ell_\nu,\ell_\mu)\\ \mu>\nu}} \tilde{\alpha}_{\ell_\nu\ell_\mu}\xi_{\ell_\nu\ell_\mu} + \tilde{u}(\ell^{(n)})) - \tilde{u}(\ell^{(1)})).\end{aligned} \tag{5.41}$$

The conditions in which the FR above holds are the reversibility of each observable transition, observation of a number N of edges lesser than the number of cycles in the graph and the condition of hidden irreducibility, that is, there exist at least one path connecting each pair of states through only hidden transitions. This path can also be irreversible if there is at least another path connecting the same states in the opposite direction. This explains why we were allowed to include an irreversible hidden transition when verifying numerically the FR for single currents in the previous section.

Before proceeding with the case where the set of observable currents is complete, we check explicitly Eq. (5.5) in the case of a single observable current by use of the solution for D given by Eq. (5.40) and the tilted matrix Eq. (4.23). The left hand side reads

$$\begin{pmatrix} e^{-\lambda} & 0 \\ 0 & e^{\lambda} \end{pmatrix} \begin{pmatrix} p(\uparrow \mid \uparrow)e^{\lambda} & p(\uparrow \mid \downarrow)e^{\lambda} \\ p(\downarrow \mid \uparrow)e^{-\lambda} & p(\downarrow \mid \downarrow)e^{-\lambda} \end{pmatrix} \begin{pmatrix} e^{\lambda} & 0 \\ 0 & e^{-\lambda} \end{pmatrix} = \begin{pmatrix} p(\uparrow \mid \uparrow)e^{\lambda} & p(\uparrow \mid \downarrow)e^{-\lambda} \\ p(\downarrow \mid \uparrow)e^{\lambda} & p(\downarrow \mid \downarrow)e^{-\lambda} \end{pmatrix}. \tag{5.42}$$

The right hand side is

$$\begin{pmatrix} e^{\frac{a}{2}} & 0 \\ 0 & e^{-\frac{a}{2}} \end{pmatrix} \begin{pmatrix} p(\uparrow \mid \uparrow)e^{-a-\lambda} & p(\uparrow \mid \downarrow)e^{-a-\lambda} \\ p(\downarrow \mid \uparrow)e^{a+\lambda} & p(\downarrow \mid \downarrow)e^{a+\lambda} \end{pmatrix}^{\perp} \begin{pmatrix} e^{-\frac{a}{2}} & 0 \\ 0 & e^{\frac{a}{2}} \end{pmatrix} = \begin{pmatrix} p(\uparrow \mid \uparrow)e^{\lambda} & p(\uparrow \mid \downarrow)e^{-\lambda} \\ p(\downarrow \mid \uparrow)e^{\lambda} & p(\downarrow \mid \downarrow)e^{-\lambda} \end{pmatrix}, \tag{5.43}$$

where we used the definition of effective affinity and applied anti-transposition, thus proving that the FR for single currents is obtained at the level of the MGF in the limit $n \to \infty$. By using the Perron-Frobenius theorem for positive matrices, the MGF is related to the Perron root $\mathrm{PR}(P(\lambda))$ of $P(\lambda)$. The Scaled Cumulant Generating Function (SCGF) is then defined as

$$g(\lambda) = \lim_{n\to\infty} \frac{1}{n} \log G_n(\lambda) = \log \mathrm{PR}(P(\lambda)). \tag{5.44}$$

for the case of a single observable transition. A symmetry of the MGF is also a symmetry of the SCGF, and this is represented in Fig. 5.4 (imported from Ref. [31]), where the SCGF is rescaled by a factor $r^{\infty} = r(\uparrow)p^{\mathrm{st}}(\mathtt{s}(\uparrow)) + r(\downarrow)p^{\mathrm{st}}(\mathtt{s}(\downarrow))$ called stationary dynamical activity, the average number of observable transitions per unit of time, so that it can be compared with the MGF for a single current observed at clock time t.

5.6 Complete sets of currents

We now address the limit case where the observable edges form a complete set. A complete set of currents, as explained in the context of cycle decompositions of graphs, is obtained when the removal of a set of observed edges

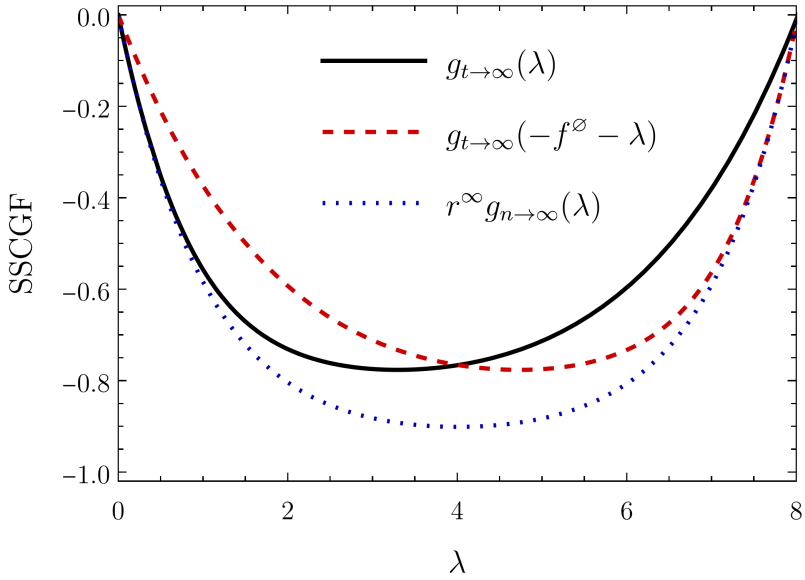

Figure 5.4: Comparison between the SCGF at stopping-t (black line) and the SCGF at stopping-n (blue dotted line) for the statistics of a single observable current. The latter presents a symmetry respect to the axis given by $\lambda^* = a/2$ with $a = \log p(\uparrow \mid \uparrow)/p(\downarrow \mid \downarrow)$ the effective affinity thus a FR holds for currents evaluated at stopping-n.

from the full graph gives a tree $\mathscr{T}$, i.e. a graph that contains no cycles. Schnakenberg analysis [41] applied to current densities evaluated at fixed time t gives a decomposition for the total entropy production in terms of cycle and tidal currents [32], the former considering closure of fundamental cycles (the set of cycles that are obtained by reinsertion of observed chords in the spanning tree $\mathscr{T}$) and the latter being a term accounting for the relaxation to the stationary state. The cycle contribution to the integrated entropy production, depending now on total integrated currents evaluated at time t, satisfies its own asymptotic fluctuation relation as proven in [33], and depends on the products of such currents with their respective cycle affinities, obtained from ratios of products of forward and backward rates along the edges constituting the cycle, as stated by Eq. (2.70).

In our description at stopping-n in terms of transitions we studied total currents evaluated up to n occurrences and we showed that they satisfy a FR when an arbitrary number of edges is accessible to observation and if their joint statistics is complemented by mixed currents. In this case the observed currents are conjugated to effective affinities that accounts for all possible hidden paths connecting the target state and the source state of the observed transition, consisting in multiple possible cycles to be closed around the observable edge without performing any other observable transition.

For complete sets, each effective affinity becomes a cycle affinity, expressed as Eq. (2.70), since the hidden graph contain no other cycle. Thus we expect that the full entropy production can be estimated by only observing such a fundamental set, without the need to track mixed currents along different edges. In this section we derive a FR for the joint statistics of a complete set of total currents by proceeding via the MGF as in the general case, and we provide an alternative proof by starting directly from the detailed FR Eq. (5.41) where the equilibrium condition on the spanning tree provides the boundedness of the contribution given by mixed currents, that can therefore be neglected in the limit $n \to \infty$. Specifically, their contribution to the integrated entropy production can be considered as generated by processes in the space of kinds, where subsequent transitions $\ell_\mu \to \ell_\nu$ along different edges ν and $\mu \neq \nu$ are treated regardless the direction of ℓ_ν and ℓ_μ. This process can be seen as a chain that can be represented on a graph where vertices represent different observable kinds and it is updated only when mixed trans-transitions occur. With these kind of considerations the mixed contribution turns out to be bounded and thus can be neglected in the limit $n \to \infty$.

5.6.1 Complete sets and hidden equilibrium

In the previous section we provided fluctuation relations for an arbitrary set of observable edges. A limit case is when the number of observable edges equals the number of fundamental cycles that can be constructed by the

Schnakenberg procedure [41], explained in Section 2.5.1, in which the observed edges, called chords, define the so-called spanning tree $\mathscr{T}$ by their removal from the full graph $\mathscr{G}$. Being a dynamics on the spanning tree at equilibrium, the currents along the observed chords constitute a minimal set of observables that provide the full information about the system, being the remaining currents linearly dependent from them, and in particular allows exact estimation of the entropy produced by the process if the cycle affinities conjugated with the currents are known. In fact, as found in [33], the statistics of currents along those edges evaluated up to some external time t satisfy a long time FR, that can be made transient (i.e. holding at all times) by selecting as initial state the stalling distribution, the stationary state of the system where the chords are removed [32].

Our objective is to derive the FR for the particular case of complete sets of currents evaluated up to n occurrences, where tracking of the mixed currents can be excluded. In particular we apply the arguments based on the MGF given above, to find that the symmetry Eq. (5.3) is satisfied even by not including counting fields associated to the mixed currents. A crucial point in the discussion is the equilibrium of the spanning tree $\mathscr{T}$, in the sense that any closed path in state space $x_1 \to x_2 \to \cdots \to x_1$ only occurring in $\mathscr{T}$ does not produce entropy. By denoting with $\pi(x|y) = r(x|y)/r(x)$ the transition probabilities of the embedded Markov chain in state space, any similar path then satisfy

$$\frac{\pi(x_1|x_{n-1})\pi(x_{n-1}|x_{n-2})\cdots\pi(x_2|x_2)}{\pi(x_1|x_2)\cdots\pi(x_{n-2}|x_{n-1})\pi(x_{n-1}|x_1)} = 1 \tag{5.45}$$

where in the denominator is the path probability of the reverse sequence, with the initial probability not contributing since the first and last visited states are the same. The relation above expresses the Kolmogorov's criterion for the equilibrium in the spanning tree, rewritten in terms of jump probability rather than transition rates.

The analogue of Eq. (5.45) can be expressed in transition space by using the trans-transition probabilities as

$$\frac{p(\ell^{(1)}|\bar{\ell}^{(n-1)})p(\ell^{(n-1)}|\bar{\ell}^{(n-2)})\cdots p(\ell^{(2)}|\bar{\ell}^{(1)})}{p(\ell^{(1)}|\bar{\ell}^{(2)})\cdots p(\ell^{(n-2)}|\bar{\ell}^{(n-1)})p(\ell^{(n-1)}|\bar{\ell}^{(1)})} = 1 \tag{5.46}$$

that holds for all sequences $\ell^{(1)} \to \ell^{(2)} \to \cdots \to \ell^{(1)}$ if the graph obtained by removing the observable edges where the $\ell^{(i)}$ occurs contains no cycles. The rewriting Eq. (5.46) is possible since in the case of complete sets the trans-transition probabilities can be written as

$$p(\ell|\ell') = \pi(\ell)\pi(\Gamma(\mathtt{t}(\ell') \to \mathtt{s}(\ell)))\sigma(\ell,\ell'), \tag{5.47}$$

where $\pi(\ell) = \pi(\mathtt{t}(\ell)|\mathtt{s}(\ell))$, $\sigma(\ell,\ell')$ is a symmetric term with $\sigma(\ell,\ell') = \sigma(\bar{\ell},\bar{\ell}')$ appearing due to failed explorations along the tree and $\pi(\Gamma(\mathtt{t}(\ell') \to \mathtt{s}(\ell)))$ is

the product of the transition probabilities along the direct (or shortest) hidden path connecting the target state of ℓ' and the source state of ℓ. Thus, by inserting the trans-transition probabilities, decomposed as Eq. (5.47) in the case of complete sets, into Eq. (5.46), the symmetric terms and the transition probabilities $\pi(\ell)$ cancel, and we are left with the products of probabilities along hidden transitions, thus recovering Eq. (5.45), that holds for all paths occurring only on the spanning tree $\mathscr{T}$. From now on, we indicate for simplicity with $\pi(\bullet)$ an operator acting on paths in state space that returns the product of the transition rates along that circuit that reduces to transition probabilities in the embedded Markov chain when the path consists of a single transition.

5.6.2 The FR for complete sets of currents

The relation Eq. (5.46) provides two properties that must be satisfied by the mixed affinities $\alpha_{\ell_\nu \ell_\mu}$ Eq. (4.10) in the case of complete sets of currents. In fact, we can consider for instance a single cyclic realization akin $\ell_\nu \to \ell_\mu \to \ell_\rho \to \ell_\nu$ in transition space, where the kinds $\nu \neq \mu \neq \rho$ are visited in succession. For such realizations, by use of Eq. (5.46) and the definition Eq. (4.10) one obtains for the mixed affinities

$$\alpha_{\ell_\nu \bar{\ell}_\rho} + \alpha_{\ell_\rho \bar{\ell}_\mu} + \alpha_{\ell_\mu \bar{\ell}_\nu} = 0. \tag{5.48}$$

Moreover, for trajectories such as $\ell_\nu \to \ell_\mu \to \bar{\ell}_\mu \to \ell_\nu$ one obtains from Eq. (5.46)

$$\alpha_{\ell_\nu \bar{\ell}_\mu} = \alpha_{\ell_\nu \ell_\mu} - a_\mu j(\ell_\mu), \tag{5.49}$$

from which one can also obtain that $\alpha_{\bar{\ell}_\nu \ell_\mu} = \alpha_{\ell_\nu \ell_\mu} - a_\nu j(\ell_\nu)$ by simply using the fact that $\alpha_{\ell_\nu \ell_\mu} = -\alpha_{\bar{\ell}_\mu \bar{\ell}_\nu}$. It is easy to check that combined usage of Eqs. (5.48) and (5.49) always verifies Eq. (5.46) for any cyclic sequence of observable transitions.

We now have all the ingredients needed to prove that in the case of complete sets of currents the statistics of total currents c_ν along their correspondant edge satisfy the FR

$$\log \frac{p_n(\{c_\nu\})}{p_n(\{-c_\nu\})} \asymp \sum_\nu a_\nu c_\nu, \tag{5.50}$$

without the need of tracking mixed occurrences along different edges, quantified by the mixed currents defined by Eq. (4.6). In fact, we prove that the diagonal matrix D satisfying

$$E(-\boldsymbol{\lambda}_c) P(\boldsymbol{\lambda}_c) E(\boldsymbol{\lambda}_c) = D^{-1} P(-\boldsymbol{f} - \boldsymbol{\lambda}_c) D \tag{5.51}$$

exists only if both conditions Eqs. (5.48) and (5.49) are verified by the mixed affinities. The equation above is rewritten after simplification as

$$\frac{d(\ell_\nu)}{d(\ell'_\mu)} = \frac{p(\bar{\ell}_\mu | \bar{\ell}'_\nu)}{p(\ell_\nu | \ell'_\mu)} e^{a_\mu j(\ell_\mu)}, \tag{5.52}$$

with $d(\ell_\nu) = D_{\ell_\nu \ell_\nu}$. By evaluating the relation above for $\ell'_\mu = \ell_\nu$ one simply finds the definition for the affinities $a_\nu = \log p(\uparrow_\nu \mid \uparrow_\nu)/p(\downarrow_\nu \mid \downarrow_\nu)$. For $\ell'_\mu = \bar{\ell}_\nu$ instead

$$\frac{d(\ell_\nu)}{d(\bar{\ell}_\nu)} = e^{-a_\nu j(\ell_\nu)}, \tag{5.53}$$

that is plugged back inside Eq. (5.52) to obtain for $\mu \neq \nu$

$$\frac{d(\ell_\nu)}{d(\ell_\mu)} = e^{-\alpha_{\ell_\nu \bar{\ell}_\mu}}, \tag{5.54}$$

where the definition of mixed affinities is used. Finally, the condition above can be plugged inside Eq. (5.52) for $\mu \neq \nu$ to obtain

$$\alpha_{\ell_\nu \bar{\ell}_\mu} = \alpha_{\ell_\nu \ell_\mu} - a_\mu j(\ell_\mu), \tag{5.55}$$

which is certainly satisfied by the mixed affinities in the case of complete sets of observable edges, as it is equivalent to Eq. (5.49). The remaining condition is found by imposing that Eq. (5.54) must hold for all pairs of kinds (ν, μ). Then

$$\frac{d(\ell_\nu)}{d(\ell_\mu)} = \frac{d(\ell_\nu)}{d(\ell_\rho)} \frac{d(\ell_\rho)}{d(\ell_\mu)} = e^{-\alpha_{\ell_\nu \bar{\ell}_\rho} - \alpha_{\ell_\rho \bar{\ell}_\mu}} = e^{-\alpha_{\ell_\nu \bar{\ell}_\mu}}, \tag{5.56}$$

which is exactly Eq. (5.48), thus proving that the statistics of monitored total currents c_ν satisfies the FR Eq. (5.50) in the case of complete sets since the conditions on the mixed affinities Eq. (4.10) required for the matrix D in Eq. (5.51) to exists are compatible with the properties emerging for the same affinities due to the equilibrium of all paths occurring in the spanning tree $\mathscr{T}$.

5.6.3 Inter-kind currents

The derivation of the FR for complete sets of currents through the symmetry Eq. (5.3) for the MGF Eq. (4.13) given in the previous section is based on connecting closed trajectories expressed in state space all occurring in the spanning tree, which are at equilibrium, with their transition space analogue. It is important to point out that the same arguments given above are still valid in the case where the set is not complete if the hidden cycles produce no entropy in average, that is, the cycle affinity evaluated along the hidden cycles vanish. We call such cycles futile cycles. In such case, removal of an edge belonging to a futile cycle does not affect the effective affinities and the mixed affinities, which then satisfy the conditions Eq. (5.48) and Eq. (5.49) and thus the FR for the total currents c_ν evaluated along the observable edges still does not require tracking of mixed currents.

Here we give a more physical interpretation on the role of mixed currents and mixed affinities in the case of complete sets of observable currents.

The starting point is the condition Eq. (5.49) which suggests that the mixed affinities $\alpha_{\ell_\nu \ell_\mu}$, $\mu \neq \nu$ defined by Eq. (4.10) can be written in this special situation as ratios of the diagonal elements of the trans-transition matrix P together with a proportionality constant only depending on the kinds ν and μ. As a consequence, the shifted mixed affinities $\tilde{\alpha}_{\ell_\nu \ell_\mu}$, defined by Eq. (5.31), now become affinities between kinds $\tilde{\alpha}_{\nu\mu}$ since shifted mixed affinities between transitions along the same pair of edges ν and μ have all the same value. As a consequence of that, we can construct a process in the space of kinds that is at equilibrium, thus its contribution to the total entropy production is bounded and therefore it can be neglected in the limit $n \to \infty$.

Mixed affinities for complete sets

As explained in the previous section, the trans-transition probabilities can be written as Eq. (5.47) in the case of complete sets of observable edges, because of the spanning tree $\mathscr{T}$ containing no cycles. By use of Eq. (5.47) the mixed affinities are then written as

$$\begin{aligned}\alpha_{\ell_\nu \ell_\mu} &= \log \frac{p(\ell_\nu|\ell_\mu)}{p(\bar{\ell}_\mu|\bar{\ell}_\nu)} \\ &= \log \frac{\pi(\ell_\nu)\pi(\Gamma(\mathtt{t}(\ell_\mu) \to \mathtt{s}(\ell_\nu)))}{\pi(\bar{\ell}_\mu)\pi(\Gamma(\mathtt{t}(\bar{\ell}_\nu)) \to \mathtt{s}(\bar{\ell}_\mu)))} \\ &= \log \frac{\pi(\ell_\nu)\pi(\Gamma(\mathtt{t}(\ell_\mu) \to \mathtt{s}(\ell_\nu)))}{\pi(\bar{\ell}_\mu)\pi(\Gamma(\mathtt{s}(\ell_\nu)) \to \mathtt{t}(\ell_\mu)))}\end{aligned} \tag{5.57}$$

where the combinatorial symmetric terms cancel because they are invariant under time reversal and since the target (source) state of $\bar{\ell}$ is the source (target) of ℓ for all observable transitions. We now consider the diagonal trans-transition probabilities and apply Eq. (5.47) to obtain

$$p(\ell_\nu|\ell_\nu) = \pi(\ell_\nu)\pi(\Gamma(\mathtt{t}(\ell_\nu) \to \mathtt{s}(\ell_\nu)))\sigma_\nu \tag{5.58}$$

so that now

$$\begin{aligned}&\log \frac{p(\ell_\nu|\ell_\mu)}{p(\bar{\ell}_\mu|\bar{\ell}_\nu)} \frac{p(\bar{\ell}_\mu|\bar{\ell}_\mu)}{p(\ell_\nu|\ell_\nu)} \\ &\quad = \log \frac{\pi(\Gamma(\mathtt{t}(\ell_\mu) \to \mathtt{s}(\ell_\nu)))}{\pi(\Gamma(\mathtt{t}(\bar{\ell}_\nu)) \to \mathtt{s}(\bar{\ell}_\mu)))} \frac{\pi(\Gamma(\mathtt{t}(\bar{\ell}_\mu) \to \mathtt{s}(\bar{\ell}_\mu)))\sigma_\mu}{\pi(\Gamma(\mathtt{t}(\ell_\nu) \to \mathtt{s}(\ell_\nu)))\sigma_\nu}.\end{aligned} \tag{5.59}$$

The right hand side of the equation above is showed in Appendix B of [82] to be a constant factor $\omega_{\nu\mu}$ not depending on ℓ_ν and ℓ_μ but only on their kinds ν and μ. Thus

$$\alpha_{\ell_\nu \ell_\mu} = \log \omega_{\nu\mu} \frac{p(\ell_\nu|\ell_\mu)}{p(\bar{\ell}_\mu|\bar{\ell}_\mu)}. \tag{5.60}$$

By consequence the mixed affinities have the following properties:

i. Mixed affinities between the same kinds ν and μ are related by a shift depending on the cycle affinities as

$$\begin{cases} \alpha_{\ell_\nu \ell_\mu} - a_\nu j(\ell_\nu) = \alpha_{\bar{\ell}_\nu \ell_\mu} \\ \alpha_{\ell_\nu \ell_\mu} - a_\mu j(\ell_\mu) = \alpha_{\ell_\nu \bar{\ell}_\mu} \end{cases}, \tag{5.61}$$

as required by the mixed affinities, analogously to Eq. (5.49);

ii. The shifted affinities $\tilde{\alpha}_{\ell_\nu \ell_\mu} \equiv \tilde{\alpha}_{\nu\mu}$ since for all ℓ_ν, ℓ_μ

$$\tilde{\alpha}_{\ell_\nu \ell_\mu} = \log \omega_{\nu\mu} \left(\frac{p(\uparrow_\nu \mid \uparrow_\nu) p(\downarrow_\nu \mid \downarrow_\nu)}{p(\uparrow_\mu \mid \uparrow_\mu) p(\downarrow_\mu \mid \downarrow_\mu)} \right)^{1/2} = \tilde{\alpha}_{\nu\mu}, \tag{5.62}$$

only depending on the kinds ν and μ, and is proven immediately by plugging Eq. (5.60) into the definition Eq. (5.31) for the shifted mixed affinities;

iii. The shifted affinities above are now antisymmetric under $\nu \leftrightarrow \mu$

$$\tilde{\alpha}_{\nu\mu} = -\tilde{\alpha}_{\mu\nu}. \tag{5.63}$$

We now use these properties to study the contribution of mixed currents to the joint FR for total currents and mixed currents in the case of complete sets.

Mixed currents in complete sets

Starting from the simple case of $N = 2$ observable transitions in both directions, we can write the mixed contributions in the right hand side of Eq. (5.41) by using Eq. (5.62)

$$\tilde{\alpha}_{12}(\xi_{\uparrow_1\uparrow_2} + \xi_{\uparrow_1\downarrow_2} + \xi_{\downarrow_1\uparrow_2} + \xi_{\downarrow_1\downarrow_2}) = \tilde{\alpha}_{12}\xi_{12}, \tag{5.64}$$

that defines the inter-kind current ξ_{12}, the net amount of times trans-transitions from kind 2 to kind 1 are observed at the end of the process after n observable transitions. It is immediate to see that for any realization of processes with only $N = 2$ observable transitions in both directions the inter-kind current can assume only values ± 1 or 0, since it only depends on the kind of the first and last transition in a given sequence of observable transitions. In the asymptotic limit $n \to \infty$, therefore, the FR Eq. (5.41) reduces to

$$\log \frac{p_n(c_1, c_2)}{p_n(-c_1, -c_2)} \asymp a_1 c_1 + a_2 c_2, \tag{5.65}$$

since the mixed contributions are bounded and it is now possible to marginalize the probabilities respect to the mixed currents $\xi_{\ell_1 \ell_2}$.

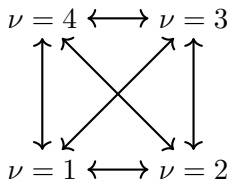

Figure 5.5: The process in the space of kinds for a process with $N = 4$ observable transitions, with nodes represent the edges where the observable transitions are occurring. The process in the space of kinds can thus be seen as a process in the space of un-directed edges. Such a process can be meaningfully constructed in the case where the N observable edges form a complete set. A peculiarity of such processes is that any cycle performed in this graph has zero affinity, and thus it can be regarded as equilibrium. Therefore, it is not contributing to the joint FR for currents and mixed currents in the asymptotic limit, allowing marginalization of mixed currents.

The argument given above in the case of $N = 2$ observable transitions can be generalized to an arbitrary number $N > 2$ of observable edges, in the case where N is also the number of fundamental cycles in the full graph and if the observable edges can be identified with chords whose removal make the graph into a spanning tree $\mathscr{T}$. To have an intuition on this, we define a process in the space of kinds. Given the process with N observable transitions we consider only events in which subsequent transitions occur along different observable edges, as the one represented in Fig. 5.5. The so-constructed process can be interpreted as a process in the space of undirected edges.

The construction of such a process is possible in the case of complete sets since the contributions from mixed currents can be rewritten in terms of inter-kind currents $\xi_{\nu\mu} = \sum_{\ell_\nu \ell_\mu} \xi_{\ell_\nu \ell_\mu}$ because of Eq. (5.62) for the shifted mixed affinities. Consider now a cyclic realization in the space of kinds

$$\nu \to \mu_1 \to \cdots \to \mu_{m-2} \to \nu \tag{5.66}$$

of some lenght $m \geq 2$. The sum of all shifted affinities in such cyclic sequences always reads

$$\tilde{\alpha}_{\mu_1 \nu} + \tilde{\alpha}_{\mu_2 \mu 1} + \cdots + \tilde{\alpha}_{\nu \mu_{m-2}} = 0 \tag{5.67}$$

because of the properties of $\tilde{a}_{\nu\mu}$ for all $\nu, \mu \neq \nu$, coming directly from the reversibility of processes occurring along the spanning tree, summarized by Eqs. (5.45) and (5.46). By consequence, each cycle in the inter-kind process has zero affinity, and thus according to Kolmogorov's criterion the net contribution by the inter-kind currents has to be bounded since the process in the space of kinds is at equilibrium. Equation (5.67) also suggests

the following ansatz for the shifted mixed affinities

$$\tilde{\alpha}_{\nu\mu} = U_\nu - U_\mu, \qquad \text{for all} \qquad \mu \neq \nu. \tag{5.68}$$

In fact, such an assumption on the shifted affinities preserves all its properties when the set of observable edges is complete. At this point, the mixed contributions to the general FR Eq. (5.41) become

$$\begin{aligned} \sum_{\substack{\mu>\nu \\ \nu,\mu}} \sum_{(\ell_\nu,\ell_\mu)} \tilde{a}_{\ell_\nu\ell_\mu}\xi_{\ell_\nu\ell_\mu} &= \sum_{\substack{\mu>\nu \\ \nu,\mu}} \tilde{a}_{\nu\mu}\xi_{\nu\mu} \\ &= -\sum_\nu U_\nu \sum_{\mu\neq\nu} \xi_{\mu\nu} \end{aligned} \tag{5.69}$$

where the used the antisymmetry property Eq. (5.63) for the shifted affinities $\tilde{a}_{\nu\mu}$ and the ansatz Eq. (5.68). In the last line, the sum $\sum_{\mu\neq\nu}\xi_{\mu\nu}$ is interpreted as the number of times the system leaves kind ν in a realization $\mathcal{L}_n$ of a process in transition space, that for cyclic sequences of kinds $\nu \to \cdots \to \nu$ reads $\sum_{\mu\neq\nu}\xi_{\mu\nu} = 0$ otherwise take values ± 1. We can then conclude that for a complete set of N observable currents the mixed contributions are bounded, and then, in the limit $n \to \infty$, their contribution to the general FR Eq. (5.41) can be neglected. The mixed currents can therefore be marginalized from the probability distributions $p_n(\{c_\nu\}, \{\xi_{\nu\mu}\})$ thus giving

$$\log \frac{p_n(\{c_\nu\})}{p_n(\{-c_\nu\})} \asymp \sum_{\nu=1}^{N} a_\nu c_\nu, \tag{5.70}$$

that is the FR for a complete set of currents only depending on the set total currents c_ν.

5.7 Transient FRs

All the FRs introduced in this Chapter are valid in specific circumstances. For instance, the FR (5.41) is valid at all n if the information about the first and last transition is included, that is, by including in the statistics only realizations with fixed endpoints. Particularly important is the case where the first and last transitions are the time-reversal of each other since the boundary terms always vanish, and in such case after sampling the total currents and the mixed currents the FR can be validated numerically by taking the ratios or probabilities $p_n(\{c_\nu\}, \{\xi_{\ell_\nu\ell_\mu}\})$ versus their symmetric analogue respect to the axes $c_\nu = 0$ and $\xi_{\ell_\nu\ell_\mu} = 0$ for all currents. The FRs obtained are also valid in general in the limit $n \to \infty$ that requires a very large sample size since, as n grows, realizations with negative entropy production become extremely rare.

To solve this issue we need to generalize the FRs obtained above to all n by also eliminating the necessity to post-select realizations $\mathcal{L}_n$ with fixed transitions at the boundaries. This can be done in general by preparing the system in a way such that the statistics of currents satisfy a FR at all n. Such choice always exists in transition space even in the most general case where an arbitrary number of edges is observed. Notice that it is also possible to define initial distributions in state space such that a FR is valid for currents at stopping-t [32]. However, this is possible uniquely in the case where a complete set of currents is observable, a particular case which restricts the study to only a few real world circumstances.

In this section we use the fact that the FR is rephrased as a symmetry of the corresponding MGF for the statistics of currents to find an initial probability $\boldsymbol{p}_1^*$, called preferred probability, such that observed currents satisfy a FR at all n. This has practical advantages since it is possible to observe very short realizations of the process in transition space to obtain a good enough statistics for outcomes with negative entropy production, thus improving the convergence of the estimator for the forward to backward probability ratios as well as the Jarzynski estimator, notoriously endowed with poor convergence properties.

5.7.1 Preferred initial probability

Consider the symmetry for the MGF at stopping-n

$$G_n(\boldsymbol{\lambda}) = G_n(-\boldsymbol{f} - \boldsymbol{\lambda}) \tag{5.71}$$

with $\boldsymbol{\lambda}$ denoting the vector of counting fields, each one conjugated to a different current, and $\boldsymbol{f}$ denoting their associated affinities. The MGF can be written in terms of a tilted matrix containing the counting fields as explained in Section 4.4.1, and the symmetry above can be reformulated as the identity

$$E(-\boldsymbol{\lambda}_c)P(\boldsymbol{\lambda})E(\boldsymbol{\lambda}_c) = D^{-1}P(-\boldsymbol{f} - \boldsymbol{\lambda})^{\perp}D \tag{5.72}$$

if there exists a diagonal matrix D that satisfy the relation. Such a matrix plays a crucial role in determining the preferred initial probability as explained in this section.

We write the left and right hand side of Eq. (5.71) in terms of tilted trans-transition matrices as

$$\mathbf{1} \cdot [P(\boldsymbol{\lambda})]^{n-1} E(\boldsymbol{\lambda}_c)\boldsymbol{p}_1 = \mathbf{1} \cdot [P(-\boldsymbol{f} - \boldsymbol{\lambda})]^{n-1} E(-\boldsymbol{a} - \boldsymbol{\lambda}_c)\boldsymbol{p}_1 \tag{5.73}$$

with $\boldsymbol{\lambda}_c$ denoting the vector of counting fields conjugated only to total currents c_ν, $\boldsymbol{a}$ containing their effective affinities and $\boldsymbol{p}_1$ the initial probability.

We can now apply the relation Eq. (5.72) to find in the left hand side

$$\mathbf{1}\cdot[P(\boldsymbol{\lambda})]^{n-1}\,E(\boldsymbol{\lambda}_c)\boldsymbol{p}_1 \tag{5.74}$$

$$=\mathbf{1}\cdot\left[E(\boldsymbol{\lambda}_c)D^{-1}P(-\boldsymbol{f}-\boldsymbol{\lambda})^{\perp}DE(-\boldsymbol{\lambda}_c)\right]^{n-1}E(\boldsymbol{\lambda}_c)\boldsymbol{p}_1 \tag{5.75}$$

$$=\mathbf{1}\cdot E(\boldsymbol{\lambda}_c)D^{-1}\left[P(-\boldsymbol{f}-\boldsymbol{\lambda})^{\perp}\right]^{n-1}D\boldsymbol{p}_1 \tag{5.76}$$

$$=\boldsymbol{p}_1\cdot DJ\,[P(-\boldsymbol{f}-\boldsymbol{\lambda})]^{n-1}\,JE(\boldsymbol{\lambda}_c)D^{-1}\mathbf{1} \tag{5.77}$$

$$=\boldsymbol{p}_1\cdot DJ\,[P(-\boldsymbol{f}-\boldsymbol{\lambda})]^{n-1}\,E(-\boldsymbol{\lambda}_c)JD^{-1}\mathbf{1}, \tag{5.78}$$

where in the fourth line we take the transposal of all quantities, being a scalar product, and applied the property $(P^{\perp})^{\top}=JPJ$. In the fifth line we used $JE(\boldsymbol{\lambda}_c)=E(-\boldsymbol{\lambda}_c)J$. By comparison with the right hand side of Eq. (5.71) we see that the two are equivalent with the choice

$$\boldsymbol{p}_1^*\propto D^{-1}\mathbf{1} \tag{5.79}$$

since also

$$E(-\boldsymbol{a})\boldsymbol{p}_1^*=J\boldsymbol{p}_1^* \tag{5.80}$$

holds. The latter equation will be proved later for explicit expressions assumed by the preferred probability in the general case and in the case where the set of observable currents is complete, which are given in the following.

Preferred probability for the general case

In Section 5.2 we derived the explicit expression for the diagonal matrix D that satisfy the relation Eq. (5.72) that is given by Eq. (5.40). Thus, for a transition ℓ_ν of kind ν the preferred initial probability reads according to Eq. (5.79)

$$p_1^*(\ell_\nu)\propto\frac{1}{p(\bar{\ell}_\nu|\bar{\ell}_\nu)\prod_{\mu\neq\nu}\left[p(\uparrow_\mu\mid\uparrow_\mu)p(\downarrow_\mu\mid\downarrow_\mu)\right]^{1/2}}, \tag{5.81}$$

that can be rewritten as

$$p_1^*(\ell_\nu)\propto\frac{e^{\frac{1}{2}a_\nu j(\ell_\nu)}}{\prod_\mu\left[p(\uparrow_\mu\mid\uparrow_\mu)p(\downarrow_\mu\mid\downarrow_\mu)\right]^{1/2}}. \tag{5.82}$$

To normalize the initial probability we impose $\sum_\nu\sum_{\ell_\nu}p_1^*(\ell_\nu)=1$, thus obtaining

$$p_{1,\mathrm{ncs}}^*(\ell_\nu)=\frac{e^{\frac{1}{2}a_\nu j(\ell_\nu)}}{2\sum_\mu\cosh\left(a_\mu/2\right)} \tag{5.83}$$

that is the preferred initial probability that grants FR at all n for an arbitrary set of N observable edges, if all the mixed currents are taken into account.

Preferred probability for complete sets

We derive here the expression for D satisfying Eq. (5.72) in the case where the mixed currents are not tracked and the set of total currents $\{c_\nu\}$ is a complete set. We proceed similarly as in the case of non-complete sets of currents, already explained in Section 5.5.2.

In this case the diagonal elements $D_{\ell_\nu \ell'_\mu} = d(\ell_\nu)\delta_{\ell_\nu \ell'_\mu}$ must satisfy the conditions

$$\frac{d(\ell_\nu)}{d(\bar{\ell}_\nu)} = e^{-a_\nu j(\ell_\nu)} \tag{5.84}$$

$$\frac{d(\ell_\nu)}{d(\ell_\mu)} = \frac{p(\ell_\mu|\bar{\ell}_\nu)}{p(\ell_\nu|\bar{\ell}_\mu)} = e^{-\alpha_{\ell_\nu \bar{\ell}_\mu}} \tag{5.85}$$

according to the definition for the mixed affinities $a_{\ell_\nu \ell_\mu}$. The first condition, as in the general case, impose that $d(\ell_\nu) \propto p(\bar{\ell}_\nu|\bar{\ell}_\nu)$. For handling the second one we make use of the ansatz Eq. (5.68) introduced before in the context of inter-kind processes, since for complete sets the shifted mixed affinities $\tilde{\alpha}_{\ell_\nu \ell_\mu} = \tilde{\alpha}_{\nu\mu}$ only depend on the kinds ν and μ. Then, by rewriting the mixed affinity in the right hand side of the second condition above as $\alpha_{\ell_\nu \bar{\ell}_\mu} = \tilde{\alpha}_{\nu\mu} + 1/2(a_\nu j(\ell_\nu) + a_\mu j(\bar{\ell}_\mu))$ we get to

$$\frac{d(\ell_\nu)}{d(\ell_\mu)} = e^{-\tilde{\alpha}_{\nu\mu}} e^{\frac{1}{2}(a_\mu j(\ell_\mu) - a_\nu j(\ell_\nu))}. \tag{5.86}$$

Again, we can use the same arguments as in the general case. Since $d(\ell_\nu) = b_\nu p(\bar{\ell}_\nu|\bar{\ell}_\nu)$ with b_ν a proportionality constant, we now have

$$\frac{p(\bar{\ell}_\nu|\bar{\ell}_\nu)b_\nu}{p(\bar{\ell}_\mu|\bar{\ell}_\mu)b_\mu} = \frac{e^{-U_\nu}}{e^{-U_\mu}} e^{\frac{1}{2}(a_\mu j(\ell_\mu) - a_\nu j(\ell_\nu))}, \tag{5.87}$$

that solved for the ratio b_ν/b_μ is

$$\frac{b_\nu}{b_\mu} = \frac{e^{-U_\nu}}{e^{-U_\mu}} \sqrt{\frac{p(\uparrow_\mu \mid \uparrow_\mu)p(\downarrow_\mu \mid \downarrow_\mu)}{p(\uparrow_\nu \mid \uparrow_\nu)p(\downarrow_\nu \mid \downarrow_\nu)}} \tag{5.88}$$

that gives

$$d(\ell_\nu) \propto e^{-U_\nu} p(\bar{\ell}_\nu|\bar{\ell}_\nu) \prod_{\mu \neq \nu} \left[p(\uparrow_\mu \mid \uparrow_\mu)p(\downarrow_\mu \mid \downarrow_\mu)\right]^{1/2}. \tag{5.89}$$

The inverse of the latter quantity is proportional to the preferred initial state, that with the same manipulations used for the general case reads

$$p^*_{1,\mathrm{cs}}(\ell_\nu) = \frac{e^{\frac{1}{2}a_\nu j(\ell_\nu) + U_\nu}}{2\sum_\mu e^{U_\mu} \cosh(a_\mu/2)}, \tag{5.90}$$

that indeed satisfy all the conditions required for the matrix D.

Before concluding this section we check the validity of both Eq. (5.83) and Eq. (5.90) in the case of a single transition, where the preferred probability was calculate simply by imposing vanishing potential in the FR Eq. (5.16). This is the only case where the two preferred probabilities are the same since in the second there is a single potential U for the single observed kind, that makes sense since there are no mixed currents in the case of a single observable current. Then, the preferred probability reads in this case

$$p_1^*(\ell) = \frac{e^{\frac{1}{2}aj(\ell)}}{e^{\frac{1}{2}a} + e^{-\frac{1}{2}a}} = \frac{p(\ell|\ell)}{p(\uparrow|\uparrow) + p(\downarrow|\downarrow)} \tag{5.91}$$

as it was already calculated in Section 5.4.

Proof of Eq. (5.80)

We prove that

$$E(-\boldsymbol{a})\boldsymbol{p}_1^* = J\boldsymbol{p}_1^* \tag{5.92}$$

for the preferred probabilities Eqs (5.83) and (5.90). In the first case, let $Z_{\rm ncs}$ denote the denominator of Eq. (5.83). Then

$$\begin{aligned}\left[E(-\boldsymbol{a})\boldsymbol{p}_{1,\rm nc}^*\right]_{\ell_\nu} &= \frac{1}{Z_{\rm ncs}}\sum_{\ell'_\mu} e^{-a_\nu j(\ell_\nu)}\delta_{\ell_\nu,\ell'_\mu}e^{\frac{1}{2}a_\nu j(\ell_\nu)} \\ &= \frac{1}{Z_{\rm ncs}}e^{\frac{1}{2}a_\nu j(\bar{\ell}_\nu)} = p_{1,\rm ncs}^*(\bar{\ell}_\nu) = \left[J\boldsymbol{p}_{1,\ \rm ncs}^*\right]_{\ell_\nu}. \end{aligned}\tag{5.93}$$

Letting $Z_{\rm cs}$ the denominator of Eq. (5.90), in the case of complete sets we have that

$$\begin{aligned}\left[E(-\boldsymbol{a})\boldsymbol{p}_{1,\rm cs}^*\right]_{\ell_\nu} &= \frac{1}{Z_{\rm cs}}\sum_{\ell'_\mu} e^{-a_\nu j(\ell_\nu)}\delta_{\ell_\nu,\ell'_\mu}e^{\frac{1}{2}a_\nu j(\ell_\nu)-U_\nu} \\ &= \frac{1}{Z_{\rm cs}}e^{\frac{1}{2}a_\nu j(\bar{\ell}_\nu)-U_\nu} = p_{1,\rm cs}^*(\bar{\ell}_\nu) = \left[J\boldsymbol{p}_{1,\rm cs}^*\right]_{\ell_\nu}. \end{aligned}\tag{5.94}$$

which prove Eq. (5.80) and thus that the preferred probability has the form Eq. (5.79).

5.7.2 Numerical verification of FRs

To give robustness to our results we proceed in proving the FRs for several observable currents Eqs. (5.41) and (5.50) via numerical experiments. Since we proved that the statistics of currents at stopping-n is generated by discrete-time processes in transition space we generate sequences of observable transitions via the function introduced in Appendix A.5.4. Once

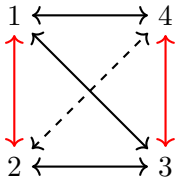

Figure 5.6: The graph used to perform the numerical experiments proving the validity of the FRs Eqs. (5.41) and (5.50). The choice of the rates is $r(1|2) = r(4|1) = 2$, $r(1|3) = r(1|4) = r(2|1) = r(2|3) = r(3|1) = r(3|2) = r(3|4) = r(4|3)$. Moreover, $r(2|4) = 4r(4|2)$ can be manipulated. In particular for $r(2|4) = r(4|2) = 0$ the number of fundamental cycles is reduced.

the sequences of observable transitions are generated, we can proceed to extrapolate the relevant current-like quantities, subject of this thesis.

The FRs are here verified in their integral version. In particular, in the case of non-complete sets of currents, denoting by $\boldsymbol{\xi}$ the joint vector of total currents and mixed currents, and $\boldsymbol{f}$ the vector of the corresponding affinities

$$\langle e^{-\boldsymbol{f}\cdot\boldsymbol{\xi}} \rangle = 1 \tag{5.95}$$

and for complete sets

$$\langle e^{-\boldsymbol{a}\cdot\boldsymbol{c}} \rangle = 1 \tag{5.96}$$

with $\boldsymbol{a}$ the vector of effective affinities conjugated with the total currents, gathered in the vector $\boldsymbol{c}$. To achieve both Eqs (5.95) and (5.96) the dynamics is prepared in their respective preferred initial probabilities, so that the expressions above holds at all n. Another advantage of this is that we are allowed to choose small values of n, and since each observable currents is in this way bounded to assume integer values $c_\nu \in [-n, n]$ the convergence of the Jarzynski estimators Eqs (5.95) and (5.96) is made faster with the use of a reasonable amount of collected data.

The numerical experiment is performed on the setup represented in Fig. 5.6. The graph has three fundamental cycles and the transitions along the edges $\boldsymbol{e}_1 : 1 \to 2$ and $\boldsymbol{e}_2 : 3 \to 4$ respectively (highlighted by red arrows in Fig. 5.6) are assumed to be observable.

Between states 2 and 4 (with dashed lines) we assume set $r(2|4) = 1$ and $r(2|4) = 4r(4|2)$. Moreover we assume that the rate $r(2|4)$ can be manipulated.

In the general case of non-complete sets of currents, the transition space Markov chain is initialized with initial probability Eq. (5.83), and we collect the currents c_1, c_2 and the mixed currents $\{\xi_{\ell_1\ell_2}\}$ after observing $n = 4$ observable transitions. For each realization $\mathcal{L}_n$ we thus evaluate the quantity $\exp(-\boldsymbol{f}\cdot\boldsymbol{\xi})$, which is then averaged over 10^5 independent outcomes. The result is showed in Fig. 5.7, where we plot the evolution of the average Eq. (5.95) as the trajectories in transition space are sampled.

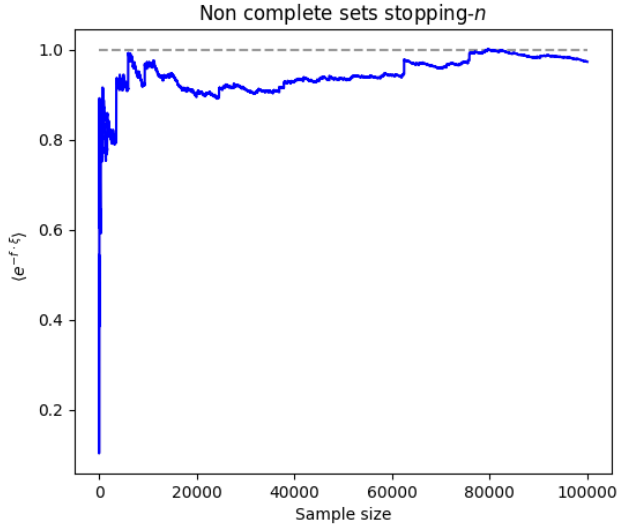

Figure 5.7: Evolution of the estimator for Eq. (5.95) with the increasing size of the sample, for a dynamics in transition space prepared with initial probability Eq. (5.83).

The same experiment is repeated by setting $r(2|4) = 0$, which also makes $r(4|2) = 0$. In this way we are eliminating a fundamental cycle, making the set of observed currents complete. Thus the transition space dynamics is now prepared with initial probability Eq. (5.90). After generating 10^5 independent realizations of $\mathcal{L}_n$, and collecting the currents c_1, c_2 for each $\mathcal{L}_n$, we average the quantities $\exp(-\boldsymbol{a} \cdot \boldsymbol{c})$ to obtain the plot in Fig. 5.8.

Figures 5.7 and 5.8 both converge to 1. However, the noise in the two cases is different, which is explained by noticing that eliminating edges affects the effective affinities and thus the statistics of the currents, while the size of the sample is the same in the two experiments. In particular, for non complete sets, the affinity a_1 conjugated with c_1 has value $a_1 \sim 1.9$, while after eliminating the edge $2 \leftrightarrow 4$ it goes down to $a_1 \sim 0.7$. Therefore, in the first case the rare occurrences $c_1(\mathcal{L}_n) = -n$ affect the average much more than in the second case. The convergence of such estimators is a well known issue, as it will be overviewed in Chapter 7.

5.7.3 Interpreting preferred probabilities

Initial probabilities in transition space are induced from the preparation in state space through the relation Eq. (3.20). However, it is not granted that the preferred initial probabilities, as defined in the previous section, can be obtained by manipulating state space probabilities at initial time $t = 0$, apart from a few limit cases, and there is no correspondance with

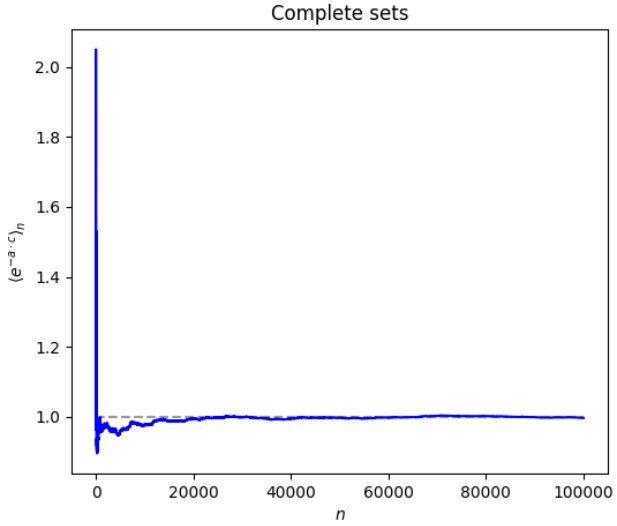

Figure 5.8: Evolution of the estimator for Eq. (5.96) with the increasing size of the sample, for a dynamics in transition space prepared with initial probability Eq. (5.90).

any stationary state in state space. So far, the preferred initial probabilities in transition space Eqs. (5.83) and (5.90) can only be used in numerical simulations since we showed that the trans-transition process at stopping-n can be formulated in terms of a discrete time stochastic process in the space of transitions, providing nothing more than statistical advantages due to the fact that we are allowed to acquire sequences of just a few transitions for the statistics of currents to satisfy a FR. This fact opens a research line around the physical interpretation of such probabilities, which hopefully are related to some physical system with particular properties. A discussion around this issue is reported in Section 6.2 when discussing potential followups of the theory presented in this thesis.

Chapter 6

Followups and other research: Part I

What discussed so far in this thesis represents just a part (the most successful one) of the work done during my PhD, and constitutes about the last two years of research done in the group. At the beginning of the research experience, I was in fact assigned to work with my advisor on a project about thermodynamic efficiency in computation, a work that was left behind by a precedent PhD candidate. The goal of the project was to find the optimal compromise between speed, dissipation and reliability in electronic computation with the use of tools from stochastic thermodynamics. In parallel to this, I spent some months working on a small project about the cost of maintaining temperature gradients in harmonic chains, which was successfully completed with the publication of the article Ref. [35]. The result of the paper can be seen as a self-consistent derivation of Fourier's law of thermal conduction, starting from microscopic models obeying Langevin dynamics, and in particular Ornstein-Uhlenbeck processes, which can be solved analitically, a framework which was not described nor introduced in the present thesis.

In the meantime, our focus shifted and the project was abandoned after a few months. Then I turned on the study of FRs in systems described by a finite number of states, thus entering the realm of continuous-time Markov chains.

In particular, I addressed the problem of sampling useful data for experimental verifications of FRs, which relies on collecting a sufficient (whatever it means) amount of data from rare events falling on the tails of distributions. More precisely, the objective was to provide a consistent statistical analysis on the distribution of the outcomes of entropy production, via the use of statistical estimators which are sensible in distinguishing a statistics which satisfy an out of equilibrium FR, which can be valid for distributions which are not merely Gaussian, which is the expected distribution in close-

to-equilibrium settings or at large times, where in such case it can be seen as a manifestation of the Central Limit Theorem. Objective of the project was also to study the role of the tails of distributions for stochastic quantities as currents and entropy production as outcomes of single realizations of stochastic processes between a finite number of states, when the purpose is to verify FRs from numerical experiments. In fact, the tails of distributions with unbounded spectrum contain very few data compared to the bulk, and consequently ratios of empirical frequencies become very noisy far from those points which correspond to close-to-equilibrium settings, thus making verification of FRs not easily achievable far away from equilibrium. In particular, in stopping-t settings, where the distributions of currents or entropy production have unbounded spectrum, the noise generated by the tails always provide an underestimation of the slope where the points $\log \hat{p}_t(\sigma)/\hat{p}_t(-\sigma)$ lie, with $\sigma := \sigma_{\rm tot}$ the total entropy production, estimated from Gillespie simulations, and $\hat{p}$ its empirical frequency. In the case of Gaussian distributions, it is possible to predict how the points in correspondance of the tails are affected and eventually corrected. The problem of the convergence for the Jarzynski estimator was addressed in this context.

Finally I joined the project about transition space thermodynamics by contributing to the article [31] in particular by performing the numerical simulations and providing the formula connecting total currents and loop currents in transition space, an essential step in the derivation for the single current FR at stopping n. The details of the research are largely addressed in this thesis. From there, the extension of such FRs to the case of multiple observable currents came as a natural followup (summarized in Ref. [82]) together with other research lines that were explored in parallel to this.

The abovementioned followups and previous unpublished research done in the group are gathered in this and the next Chapter, and are treated in a non-rigorous way with the purpose of giving an overview and formulate some open questions. The reason why I choose to first introduce the followups is to not interrupt the flow with the previous chapters. They consist mainly in

1. *Stochastic complementation*: a method to reduce the state space of a stochastic process, introduced to reduce the computational cost in the evaluation of stationary distributions for processes which are described by large transition matrices. I will show that it is strictly related to first-exit-time problems and that it provides an alternative way to derive trans-transition matrices for reduced systems in transition space;

2. *Interpretation of initial probabilities*: an attempt to interpret the preferred initial probabilities that provide exact FR at all n, and in particular to connect such probabilities with a physically meaningful state space probability at time $t = 0$ as for instance the stationary state of

some subgraph obtained by removing some edges, as it is done in the case of stopping-t processes in state space where the preferred state is the stalling probability [32, 56].

After the abovementioned followups, the study of the convergence of estimators used to verify FRs is discussed, in Chapter 7 and in particular we discuss how the stopping-n criterion, which was presented in this thesis, solves the problem only partially.

6.1 Stochastic Complementation

Stochastic Complementation (SC) was initially introduced to compute the stationary probability distribution for Markov chains on a large number of states, and in particular to reduce the computational complexity when dealing with large stochastic matrices [34, 57, 58, 59].

We begin the study by considering processes in state space at discrete time, for which SC was initially introduced, but it can be straightforwardly extended to any process in any space, if the irreducibility condition is granted.

Consider a discrete-time Markov chain in state space with stochastic matrix $\Pi_{x,y} = \pi(x|y)$ with $x, y \in \mathcal{X}$ states, $\pi(x|y)$ the transition probability from state y to state x, and let $q_{\text{st}}(x)$ denote the stationary probability of being in state x, which satisfies

$$q_{\text{st}}(x) = \sum_y \Pi_{x,y} q_{\text{st}}(y). \tag{6.1}$$

The stationary state can be computed directly from the transition matrix Π by computing the normalized eigenvector associated with eigenvalue 1. If the task is easily achievable for processes with a small number of states, the same can't be said when the state space becomes large. In fact, calculation of the stationary distribution of large stochastic processes can be computationally very expensive in terms of time and memory, if one makes use of sequential algorithms. SC was initially introduced to decrease the computational complexity of such calculations, and it is based on computing the stationary distribution of smaller modules of the system independently, allowing parallelization, which are then re-assembled together.

We start from the case of two partitions of the state space, which can be easily extended to any number $m \geq 2$ of partitions.

Let us separate the state space $\mathcal{X}$ into two non-overlapping sub partitions $\mathcal{X}_1$ and $\mathcal{X}_2$ such that now the stochastic matrix can be expressed as

$$\Pi = \begin{pmatrix} \Pi_{\mathcal{X}_1\mathcal{X}_1} & \Pi_{\mathcal{X}_1\mathcal{X}_2} \\ \Pi_{\mathcal{X}_2\mathcal{X}_1} & \Pi_{\mathcal{X}_2\mathcal{X}_2} \end{pmatrix}. \tag{6.2}$$

Given that the full process is at some state $x \in \mathcal{X}_i$ at step k, the submatrix $\Pi_{\mathcal{X}_i\mathcal{X}_i}$ in the diagonal of Π encodes the probability of remaining in

$\mathcal{X}_i$ at the next step $k+1$, while $\Pi_{\mathcal{X}_j\mathcal{X}_i}$, with $j \neq i$, contains the transition probabilities from states $x \in \mathcal{X}_i$ to a state $y \in \mathcal{X}_j$. What we are interested in is an effective process living in one of the partitions $\mathcal{X}_i$, where the *clock*, i.e. a natural number n (notice that we distinguished the step k for the full process generated by Π and the step n for the reduced process given by SC) determining the *step* of the effective process, ticks only when a state $x \in \mathcal{X}_i$ is reached. In the case of two partitions $\mathcal{X}_1$ and $\mathcal{X}_2$ we are interested in the reduced process in $\mathcal{X}_1$. The stochastic complement $\Pi_{\mathcal{X}_1} = \mathrm{SC}_{\mathcal{X}_1}(\Pi)$ of Π respect to $\mathcal{X}_1$ is then defined by

$$\Pi_{\mathcal{X}_1} = \Pi_{\mathcal{X}_1\mathcal{X}_1} + \Pi_{\mathcal{X}_1\mathcal{X}_2}(I - \Pi_{\mathcal{X}_2\mathcal{X}_2})^{-1}\Pi_{\mathcal{X}_2\mathcal{X}_1}. \tag{6.3}$$

And it is proved to be a well defined irreducible stochastic process at discrete-time [34]. Given the probability $\tilde{q}_n(x)$ that the effective process is found in state $x \in \mathcal{X}_1$ at step n, its evolution is then

$$\tilde{q}_{n+1}(x) = \sum_{y\in\mathcal{X}_1} [\Pi_{\mathcal{X}_1}]_{x,y}\, \tilde{q}_n(y). \tag{6.4}$$

Analogously, one can construct the effective process by complementing the full process Π with respect to $\mathcal{X}_2$, thus obtaining another process whose time ticks when states in $\mathcal{X}_2$ are reached. The effective stochastic matrix is in this case given by

$$\Pi_{\mathcal{X}_2} = \Pi_{\mathcal{X}_2\mathcal{X}_2} + \Pi_{\mathcal{X}_2\mathcal{X}_1}(I - \Pi_{\mathcal{X}_1\mathcal{X}_1})^{-1}\Pi_{\mathcal{X}_1\mathcal{X}_2}. \tag{6.5}$$

The fact that the stationary state of the full process can be computed from the stochastic complements defined above is summarized by the following properties:

i. The columns of $\Pi_{\mathcal{X}_i}$ for all partitions $\mathcal{X}_i$ are normalized to unity

$$\sum_x [\Pi_{\mathcal{X}_i}]_{x,y} = 1, \qquad x, y \in \mathcal{X}_i; \tag{6.6}$$

ii. Given $\boldsymbol{q}_{\mathrm{st}}$ the stationary distribution vector of the full uncomplemented process and $\tilde{\boldsymbol{q}}_{\mathrm{st}}$ the stationary distribution for the reduced process obtained by SC respect to a partition $\mathcal{X}_i$, we have

$$\frac{q_{\mathrm{st}}(x)}{q_{\mathrm{st}}(y)} = \frac{\tilde{q}_{\mathrm{st}}(x)}{\tilde{q}_{\mathrm{st}}(y)}, \tag{6.7}$$

with $x, y \in \mathcal{X}_i$ and $x \neq y$;

iii. Successive complementations over different subsets are composable, i.e. given subsets $\mathcal{X}_1$ and $\mathcal{X}_2$ with $\mathcal{X} = \mathcal{X}_1 \cup \mathcal{X}_2$ and $\mathcal{X}_3, \mathcal{X}_4$ such that $\mathcal{X}_3 \cup \mathcal{X}_4 = \mathcal{X}_2$ then

$$\mathrm{SC}_{\mathcal{X}_1}(\Pi) = \mathrm{SC}_{\mathcal{X}_1}(\mathrm{SC}_{\mathcal{X}_1\cup\mathcal{X}_3}(\Pi)). \tag{6.8}$$

The first property Eq. (6.6) says that the stochastic complement defines a discrete time stochastic process on a reduced state space $\mathcal{X}_i \subset \mathcal{X}$ where the time ticks when the system enters any state $x \in \mathcal{X}_i$. The second property Eq. (6.7) says that the ratios between stationary probabilities for pairs of states $x, y \in \mathcal{X}_i$ are the same as the ratio of stationary distributions on the same pair of states for the full process with transition matrix Π. The third property Eq. (6.8) says that fixed a partition, say $\mathcal{X}_1$, and its complementary subspace $\mathcal{X}_2$ it is possible to complement directly on $\mathcal{X}_2$ or first on $\mathcal{X}_3$ (or $\mathcal{X}_4$) then on $\mathcal{X}_4$ ($\mathcal{X}_3$) to obtain the same stochastic matrix. This is an advantage, since complementation requires the computation of inverse matrices: if the partitioning on the complemented space becomes finer, then the computational effort to compute the full complementation decreases. The properties above are the reason why SC can be used to compute stationary distributions for large stochastic matrices [34, 57, 58]. In fact, by property Eq. (6.7) it is possible to derive the stationary distribution of each complement, such that the stationary distribution of the full process can be reconstructed as

$$\boldsymbol{p}_{\text{st}} = (\xi_1 \tilde{\boldsymbol{p}}_1, \xi_2 \tilde{\boldsymbol{p}}_2, \ldots, \xi_m \tilde{\boldsymbol{p}}_m) \tag{6.9}$$

with $\tilde{\boldsymbol{p}}_i$, $i = 1, \ldots, m$, denoting the stationary distribution of the i-th reduced process obtained by complementing respect to partition $\mathcal{X}_i$ and ξ_i the elements of a coupling vector that represents intuitively the probability of being in the subset $\mathcal{X}_i$ respect to the full system, when the state space $\mathcal{X}$ is divided into m partitions. By property Eq. (6.8) instead, a stochastic matrix can be partitioned in arbitrarily small blocks, thus the computation for reconstructing the full stationary distribution can be done in parallel.

6.1.1 Reconstructing the stationary distribution

The stationary probability for the full process can be reconstructed from the stationary state of each complemented subspace in which we partition the original state space. The probability of the full process is obtained from Eq.(6.9) where the coefficients ξ_i are coupling factors that are related to the dynamics between partitions, thus it can be interpreted as the stationary state of a dual process, generated by another stochastic matrix C called coupling matrix. This is defined as

$$C_{\mathcal{X}_i \mathcal{X}_j} = \mathbf{1} \cdot \Pi_{\mathcal{X}_i \mathcal{X}_j} \tilde{\boldsymbol{q}}_{\text{st},i} \tag{6.10}$$

with $\mathcal{X}_i$ denoting the i-th partition of the state space $\mathcal{X}$ and $\tilde{\boldsymbol{q}}_{\text{st},i}$ the stationary distribution of the complemented process respect to the same partition.

Now, the process generated by Eq. (6.10) is a discrete time process that ticks everytime the system transitions between coarse grained macro states, identified by the m partitions $\mathcal{X}_i$, $i = 1, \ldots, m$. The resulting process is markovian since non-markovianity only arises on the time distributions that

now are integrated out of the picture. Its stationary state is then the fraction of time spent by the system in partition $\mathcal{X}_i$, hence the full stationary state can now be reconstructed as Eq. (6.10)

6.1.2 Reduced dynamics on states

Given its properties introduced earlier, the stochastic matrix obtained by SC respect to some partition $\mathcal{X}_i$ in state space, represents an irreducible Markov chain in a reduced set of states. We can imagine that the subset $\mathcal{X}_i$ which is considered collects all states that are somehow accessible to observation. Thus we call the states $x \in \mathcal{X}_i$ observable states, that is, when monitoring the system one is able to distinguish observable states among themselves and when they are first reached after the system visited the complementary partition, whose states are said to be hidden. As discussed above, the time step in the complemented process is updated only when it is hitted regardless the system was already in a set of observable states or the system visited some hidden states before reaching another observable state. The first case is represented by the first term in Eq. (6.3) and the second case by the second one, that represents the probability of having an arbitrarily long sequence of hidden visited states before returning to an observable state. SC can then be interpreted as the solution of a discrete-time analogue of a first-exit time in state space [34]. More precisely, the abovementioned first-exit process is stopped when an observable state is first reached (and thus it is an absorbing state) and the process is initialized to be in the subset of observable transitions at initial time, thus representing a first-return problem.

The reduced process is then obtained by complementing the full process respect to the observable states where the hidden ones are integrated out of the picture. The so obtained process accounts only for the events where the system enters observable states. The discrete-time step for the new process, which ticks only when observable events occur, defines a notion of internal time which depends on the chosen partition and thus on the set of observable states.

The considerations given above hold for all Markov chains generated by stochastic matrices, even in the case where the diagonal elements of the matrix Π defining the full process are positive, which is $\Pi_{x,x} > 0$ for some $x \in \mathcal{X}$. However, in the following we focus on processes with $\Pi_{x,x} = 0$ for all $x \in \mathcal{X}$, which is the case where Π is the embedded Markov chain associated to a continuous time process with generator R. In fact, such processes are updated only when a transition to a different state occur, which is reminescent of the fact that in continuous time processes we invoke the notion of permanence time, which is an exponentially distributed time if the chain is markovian.

Let us consider a partition $\mathcal{X}_i$ in state space which only contains observ-

able states in the sense explained above. Thus, by renaming it $\mathcal{X}_{\rm v} = \mathcal{X}_i$, is the space of observable states, where diagonal terms $[\Pi_{\mathcal{X}_{\rm v}}]_{x,x}$, with $x \in \mathcal{X}_{\rm v}$, may also appear to be positive and represents the events where the system explores hidden states before returning to x, and without entering any other observable state $y \in \mathcal{X}_{\rm v}$. The complementary partition $\mathcal{X}_{\rm h}$ contains the states that are not observable, i.e. the hidden states. If the full process is the embedded chain associated to a continuous time process, however, the reduced chain obtained by SC generates some ambiguities since we assume that we are not able to detect transitions from a state x to itself, a problem that is solved with the introduction of an exponentially distributed permanence time in fully observable continuous-time Markov chains. In fact, the reduced chain will have positive diagonal elements if the observable states are connected to hidden states. This means that when observing the system we are actually not able to access those probabilities, since, given an observable state x, it is not possible to discern whether the system didn't jump or it jumped back to itself after visiting hidden states, since hidden states are not observable by definition. Moreover, a notion of permanence time in the reduced process would result in non-exponentially distributed times.

For this reason, the notion of observable state is sloppy and thus makes SC applied to state space processes not a good candidate to describe partially accessible stochastic systems. The usual approach consists in fact in grouping several micro states with similar properties under the same macro state, and by assuming a separation in the relaxation timescales for the micro states inside each macro state and between each macro state [23, 24]. However, in this thesis we discussed a transition based coarse-graining with which it is possible to give a thermodynamically consistent description of systems where only a few transitions can be observed. In the following section we prove that first-return time problems in transition space is equivalent to SC, as expected. Moreover, the reduced chain obtained by applying SC with respect to observable transitions is equivalent to the coarse-graining scheme largely discussed in this thesis.

6.1.3 SC on observable transitions

We start from the dynamics on the full transition space, introduced in Section 3.2.5, and show that SC in transition space recovers the trans-transition probabilities obtained from first-exit time processes.

As stated by Eq. (3.34), the trans-transition probabilities in the case where all transitions are observable are expressed as

$$p(\ell|\ell') = \begin{cases} \pi(\ell), & \text{if} \quad \mathtt{t}(\ell') = \mathtt{s}(\ell), \\ 0, & \text{otherwise.} \end{cases} \tag{6.11}$$

Notice that all diagonal terms in the trans-transition matrix vanish, as the trans-transition matrix above is obtained directly from the embedded ma-

trix in state space. We now consider the set $\mathcal{O}$ of observable transitions, complementary to a set of hidden transitions $\mathcal{H}$. We are interested in finding the probabilities of observing a succession of observable transitions. The full trans-transition matrix then reads

$$P = \begin{pmatrix} P_{\mathcal{O}\mathcal{O}} & P_{\mathcal{O}\mathcal{H}} \\ P_{\mathcal{H}\mathcal{O}} & P_{\mathcal{H}\mathcal{H}} \end{pmatrix}. \tag{6.12}$$

What we want to get is a reduced dynamics occurring only on the subset of observable transitions $\mathcal{O}$, and thus we calculate the probability of returning to the subset $\mathcal{O}$ after k steps of the full process, conditioned on the first transition at $k = 1$ being in $\mathcal{O}$. We distinguish here two situations:

i. the second transition at time $k = 2$ occurs in $\mathcal{O}$ thus stopping the process, that is, if the first transition is $\ell^{(1)} \in \mathcal{O}$ the second one is also $\ell^{(2)} \in \mathcal{O}$;

ii. the case where the second transition occur in the hidden subset $\mathcal{H}$, i.e. $\ell^{(2)} \in \mathcal{H}$.

In the former case, the probability of two consecutive transitions being in the observable subset $\mathcal{O}$ is contained in the block $P_{\mathcal{O}\mathcal{O}}$. In the following, we use the initial probability $p_1(\ell) = \delta_{\ell\ell_\mathrm{v}}$ with $\ell_\mathrm{v} \in \mathcal{O}$, so that the initial probability vector has null entries in correspondance of hidden transitions, and, for simplicity, $\boldsymbol{p}_1$ now indicates a vector with $2N$ entries with N the number of observable transitions in both directions, i.e. the restriction of the initial vector to the visible subspace. The probability that the second transition, which occur consecutively to the first one, is observable can therefore be written as

$$\boldsymbol{p}_2 = P_{\mathcal{O}\mathcal{O}}\boldsymbol{p}_1, \tag{6.13}$$

$\boldsymbol{p}_2$ also having $2N$ entries.

In the latter case, we consider sequences of transitions in the full space $\mathcal{O} \cup \mathcal{H}$ with $k > 2$ that end up in $\mathcal{O}$. For this case we then calculate the probability of not observing any observable transitions at time k as

$$p_\varnothing(k|\ell^{(1)} \in \mathcal{O}) = \sum_{\ell_\mathrm{h} \in \mathcal{H}} p^{(1)}_{\ell_\mathrm{h}} = \sum_{\ell_\mathrm{h} \in \mathcal{H}} \left[P^{k-2}_{\mathcal{H}\mathcal{H}} P_{\mathcal{H}\mathcal{O}} \boldsymbol{p}_1 \right]_{\ell_\mathrm{h}}, \tag{6.14}$$

since in this case the process performs at least one hidden transition. The probability of observing the second observable transition at time $k + 1$ is then

$$p_\varnothing(k|\ell^{(1)} \in \mathcal{O}) - p_\varnothing(k+1|\ell^{(1)} \in \mathcal{O}) = \sum_{\ell_\mathrm{h} \in \mathcal{H}} \left[(P^{k-2}_{\mathcal{H}\mathcal{H}} - P^{k-1}_{\mathcal{H}\mathcal{H}}) P_{\mathcal{H}\mathcal{O}} \boldsymbol{p}_1 \right]_{\ell_\mathrm{h}}, \tag{6.15}$$

if at previous times the process visited hidden transitions. The equation above can be rewritten as

$$p_{\varnothing}(k|\ell^{(1)} \in \mathcal{O}) - p_{\varnothing}(k+1|\ell^{(1)} \in \mathcal{O}) = \sum_{\ell_{\rm h},\ell'_{\rm h},\ell''_{\rm h} \in \mathcal{H}} \sum_{\ell_{\rm v} \in \mathcal{H}} (I - P_{\mathcal{H}\mathcal{H}})_{\ell_{\rm h}\ell'_{\rm h}} \left[P_{\mathcal{H}\mathcal{H}}^{k-2}\right]_{\ell'_{\rm h}\ell''_{\rm h}} [P_{\mathcal{H}\mathcal{O}}]_{\ell''_{\rm h}\ell_{\rm v}} \boldsymbol{p}_1(\ell_{\rm v}). \quad (6.16)$$

Noticing that $\sum_{\ell_{\rm h}\in\mathcal{H}}(I - P_{\mathcal{H}\mathcal{H}})_{\ell_{\rm h}\ell'_{\rm h}} = \sum_{\ell_{\rm v}\in\mathcal{O}} [P_{\mathcal{O}\mathcal{H}}]_{\ell_{\ell_{\rm v}}\ell'_{\rm h}}$, and by summing over $k \in [2, +\infty)$ we finally obtain

$$\sum_{\ell_{\rm v}\in\mathcal{O}} \left[P_{\mathcal{O}\mathcal{H}} \left(I - P_{\mathcal{H}\mathcal{H}}\right)^{-1} P_{\mathcal{H}\mathcal{O}} \boldsymbol{p}_1\right]_{\ell_{\rm v}} = 1 - \sum_{\ell_{\rm v}\in\mathcal{O}} [P_{\mathcal{O}\mathcal{O}}\boldsymbol{p}_1]_{\ell_{\rm v}} \quad (6.17)$$

where where we used the operator-valued geometrical series $\sum_k [P_{\mathcal{H},\mathcal{H}}]^k = (I - P_{\mathcal{H},\mathcal{H}})^{-1}$, which is well defined because the spectral radius of $P_{\mathcal{H},\mathcal{H}}$ is $\rho(P_{\mathcal{H},\mathcal{H}}) < 1$ (see Section 2.1.4), and used Eq. (6.13) in the right-hand side. By using that the initial probability $\boldsymbol{p}_1$ only accounts for observable transitions, the identity Eq. (6.17) can be seen as the normalization condition on the columns of the stochastic matrix

$$P_{\mathcal{O}} = P_{\mathcal{O}\mathcal{O}} + P_{\mathcal{O}\mathcal{H}} \left(I - P_{\mathcal{H}\mathcal{H}}\right)^{-1} P_{\mathcal{H}\mathcal{O}}, \quad (6.18)$$

that is indeed the stochastic complement on the full transition space matrix with respect to the observable transitions.

6.1.4 Equivalence with trans-transition matrices

The final step is to show that the stochastic matrix Eq. (6.18) is the same as the trans-transition matrix that we used in the previous chapters to study the thermodynamical properties of partially accessible systems that was obtained by arguments based on first-exit time processes at continuous time.

The following proof consists on comparing the SC respect to an observable set of transitions $\ell \in \mathcal{O}$ and the trans-transition matrix with elements Eq. (3.17) introduced in Chapter 3 by expressing the two matrices in terms of path probabilities in state space.

Let us consider the trans-transition matrix elements $[P_{\mathcal{O}}]_{\ell,\ell'}$ expressed by Eq. (6.18). Here, $\ell, \ell' \in \mathcal{O}$ indicate observable transitions, and $\ell_{\rm h}^{(k)}$ the k-th hidden transition in $\mathcal{H}$. Since the non-zero elements in the trans-transition matrix in the full transition space are the state space transition probabilities of the embedded Markov chain, the rightmost term can be interpreted as

$$\left[P_{\mathcal{O}\mathcal{H}} \left(I - P_{\mathcal{H}\mathcal{H}}\right)^{-1} P_{\mathcal{H}\mathcal{O}}\right]_{\ell,\ell'} = p(\ell|\ell_{\rm h}^{(k)}) \left[\sum_{k=1}^{\infty} \sum_{\ell_{\rm h}^{(1)},\cdots,\ell_{\rm h}^{(k)}} p(\ell_{\rm h}^{(k)}|\ell_{\rm h}^{(k-1)}) \cdots p(\ell_{\rm h}^{(1)}|\ell')\right], \quad (6.19)$$

where the sum from $k = 1$ is motivated from the fact that the second term in the right hand side of Eq. (6.18) requires that at least one hidden transition is performed. Since $\pi(\ell) = \pi(\mathtt{t}(\ell)|\mathtt{s}(\ell))$ and by use of Eq. (6.11), the equation above can be re-written in terms of state space paths as

$$\begin{aligned}&\left[P_{\mathcal{OH}}\left(I - P_{\mathcal{HH}}\right)^{-1} P_{\mathcal{HO}}\right]_{\ell,\ell'} \\ &\quad = \pi(\mathtt{t}(\ell)|\mathtt{s}(\ell)) \left[\sum_{k=1}^{\infty} \sum_{\mathtt{t}(\ell_{\mathrm{h}}^{(1)}),\cdots,\mathtt{t}(\ell_{\mathrm{h}}^{(k)})} \pi(\mathtt{t}(\ell_{\mathrm{h}}^{(k)})|\mathtt{t}(\ell_{\mathrm{h}}^{(k-1)})) \cdots \pi(\mathtt{t}(\ell_{\mathrm{h}}^{(1)})|\mathtt{t}(\ell'))\right],\end{aligned} \tag{6.20}$$

where the sum over all possible hidden transitions can be replaced with a sum over their respective target states, and where the target state of the last hidden transition is the source of the observable transition ℓ. Thus the matrix elements of the complemented matrix $P_{\mathcal{O}}$ are given by including the probability of performing two consecutive observable transitions without any hidden transition in between that is obtained by adding $\pi(\mathtt{t}(\ell)|\mathtt{s}(\ell))\delta_{\mathtt{s}(\ell),\mathtt{t}(\ell')}$ to the quantity above, since this is possible only when the target of ℓ' is the source of ℓ.

Let us now consider the trans-transition probabilities which we used throughout this thesis, which can be written as Eq. (3.17) in terms of a survival matrix S. Given the interpretation of S in terms of hidden paths, the trans-transition probabilities can be rewritten in terms of the survival transition matrix Σ for the embedded chain associated with the process, and whose powers are expressed by Eq. (3.23). So now it is clear that from that expression we can isolate the term with $k = 0$, corresponding to no hidden transitions, and sum over $k \in [1, +\infty)$, thus proving that the trans-transition matrix derived as a solution of a first-exit time problems in state space at continuous time is equivalent to the trans-transition matrix obtained by taking the SC in the full transition space respect to the observable transitions, which was discussed in this section.

6.1.5 Hybrid complementation

In the previous sections we provided an interpretation of complemented processes as effective processes where only some of the degrees of freedom can be tracked. In the case of SC in state space, however, it requires the possibility to detect when the system enters an observable state, which is against the standard interpretation of continuous-time Markov chains where it is not possible to distinguish transitions from a certain state to itself, while in the complemented process such self-transition probabilities may appear.

This issue is proven not to be present in the case where SC is performed in transition space, since occurring of observable transitions are associated to

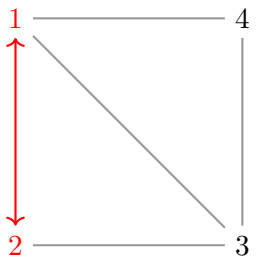

Figure 6.1: A graph where states 1 and 2 and the direct transition in both directions between them is observable. The process in the reduced set of states is given by SC respect to 1 and 2, and it includes the probability to come back to an observable state after visiting hidden states. The observable transition, denoted as the red line, connects the observable states and introduces the possibility to discern whether the transition between states in the effective model is occurring through the direct channel or not.

a measurable quantity which can be directly observed (see Section 4.1). The so obtained process, which we proved in the previous section to be equivalent to the discrete-time chain obtained from first-exit problems which was the subject of this thesis, is well defined from a thermodynamical point of view, since from sequences of transitions we can extract extensive quantities which satisfy FRs.

In this section, we imagine a situation where states can at least be observed when they are first reached after another state, thus ignoring the fact that self-transition appear when taking the SC respect to such observable states. Moreover, we add the possibility to discern whether the transition from the two observable states occur through the direct transition connecting them, which is assumed to be observable. The problem becomes related then to SC which is made both in state space and transition space.

Here, we consider the simplest case where two observable states are connected by an observable transition, and the remaining part of the graph is hidden to observation. As a result, by combining observation of the two observable states and the observable transition, it is possible to derive the transition probability of directly performing the observable transition from its source state, and so its transition rate.

As a reference example, consider the graph represented in Fig. 6.1. The states 1 and 2 are assumed to be observable, i.e. it is possible to track events where 1 and 2 are reached. We thus call $\mathcal{X}_{\mathrm{v}} = \{1, 2\}$ the set of observable states and $\mathcal{X}_{\mathrm{h}}$ the set containing the remaining states which are hidden. Moreover, we consider a transition $\ell = \{\uparrow, \downarrow\}$ occurring in both directions, with $\uparrow$: $2 \to 1$ and $\downarrow$: $1 \to 2$. According to this setting, we can imagine to be able to distinguish when observable states are first reached after another observable state, and this occurs with probabilities $q(x|y)$ obtained by SC

respect to the observable states $x, y = 1, 2$, and thus are the elements of the complemented matrix $\tilde{\Pi}$

$$\tilde{\Pi} = \Pi_{\mathcal{X}_{\rm v},\mathcal{X}_{\rm v}} + \Pi_{\mathcal{X}_{\rm v},\mathcal{X}_{\rm h}}(I - \Pi_{\mathcal{X}_{\rm h},\mathcal{X}_{\rm h}})^{-1}\Pi_{\mathcal{X}_{\rm h},\mathcal{X}_{\rm v}} \tag{6.21}$$

We discussed previously that with standard approaches to the theory of continuous-time Markov chains it is assumed that self transitions $x \to x$ in the effective model can not be observed practically. However, we assume for the moment that this is possible, and at the end we will only need to take into account the complemented probabilities $q(x|y)$ with $x \neq y$, which accounts for the probabilities of going from y to x through the direct transition or hidden paths, which becomes a problem of comparing the stationary probabilities on observable states.

The elements of the trans-transition matrix P are the trans-transition probabilities for the observable transition, which connects the observable states, given by

$$p(\ell|\ell') = \pi(\ell)(I - \Sigma)^{-1}_{\mathtt{s}(\ell)\mathtt{t}(\ell')}, \tag{6.22}$$

with $\pi(\ell) = \pi(\mathtt{t}(\ell)|\mathtt{s}(\ell))$ and Σ the survival matrix for the embedded chain in state space. The first factor $\pi(\ell) = \pi(\mathtt{t}(\ell)|\mathtt{s}(\ell))$ is the probability that given the system is in state $\mathtt{s}(\ell)$ the next state will be $\mathtt{t}(\ell)$ through the direct channel connecting the two states. The second one is interpreted from Eq. (3.23) and it is not necessarily smaller than one. In fact, this is not a probability, but the sum of all probabilities of paths starting from $\mathtt{t}(\ell')$ and ending in $\mathtt{s}(\ell)$ through all the channels containing only hidden transitions regardless of their lenghts. The fact that the system, after hitting the observable states $\mathtt{s}(\ell)$ or $\mathtt{t}(\ell')$ can return in the hidden part of the graph allows the process hitting the same states once again. This is then not interpretable as a first-hitting problem. If we wish to connect complementation on states and on transitions we have to start from this consideration.

Any path of this kind has probability

$$q(1|1)^{\alpha_1}\bar{q}(1|2)^{\alpha_2}\bar{q}(2|1)^{\alpha_3}q(2|2)^{\alpha_4}, \tag{6.23}$$

with $\bar{q}$ denoting probabilities on the hidden paths obtained from the stochastic complemented analogue q by

$$\bar{q}(1|2) = q(1|2) - \pi(1|2), \tag{6.24}$$

and α_1, α_4 the number of times $1 \to 1$ and $2 \to 2$ occurs respectively in the complemented process before performing an observable transition, and α_2, α_3 the number of times $2 \to 1$ and $1 \to 2$ respectively via hidden transitions. The abovementioned exponents are not independent on each other, as it will be clear later.

The term $(I-\Sigma)^{-1}_{\mathtt{s}(\ell),\mathtt{t}(\ell')}$ can be written as

$$\left[(I-\Sigma)^{-1}\right]_{\mathtt{s}(\ell)\mathtt{t}(\ell')} = \sum_{\{\alpha_i\}} C^{\mathtt{s}(\ell)\mathtt{t}(\ell')}(\{\alpha_i\}) q(1|1)^{\alpha_1} \bar{q}(1|2)^{\alpha_2} \bar{q}(2|1)^{\alpha_3} q(2|2)^{\alpha_4} \tag{6.25}$$

with some combinatorial factor $C^{\mathtt{s}(\ell,)\mathtt{t}(\ell')}(\{\alpha_i\})$ depending on the involved initial and final state. Also, fixing the endpoints $\mathtt{s}(\ell), \mathtt{t}(\ell)$ gives relationships between the exponent α_2 and α_3. Consider for instance the diagonal element $\left[(I-\Sigma)^{-1}\right]_{1,1}$. This is the sum over all the path probabilities of cyclic trajectories $1 \to \Gamma_h \to 1$ with Γ_h a trajectory which does not occur in the observable part of the system. For this reason, everytime the system goes from 1 to 2 through hidden paths, the trajectories from 1 to 1 must contain the sequence $2 \to 1$ through hidden channels as well. Then, we set $\alpha = \alpha_2 = \alpha_3$. Analogously, the elements $\left[(I-\Sigma)^{-1}\right]_{2,1}$ require that $1 \to 2$ through the hidden channel must happen at least once. Whereas the opposite hidden sequence of non observable transitions from 2 to 1 occurs, another $1 \to 2$ must happen. Then in this case $\alpha_3 = \alpha_2 - 1$.

Consider $\left[(I-\Sigma)^{-1}\right]_{1,1}$ and let $\alpha_1 = \beta_1, \alpha_4 = \beta_2, \alpha_2 = \alpha_3 = \alpha$. At this point, finding the correct combinatorial factors $C^{\mathtt{s}(\ell),\mathtt{t}(\ell')}(\{\alpha_i\})$ appearing in Eq. (6.25) becomes equivalent to the problem of disposing β_1 indistinguishable particles in $\alpha+1$ states and β_2 particles in α states in an independent way. Then, the explicit writing of $(I-\Sigma)^{-1}_{1,1}$ with Eq. (6.25) becomes for $\alpha \neq 0$

$$\left[(I-\Sigma)^{-1}\right]_{1,1} = \sum_{\alpha,\beta_1\beta_2} \binom{\beta_1+\alpha}{\beta_1} \binom{\beta_2+\alpha-1}{\beta_2} q(1|1)^{\beta_1} q(2|2)^{\beta_2} \left[\bar{q}(1|2)\bar{q}(2|1)\right]^{\alpha} \tag{6.26}$$

When $\alpha = 0$ then also $\beta_2 = 0$ and β_1 can freely take all the values between zero to infinity:

$$\sum_{\beta_1=0}^{\infty} p(1|1)^{\beta_1} = \frac{1}{1-p(1|1)} \tag{6.27}$$

Together with the other contributions one can show that

$$[(I-\Sigma)]^{-1}_{1,1} = \frac{1}{1-q(1|1)} + \sum_{\alpha=1}^{\infty}\sum_{\beta_1\beta_2}\binom{\beta_1+\alpha}{\beta_1}\binom{\beta_2+\alpha-1}{\beta_2} q(1|1)^{\beta_1} q(2|2)^{\beta_2} [\bar{q}(1|2)\bar{q}(2|1)]^{\alpha} \tag{6.28}$$

$$= \sum_{\alpha=0}^{\infty} [\bar{q}(1|2)\bar{q}(2|1)]^{\alpha} \frac{1}{(1-q(2|2))^{\alpha}} \frac{1}{(1-q(1|1))^{\alpha+1}} \tag{6.29}$$

$$= \frac{1}{q(2|1)} \sum_{\alpha=0}^{\infty} \left[\frac{\bar{q}(2|1)}{q(2|1)} \frac{\bar{q}(1|2)}{q(1|2)}\right]^{\alpha} \tag{6.30}$$

$$= \frac{1}{q(2|1)} \frac{1}{1-\frac{\bar{q}(2|1)}{q(2|1)}\frac{\bar{q}(1|2)}{q(1|2)}}. \tag{6.31}$$

From Eq. (6.28) to Eq. (6.29) we used the Stirling's polynomials

$$\binom{\beta_1+\alpha}{\beta_1}\binom{\beta_2+\alpha-1}{\beta_2} = \frac{(\beta_1+\alpha)!}{\beta_1!\alpha!}\frac{(\beta_2+\alpha-1)!}{\beta_2!(\alpha-1)!} \tag{6.32}$$

$$= \frac{1}{\alpha!(\alpha-1)!}\prod_{k=1}^{\alpha}(\beta_1+k)\prod_{j=1}^{\alpha-1}(\beta_2+j) \tag{6.33}$$

Then, the trans-transition probability $p(\downarrow \mid \uparrow) = \pi(2|1)\left[(I-\Sigma)^{-1}\right]_{1,1}$ can be written as

$$p(\downarrow \mid \uparrow) = \frac{\pi_{21}\bar{q}(1|2) + \pi_{12}\pi_{21}}{\pi_{21}\bar{q}(1|2) + \pi_{12}\bar{q}(2|1) + \pi_{12}\pi_{21}} \tag{6.34}$$

with $\pi_{xy} = \pi(x|y)$ in short for the probabilities that the transition $y \to x$, $y \neq x$, occurs through the direct observable channel. By normalization of probabilities we have that

$$p(\uparrow \mid \uparrow) = \frac{\pi_{12}\bar{q}(2|1)}{\pi_{21}\bar{q}(1|2) + \pi_{12}\bar{q}(2|1) + \pi_{12}\pi_{21}} \tag{6.35}$$

Finally, $p(\uparrow \mid \downarrow)$ and $p(\downarrow \mid \downarrow)$ are obtained by symmetry from the previous two. Since the probabilities $\bar{q}(x|y)$ are the probabilities of reaching x from y through the hidden channel, we can decompose the trans-transition probabilities in terms of the elementary diagrams

$\pi_{12}\bar{q}(2|1) =$ 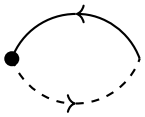 $\pi_{21}\bar{q}(1|2) =$ 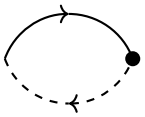 $\pi_{12}\pi_{21} =$ 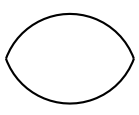 (6.36)

here we intend the full lines as observable transitions and the dashed lines as the hidden transitions, with the dot denoting the starting point of the loop, state 1 being at the left and state 2 at the right.

The trans-transition probabilities are then, after normalization

$p(\uparrow \mid \uparrow) =$ 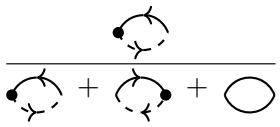 $p(\uparrow \mid \downarrow) =$ 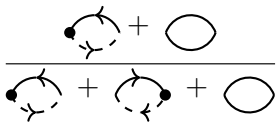 (6.37)

$p(\downarrow \mid \uparrow) =$ 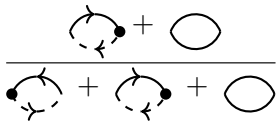 $p(\downarrow \mid \downarrow) =$ 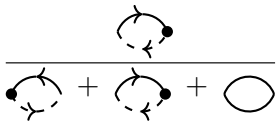 (6.38)

We notice that all the trans-transition probabilities are built by combining the trans-transition probabilities $p(\uparrow \mid \uparrow)$, $p(\downarrow \mid \downarrow)$ and the leftover

$\gamma =$ 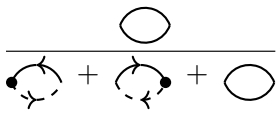 (6.39)

Then we notice $0 < \gamma = p(\uparrow \mid \downarrow) - p(\uparrow \mid \uparrow) = p(\downarrow \mid \uparrow) - p(\downarrow \mid \downarrow)$ because of the positivity of the probabilities π_{12} and π_{21}. Also $\gamma = -\det P$. By manipulating the explicit expression of the trans-transition probabilities in terms of the elements $q(x|y)$, $x, y = 1, 2$ of the stochastic complement in state space, one finds

$$\pi_{12} = \frac{\gamma\, q(1|2)}{p(\downarrow \mid \uparrow)} \qquad \pi_{21} = \frac{\gamma\, q(2|1)}{p(\uparrow \mid \downarrow)} \tag{6.40}$$

Assume that it is possible to distinguish the two states 1 and 2 and we are able to track when states 1 or 2 are first reached after one another. Then the direct transition probabilities from the original full system can be estimated. This is true also for the continuous time case. By taking the left expression in Eq. (6.40)

$$r_2\pi_{12} = r(1|2) = \frac{\gamma\, r_2 q(1|2)}{p(\downarrow \mid \uparrow)} = \frac{\gamma\, \tilde{R}_{1,2}}{p(\downarrow \mid \uparrow)} \tag{6.41}$$

where $\tilde{R}_{12}$ is the SC of the continuous time generator R of the full process in state space

$$\tilde{R} = R_{\mathcal{X}_\mathrm{v},\mathcal{X}_\mathrm{v}} - R_{\mathcal{X}_\mathrm{v},\mathcal{X}_\mathrm{h}} (R_{\mathcal{X}_\mathrm{h},\mathcal{X}_\mathrm{h}})^{-1} R_{\mathcal{X}_\mathrm{h},\mathcal{X}_\mathrm{v}}. \tag{6.42}$$

Thus, a combined observation of observable states and the transition which connects them, allows exact estimation of the transition probabilties via Eq. (6.40) and the transition rates by use of Eq. (6.41) via estimation of the effective rates of jumping between observable transitions regardless this is happening via the direct channel or not.

6.2 Interpretation of initial probabilities

The preferred probabilities in transition space $\boldsymbol{p}_1^*$, as discussed in Section 5.7.1, provide transient FRs for a reduced set of observable currents at stopping-n. When we can access a a subset of transitions, occurring in both directions, we track the total currents $\{c_\nu\}$ and the mixed currents $\{\xi_{\ell_\nu \ell_\mu}\}$ so that the following the exact FR holds

$$\log \frac{p_n(\{c_\nu\}, \{\xi_{\ell_\nu \ell_\mu})}{p_n(\{-c_\nu\}, \{-\xi_{\ell_\nu \ell_\mu})} = \sum_\nu a_\nu c_\nu + \sum_{\substack{(\ell_\nu, \ell_\mu) \\ \mu > \nu}} \alpha_{\ell_\nu \ell_\mu} \xi_{\ell_\nu \ell_\mu}, \tag{6.43}$$

with vanishing boundary term, $\{a_\nu\}$ and $\{\alpha_{\ell_\nu \ell_\mu}\}$ denoting the affinities conjugated with the total currents and the mixed currents respectively.

The preferred probability in this case is expressed as

$$p^*_{1,\mathrm{nc}}(\ell_\nu) = \frac{\exp\left(\frac{1}{2} a_\nu j(\ell_\nu)\right)}{2 \sum_\mu \cosh\left(\frac{a_\nu}{2}\right)}. \tag{6.44}$$

Complete sets of currents, instead, satisfy the FR Eq. (5.50) with equality according to the preferred distribution

$$p^*_{1,\mathrm{c}}(\ell_\nu) = \frac{e^{\frac{1}{2} a_\nu j(\ell_\nu) + U_\nu}}{2 \sum_\mu e^{U_\mu} \cosh\left(\frac{a_\nu}{2}\right)}, \tag{6.45}$$

with a potential U_ν associated with the kind ν, when only the statistics of the total currents $\{c_\nu\}$ is taken into account.

A generic initial probability $\boldsymbol{p}_1$ in transition space is in relation with the initial probability $\boldsymbol{q}_0$ at time $t = 0$ in state space via the relation Eq. (3.20), which we recall for convenience:

$$p_1(\ell) = -r(\ell) \sum_x \left[S^{-1}\right]_{s(\ell), x} q_0(x). \tag{6.46}$$

We are interested in finding a state space probability $\boldsymbol{q}_0^*$ at initial time $t = 0$ which provides the preferred $\boldsymbol{p}_1^*$ in transition space by use of the relation above. In the following we discuss some arguments to disprove the stalling probability [32, 55, 56] as a candidate to represent the preparation at initial time in state space such that the first observable transition occurs with the preferred probability Eq. (6.44) for non complete sets and Eq. (6.45) for complete sets, in some very specific situations.

6.2.1 Single observable transition

We first consider the case of a single observable transition in both directions $\ell = \uparrow, \downarrow$, where Eq. (6.44) is expressed as

$$p_1^*(\ell) = \frac{p(\ell|\ell)}{p(\uparrow \mid \uparrow) + p(\downarrow \mid \downarrow)}. \tag{6.47}$$

Since the observable transition ℓ connects only a pair of states $\mathtt{s}(\ell)$ and $\mathtt{t}(\ell)$ referred as source and target states of ℓ, then we can find easily a distribution $\boldsymbol{q}_0$ which provides Eq. (6.46) by just imposing that $q_0(x) = 0$ for all $x \neq \mathtt{s}(\ell), \mathtt{t}(\ell)$, thus finding that

$$q_0^*(\mathtt{s}(\ell)) = p_1^*(\bar{\ell}). \tag{6.48}$$

However, preparing the system in such a way requires full access to all states of the full system in order to manipulate their occupations. It is preferrable, in fact, to prepare the system at some stationary probability on the same state space where only the observable transition rates are manipulated, analogously to the case of systems where a complete set of currents is observable. In fact, such currents will satisfy the fluctuation relation Eq. (2.73) at stopping-t with vanishing boundary term if the system is prepared in the so-called stalling state which consists on the stationary state of the same system where the observable rates are set to zero [32]. Therefore we look for a similar way to prepare the system to obtain the preferred probabilities in state space Eq. (6.44).

Eq. (6.48) provides that for single observable transitions in the two directions $\uparrow$ and $\downarrow$ the preferred probability can be obtained from the following relation

$$\boldsymbol{p}_1^* = P^{\leftrightarrow}\boldsymbol{p}_1^*, \tag{6.49}$$

that is, the preferred probability is the stationary probability for the Markov chain with trans-transition matrix $P^{\leftrightarrow} = PJ$, obtained from the trans-transition matrix P by swapping their columns, with J denoting the swapping matrix defined in Section 3.4.1 that reads in the case of a single observable transition in both directions

$$J = \begin{pmatrix} 0 & 1 \\ 1 & 0 \end{pmatrix}. \tag{6.50}$$

Consider now the same process expressed as a discrete time process in the full transition space where the trans-transition probabilities are given in this case by Eq. (3.34). The reduced process, with trans-transition matrix P, is then obtained by use of SC, explained in the previous section, with respect to the observable transitions $\uparrow$ and $\downarrow$. We can imagine that the matrix $P^{\leftrightarrow} = PJ$ is also obtained though SC of another process whose stationary state hopefully provides the preferred probability $\boldsymbol{p}_1^*$ which gives a FR for currents evaluated at all number n of observed transitions. In fact, letting $\mathcal{O} = \{\uparrow, \downarrow\}$ denoting the set of observable transitions and $\mathcal{H}$ the complementary set of hidden transitions

$$P^{\leftrightarrow} = PJ = P_{\mathcal{O}\mathcal{O}}J + P_{\mathcal{O}\mathcal{H}}(I - P_{\mathcal{H}\mathcal{H}})^{-1}P_{\mathcal{H}\mathcal{O}}J, \tag{6.51}$$

saying that $P^{\leftrightarrow}$ is obtained by complementing the full process in transition space where the columns labeling the observable transition in the two directions are swapped, which is also associated to a process in state space where

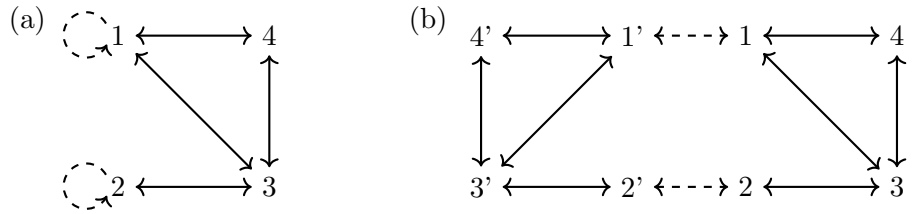

Figure 6.2: (a) The process in state space that corresponds to the process in transition space where the columns corresponding to the observable transition (that connects states 1 and 2) are swapped is a process where the observable transitions are redirected to the source states for a single observable transition. (b) The same process can be seen as another equivalent process between the original process and a mirrored process with states $x' \in \mathcal{X}$ connected by the observable transitions. The stationary probability of being in x is then given by summing the probabilities of being in x and x' in the new process.

the observable transitions ℓ are redirected to its source state $\ell : \mathtt{s}(\ell) \to \mathtt{s}(\ell)$, as in Figure 6.2(a).

The stationary state of the so obtained process in state space is in fact the stalling state [32, 56] of the original process where the observable edge is removed, both in the case of non-complete and complete sets of currents. This can be seen in the simple case of a single observable transition in both directions as in the following. With reference to Fig. 6.2(a), we can imagine the self transition $1 \to 1$ as a transition to a fictitious state $1 \to 1'$ with rate $r(2|1)$ followed by an instantaneous transition $1' \to 1$ with rate λ for which we take the limit $\lambda \to \infty$ later, and similarly for state 2. Let us define the matrices

$$\Lambda = \begin{pmatrix} \lambda & 0 \\ 0 & \lambda \end{pmatrix} \qquad V = \begin{pmatrix} r(2|1) & 0 \\ 0 & r(1|2) \end{pmatrix}, \tag{6.52}$$

and we divide the survival matrix S for the original first-exit time problem in blocks as

$$S = \begin{pmatrix} S_{vv} & S_{vh} \\ S_{hv} & S_{hh} \end{pmatrix}. \tag{6.53}$$

Given the generator of the stalling process R^{stal} where the observable edge is removed, we have that [55, 56]

$$S_{vv} + V = R^{\mathrm{stal}}_{vv}, \tag{6.54}$$

and $S_{vh} = R^{\mathrm{stal}}_{vh}$, $S_{hv} = R^{\mathrm{stal}}_{hv}$, $S_{hh} = R^{\mathrm{stal}}_{hh}$. The generator of the modified process is then

$$\tilde{R} = \begin{pmatrix} -\Lambda & V & O \\ \Lambda & S_{vv} & S_{vh} \\ O & S_{hv} & S_{hh} \end{pmatrix}, \tag{6.55}$$

with O the null matrix, and its stationary state is obtained from $\tilde{R}\tilde{\boldsymbol{q}} = 0$. By defining the vectors $\tilde{\boldsymbol{q}}_\lambda^\top = (\tilde{q}_{1'}, \tilde{q}_{2'})$, $\tilde{\boldsymbol{q}}_v^\top = (\tilde{q}_1, \tilde{q}_2)$ and $\tilde{\boldsymbol{q}}_h^\top = (\tilde{q}_3, \tilde{q}_4)$, the stationary state is the solution of the following system of equations

$$\begin{cases} -\Lambda\tilde{\boldsymbol{q}}_\lambda + V\tilde{\boldsymbol{q}}_v = \boldsymbol{0} \\ \Lambda\tilde{\boldsymbol{q}}_\lambda + S_{vv}\tilde{\boldsymbol{q}}_v + S_{vh}\tilde{\boldsymbol{q}}_h = \boldsymbol{0} \\ S_{hv}\tilde{\boldsymbol{q}}_v + S_{hh}\tilde{\boldsymbol{q}}_h = \boldsymbol{0}. \end{cases} \tag{6.56}$$

By inserting the first equation in Eq. (6.56) inside the second, and using Eq. (6.54), we get to

$$\begin{cases} R_{vv}^{\mathrm{stal}}\tilde{\boldsymbol{q}}_v + R_{vh}^{\mathrm{stal}}\tilde{\boldsymbol{q}}_h = \boldsymbol{0} \\ R_{hv}^{\mathrm{stal}}\tilde{\boldsymbol{q}}_v + R_{hh}^{\mathrm{stal}}\tilde{\boldsymbol{q}}_h = \boldsymbol{0} \\ \tilde{\boldsymbol{q}}_\lambda = \Lambda^{-1}V\tilde{\boldsymbol{q}}_v. \end{cases} \tag{6.57}$$

Since the last equation gives $\tilde{\boldsymbol{q}}_\lambda = \boldsymbol{0}$ when taking the limit $\lambda \to \infty$, then

$$\begin{pmatrix} \tilde{\boldsymbol{q}}_v \\ \tilde{\boldsymbol{q}}_h \end{pmatrix} = \boldsymbol{q}^{\mathrm{stal}}, \tag{6.58}$$

such that $R^{\mathrm{stal}}\boldsymbol{q}^{\mathrm{stal}} = \boldsymbol{0}$, thus the stationary state of the process where observable transitions are redirected to their source state is the stalling state associated with the full process, obtained from the original process by eliminating observable edges.

However it can be checked numerically that such initial probability in state space does not correspond to the initial probability that provides the preferred probability in transition space when plugged inside Eq. (6.46), thus we must exclude the stalling probability as a candidate to provide exact transient fluctuation relations at stopping-n for processes in the observable transition space. In the next subsection we extend this to the case of an arbitrary number of observable transitions.

6.2.2 Multiple observable transitions

As done in the case of a single observable transition we check that a system prepared at the stalling state at time $t = 0$ does not provide the preferred initial probability in the case of an arbitrary number of observable transitions in both directions.

Let $\boldsymbol{q}^{\mathrm{stal}}$ be the stationary probability vector of the full system described in state space where the observable edges $\boldsymbol{e}_\nu$ are removed, also known as stalling state [32, 55, 56]. The effective affinities $\{a_\nu\}$ can be expressed in terms of stalling probabilities as [55, 56]

$$f_\nu = \ln \frac{r(\uparrow_\nu) q^{\mathrm{stal}}(\mathtt{s}(\uparrow_\nu))}{r(\downarrow_\nu) q^{\mathrm{stal}}(\mathtt{t}(\downarrow_\nu))}. \tag{6.59}$$

When a complete set of currents is observed, and if all $x \in X$ are source states for an observable transition we can check on explicit examples that the probability ratio of the first transition being $\uparrow_\nu$ against $\downarrow_\nu$ is, when the system is prepared at the stalling state $\boldsymbol{q}^{\rm stal}$

$$\frac{p_1(\uparrow_\nu)}{p_1(\downarrow_\nu)} = \frac{r(\uparrow_\nu)}{r(\downarrow_\nu)} \frac{q^{\rm stal}(\mathtt{s}(\uparrow_\nu)}{q^{\rm stal}(\mathtt{s}(\downarrow_\nu))} \frac{\sum_\ell S^{-1}_{\mathtt{s}(\ell),\mathtt{s}(\uparrow_\nu)}}{\sum_\ell S^{-1}_{\mathtt{s}(\ell),\mathtt{s}(\downarrow_\nu)}}. \tag{6.60}$$

For preferred probabilities, the following relation holds

$$\frac{p_1^*(\ell)}{p_1^*(\bar{\ell})} = e^{a_\nu j(\ell_\nu)}, \tag{6.61}$$

when both non-complete and complete sets are observed, which is only achieved by Eq. (6.60) when $p(\ell|\ell') = 1/2N$ and $r(\uparrow_\nu) = r(\downarrow_\nu)\ \forall\ \nu$. Hence, for complete sets the initial distribution at initial time of the full process in state space which provides the FR with vanishing potential is not the stalling state.

These arguments are supported by numerical evidence. In particular, in the specific case where the number of observable transitions in both directions equals the number of states and the sources of observable transitions spans the full state space of the system, relation Eq. (6.46) connects initial probabilities in state space with initial probabilities in transition space via an invertible relation. With reference to Fig. 6.3, certain choices of positive orientation for the observable transitions allow definition of a matrix

$$V = \begin{pmatrix} -r(2|1) & 0 & 0 & 0 \\ 0 & -r(1|2) & 0 & 0 \\ 0 & 0 & -r(4|3) & 0 \\ 0 & 0 & 0 & r(3|4) \end{pmatrix} \tag{6.62}$$

such that Eq. (6.46) can be inverted as

$$\boldsymbol{q}_0^* = SV^{-1}\boldsymbol{p}_1^* \tag{6.63}$$

with $\boldsymbol{p}_1^*$ the preferred probability in transition space, which for this specific example is given by Eq. (6.45) which for the choice of rates in the model in Fig. 6.3 reads

$$\boldsymbol{q}_0^* = \begin{pmatrix} 0.232558 \\ 0.0930233 \\ 0.0232558 \\ 0.651163 \end{pmatrix}, \tag{6.64}$$

whereas the stalling probability for the same process is

$$\boldsymbol{q}^{\rm stal} = \begin{pmatrix} 0.25 \\ 0.125 \\ 0.125 \\ 0.5 \end{pmatrix}. \tag{6.65}$$

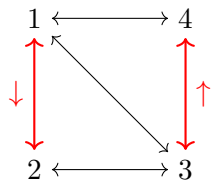

Figure 6.3: A graph with two observable transitions (in red) where positive orientations are indicated by the arrows next to the observable edges. The assigned transition rates are $r(1|2) = 4$, $r(2|1) = 5$, $r(3|4) = 3$, $r(1|3) = r(4|1) = 2$, $r(1|4) = r(2|3) = r(3|1) = r(3|2) = r(4|3) = 1$.

With the same arguments we can check that it is the case also for the case of non-complete sets of currents, obtained by adding the edge connecting states 2 and 4.

This section, dedicated to the preferred initial probability $\boldsymbol{p}_1^*$, gathered the attempts made in trying to give them an interpretation by finding initial states in state space that are the stationary state of some process obtained by manipulating the original one. This a very important point, since

1. This would provide an operational way of preparing the system for the currents to satisfy exact fluctuation relations at stopping-n without the need to post select realizations so that less experiments can be ran to gather enough data for the estimated log.ratio of forward to backward probabilities, or the Jarzynski estimator, to converge to a FR;

2. Gathering of short trajectories is convenient for such convergence since, being the spectrum of possible outcomes for the currents being bounded at stopping-n, the rarest outcomes in the tails are observed a reasonable amount of times, thus making a fluctuation relation easier to observe both in its detailed version and in the form of a Jarzynski equality, notoriously provided of poor convergence properties.

A physically meaningful interpretation must exist, since by looking at the preferred initial probability, especially in the case of complete sets of currents, the numerators in Eq. (5.90) shows exponentials of quantities that can be interpreted as a kinetic term (given by the cycle affinities) and a potential term associated to the transition types. However, little progress has been made in this direction.

As a final comment, the importance of interpreting preferred probabilities is connected to another open research direction present in this thesis, as in the following Section. 7.1 we address the problem of the convergence of estimators related with fluctuation relations and in particular how the tails of distributions always lead to an underestimation of the slope where the points lie when estimating the entropy production of single realization of Markov chains out of equilibrium.

Chapter 7

Followups and other research: Part II

As anticipated in the introduction of the previous Chapter, we discuss here the importance of statistical estimators in verifying FRs and in particular how some issues such as the poor convergence of averaged exponentiated quantities and the incidence of noise in the tails of distributions are contextualized in the present Thesis.

7.1 The problem of sampling

Experimental verification of fluctuation relations for discrete state space Markov chains, central object of this thesis, requires observation of a large number of single realizations of such processes all prepared in the same initial state. The fluctuation relations discussed in this work concern mainly observation of currents, as their product with the affinities provides the contribution to the total entropy production that comes from the coupling with reservoirs, which dominates at large times.

In this section we discuss an attempt of providing a consistent verification of fluctuation relations by investigating the statistical properties of the estimators involved in its formulation, i.e. the log-ratio of probabilities for the detailed version and the mean value of the exponential of entropy production estimators in the case of integral fluctuation relations, also known as Jarzynski equality.

In the first case, we consider the exact fluctuation relation Eq. (2.57) for the total entropy production $\sigma := \sigma_{\mathrm{tot}}$ evaluated at stopping time t according by an external clock, and given a realization of a process its entropy production is estimated by considering the extensive contribution from the currents along edges and the bounded contribution given by the state space probabilities at initial and final times, that are sampled from the stationary

distribution. Then

$$\log \frac{p_t(\sigma)}{p_t(-\sigma)} = \sigma. \tag{7.1}$$

The entropy outcomes are then collected into an histogram with bin size chosen arbitrarily, obtaining an empirical probability density $\hat{p}_t(\sigma)$ which approximates the real distribution $p_t(\sigma)$ for the total entropy production σ. The empirical distribution $\hat{p}_t(-\sigma)$ is obtained by symmetry with respect to the axis defined by $\sigma = 0$, thus we can evaluate the log-ratio by considering the bin-by-bin ratio of $\hat{p}_t(\sigma)$ and $\hat{p}_t(-\sigma)$. The fluctuation relation Eq. (7.1) is then verified if the so-obtained points lie on the line with unitary slope. We show here that the unboundedness of the spectrum of total entropy production outcomes at stopping-t always provides an underestimation of such slope, thus making such fluctuation relation harder to verify because of systematic effects which depend both on the sample size and the bin width chosen to represent the probability distributions $p_t(\sigma)$ and $p_t(-\sigma)$.

Moreover, we address an important point about distinguishing the central limit theorem from fluctuation relations, by providing a statistical test to discern whether distributions of probabilities satisfying fluctuation relations are Gaussian or not.

Jarzynski equalities on the other hand are notoriously endowed poor convergence properties, since exponentiation of entropy production estimators, which can assume both positive and negative values in single realizations of a process, need a sufficient number of typical negative outcomes to ensure

$$\langle e^{-\sigma} \rangle = 1, \tag{7.2}$$

that requires a huge amount of sample data. In the case where the total entropy σ is distributed as a Gaussian, for instance, the function $e^{-\sigma}$ follows a log-normal distribution, whose cumulants scale as

$$\kappa_j \overset{\text{leading}}{\sim} \left(\frac{e^{\bar{\sigma} j}}{N_{\text{sample}}} \right)^{j-1}, \tag{7.3}$$

with $\bar{\sigma}$ denoting the average entropy production. Since the numerator of the j-th cumulant scales exponentially as j^2, its denominator as N_{sample}^j, and since $\bar{\sigma}$ is positive, an increasingly number of data is required to grant each cumulant with $j > 2$ to vanish so that the central limit theorem can be applied. Moreover, the unboundedness of the outcome space of the entropy production kicks the average Eq. (7.2) above 1 whenever a very rare event with negative entropy production occurs, thus the size of the sample has to be increased with no warranty that another even more rare event will occur in later measurements.

7.1.1 Systematic deviation at the tails

As previously mentioned, the verification of a detailed FR for the total entropy production requires approximating the probability density $p(\sigma)$ by

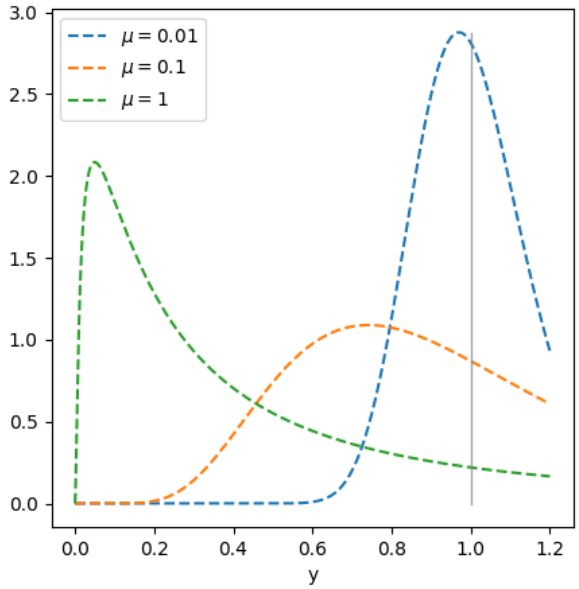

Figure 7.1: Log-normal distributions obtained from Gaussians with average μ. If the entropy production σ is distributed as a Gaussian, $y = \exp -\sigma$ is distributed according to such distributions with $\mu = \bar{\sigma}$. The mean value of the log-normal distribution is highlighted with the vertical line at $y = 1$.

choosing an arbitrary (yet meaningful) bin size, so that the ratio $\hat{p}_t(\sigma)/\hat{p}_t(-\sigma)$ can be evaluated for each bin, required that the binnings for the forward and backward empirical densities are the same. However, the poor acquisition of data in the tails of distributions lead to effects affecting negatively the evaluation of the slope of the line where the points $\log \hat{p}_t(\sigma)/\hat{p}_t(-\sigma)$ should lie. In Fig. 7.2 we see in fact that in processes prepared at stationarity where the total entropy production is evaluated with Eq. (2.47), the slope of the fitting line is underestimated with respect to the expected unitary slope.

This is due to effects emerging from the poor statistics at the tail of distributions. Let $p_t(\sigma)$ denote the true probability density for the total entropy production σ, and assume we observe a very rare event falling into the bin σ^* in a sample with N_{sample} elements. If σ^* has only one element, the empirical density in that range is $\hat{p}(\sigma^*) = (\Delta\sigma N_{\text{sample}})^{-1}$, with $\Delta\sigma$ denoting the bin width. Let us consider outcomes falling inside σ^* such that $\int_{\sigma^*} p_t(\sigma)d\sigma < 1/N_{\text{sample}}$, which is, the area contained below the curve $p_t(\sigma)$ in the interval σ^* is smaller than the area below the bin σ^*, which is $1/N_{\text{sample}}$.

If now σ^* is in the left tail of the density $\hat{p}_t(\sigma)$, assuming that the time reversed empirical density in the same bin is approximating the real density $p_t(-\sigma)$ with a small relative error, then the fact above leads to an overestimation of the point $\log \hat{p}_t(\sigma^*)/\hat{p}_t(-\sigma^*)$. By symmetry, the points at the right tail of $\hat{p}_t(\sigma)$ are underestimated. Thus, the global effect is that by performing a linear regression on data one will find a line whose slope is underestimated, since the points at the correspondance of the tails of the probability density are tilting the fitting curve clockwise.

For such reason, we attempt answering the following questions:

- Is it possible to predict how much the points far away from the origin are deviated due to the abovementioned effect?
- How to determine at which threshold we have to exclude data from the analysis to avoid the effect given by the poor statistics at the tails?

For the first question we consider an artificial case where we directly generate Gaussian data. If this effect emerges for Gaussian data with parameters chosen so that a FR is satisfied then we can exclude that such effects are a property of distributions not satisfyng FRs. Moreover, since in this case we can write analitically the probability density, we are able to predict how the points are affected by the noise at the tails.

7.1.2 Gaussian case

We consider the simplest case of data generated according to a Gaussian distribution with mean $\bar{\sigma}$ and variance $2\bar{\sigma}$

$$p_t(\sigma) = \frac{1}{2\sqrt{\pi\bar{\sigma}}} e^{-\frac{(\sigma-\bar{\sigma})^2}{4\bar{\sigma}}}. \tag{7.4}$$

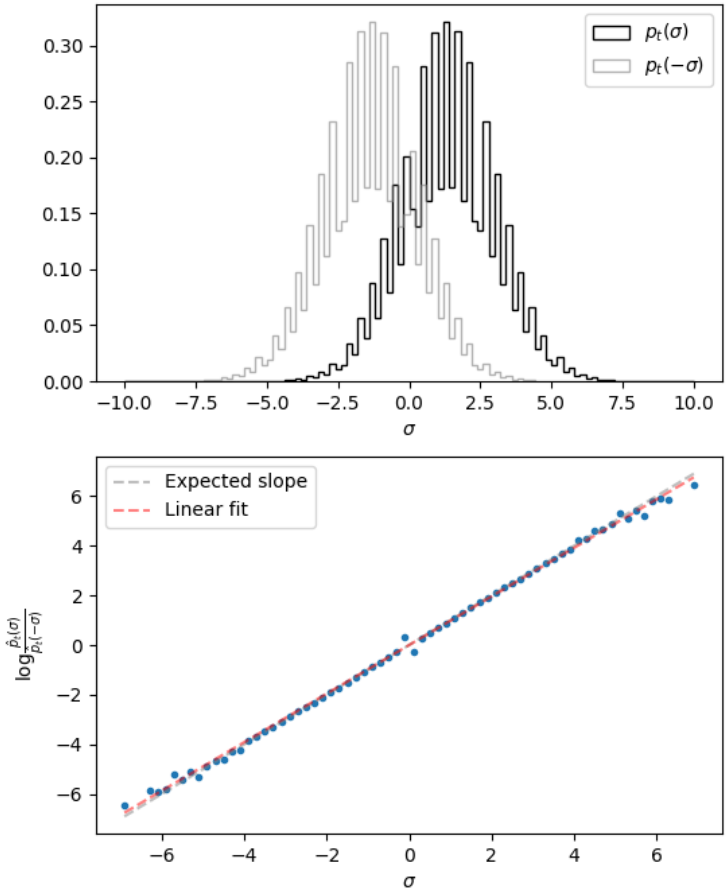

Figure 7.2: Top panel: distribution of the total entropy production in a Markov chain up to time t (black) and its analogue for the time-reversed process (light grey). Bottom panel: bin-by-bin log ratio of the forward to backward probabilities. The estimated slope (red line) is slightly underestimated with respect to the expected slope (light grey line)

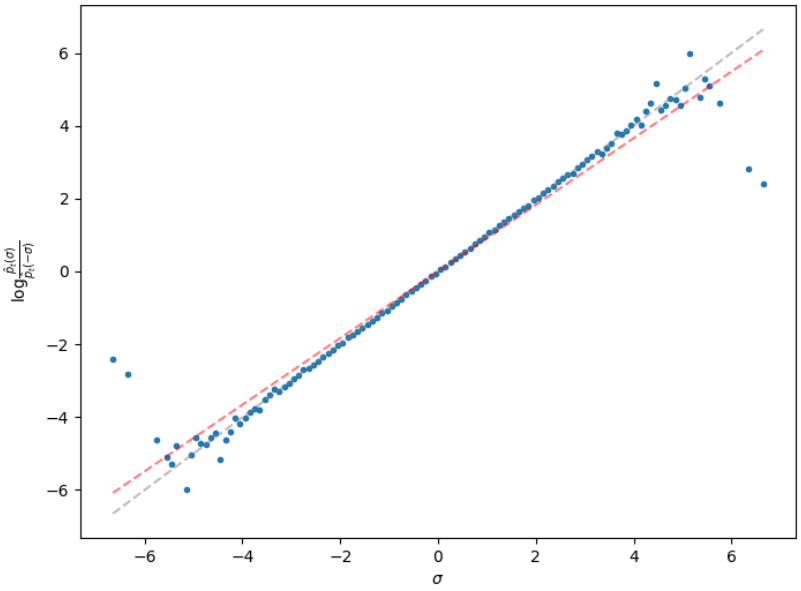

Figure 7.3: An example obtained by generating data from Gaussian distributions with average $\bar{\sigma} = 1$ and variance $2\bar{\sigma}$. Despite the fact that the points closer to $\sigma = 0$ are lying on the line with unitary slope (gray dashed line), the fitting line (red dashed line) is tilted clockwise, as a manifestation of the poor statistics at the tails of distributions.

Such a distribution, in fact, always satisfy a FR if $\bar{\sigma}$ grows linearly in time, as it can be verified explicitly.

We now consider randomly generated data according to the Gaussian distribution Eq. (7.4). As it can be seen in Fig. 7.3 most of the points lie on the line with unitary slope, since the distribution above satisfies the FR Eq. (7.1). Since in this case we know the probability density, it is possible to give a rough quantification of such effect. This is done with the following empirical argument. With reference to Fig. 7.4, all the rarest outcomes of the total entropy production of forward realizations will be roughly uniformly distributed with height $1/(N_{\text{sample}}\Delta\sigma)$, with $\Delta\sigma$ the bin size, since the bins at the tails will very likely contain at most one single outcome. The distribution corresponding to the time-reversed outcomes, obtained by symmetry, are better approximating the Gaussian distribution Eq. (7.4). This is also true for events which are slightly less rare than the ones previously considered, and they will be uniformly distributed with height $2/(N_{\text{sample}}\Delta\sigma)$. In general, we can repeat the argument as far as there are groups of bins which are uniformly distributed with height $k/(N_{\text{sample}}\Delta\sigma)$, with k a natural

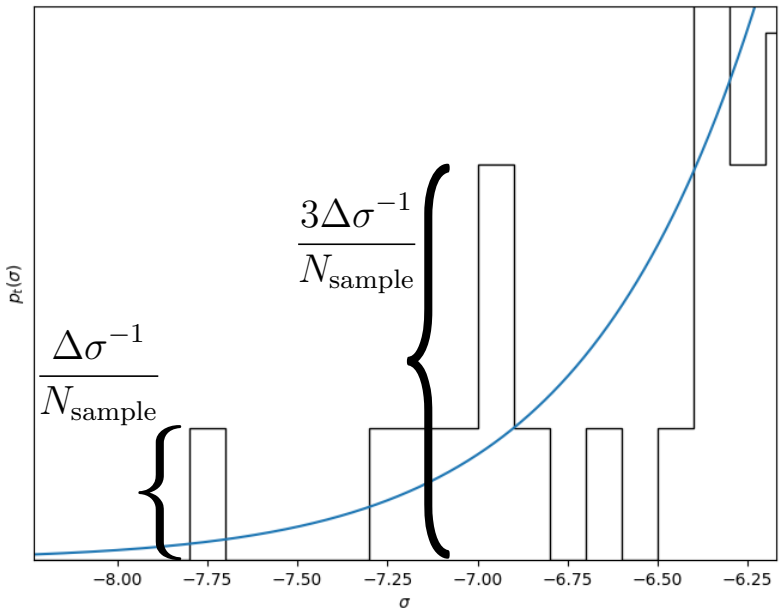

Figure 7.4: Zoom on the left tail of a Gaussian distribution. The height of the bins in the tails is $k/(N_{\text{sample}}\Delta\sigma)$ with k the amount of data falling inside the bin, with size $\Delta\sigma$. In the tails of distributions it is then very common to have bins with just a few data separated by empty bins. The overall effect is that flat regions in the histogram are created.

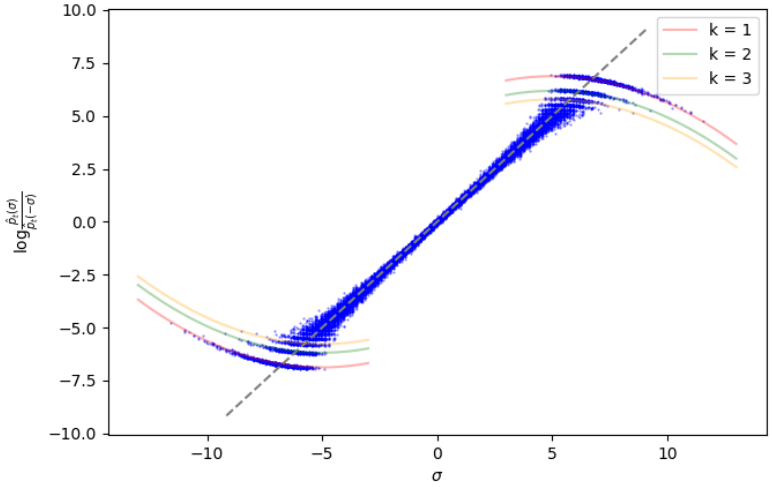

Figure 7.5: By taking 100 sets of experiments, each containing 10^8 randomly generated Gaussian data, we see that the ratios $\log \hat{p}(\sigma)/\hat{p}(-\sigma)$ in correspondance to the tails of distributions are deviated by an amount given by Eq. (7.5) (left curves) and Eq. (7.6) (right curves) for different values of k.

number. Thus, for bins satisfying such properties, we can predict that the points $\log \hat{p}_t(\sigma)/\hat{p}_t(-\sigma)$ corresponding to rare negative events will lie around the curves defined by

$$f^{\mathrm{FWD}}(\sigma, N_{\mathrm{sample}}, k) = \log \frac{\frac{k}{N_{\mathrm{sample}}}}{\Delta\sigma \, p_t(-\sigma)}, \tag{7.5}$$

$p_t(\sigma)$ indicating the Gaussian distribution. To check numerically the expression above, we collect 100 sets of Gaussian randomly generated data, of which we then plot the bin-by-bin ratio of the corresponding forward and backward empirical distributions. The result is showed in Fig. 7.5, where we superponed the curves Eqs. (7.5) and (7.6) (see next Subsection) for $k = 1, 2, 3$, proving the argument above to be meaningful since we can easily identify groups of points lying exactly on the abovementioned curves. This suggests that in the Gaussian case the points at the tails can be corrected since they can be shifted of a quantity determined by Eq. (7.5). This is subject of the next Subsection Sec. 7.1.3.

What obtained here for the simple case of Gaussian distributions may be extended to any probability density whose tails decay exponentially to zero at their boundaries. One possible way is to estimate the true probability distributions by finding a polynomial curve to fit the groups of point at different k and then apply the arguments above.

7.1.3 Correcting data

The fact that we can identify groups of points distributed around the curves Eq. (7.5) in the case of Gaussian distributions allows the correction of the systematic effect explained in the previous subsection. Let us consider a single set of experiments with N_{sample} outcomes for σ obtained as $y(\sigma) = \log \hat{p}_t(\sigma)/\hat{p}_t(-\sigma)$. Since the expression Eq. (7.5) is applied to the tails of the forward distributions, by symmetry we say that the points corresponding to the tails of the backward distributions are obtained as

$$f^{\text{BWD}}(-\sigma, N_{\text{sample}}, k, \Delta\sigma) = -\log \frac{\frac{k}{N_{\text{sample}}}}{\Delta\sigma\, p_t(\sigma)}. \tag{7.6}$$

If the probability density is known, the points lying on the line with the same k, denoted as $y_k(\sigma)$ can be shifted by applying the transformation

$$\begin{cases} y'_k(\sigma) = y_k(\sigma) + \sigma - f^{\text{FWD}}(\sigma, N_{\text{sample}}, k, \Delta\sigma) & \text{forward outcomes} \\ y'_k(\sigma) = y_k(\sigma) + \sigma - f^{\text{BWD}}(-\sigma, N_{\text{sample}}, k, \Delta\sigma) & \text{backward outcomes,} \end{cases} \tag{7.7}$$

with σ being the value of the entropy production evaluated at the mid-point of each bin.

For instance, consider the numerical experiment in Fig. 7.6 (top panel). We identify the points corresponding to the tail of the forward and backward distributions with the same k by using the following algorithm (in Python 3)

```
levels = np.arange(1,1000,1)  # the first 1000 values of k

for j in levels:
    indlistfwd = []
    indlistbwd = []
    for k in range(len(fwdlist)):
        if fwdlist[k] == j:
            indlistfwd.append(k)
    for k in range(len(bwdlist)):
        if bwdlist[k] == j:
            indlistbwd.append(k)
    for k in indlistfwd:
        y[k] += - np.log(j*c/(nsample*gauss(-np.array(xlist)[k]
                                            ,mu,var))) + xlist[k]
    for k in indlistbwd:
        y[k] += - np.log((nsample*gauss(np.array(xlist)[k],mu,
                                        var))/(j*c)) + xlist[k]
```

With the use of this algorithm, the outcomes $y(\sigma)$ are shifted, while maintaining the statistical noise around the curves $f(\sigma, N_{\text{sample}}, k)$ in this case for $k = 1, \ldots, 1000$. As a result, the systematic effect of the tails is completely eliminated as it can be seen in the bottom panel of Fig. 7.6.

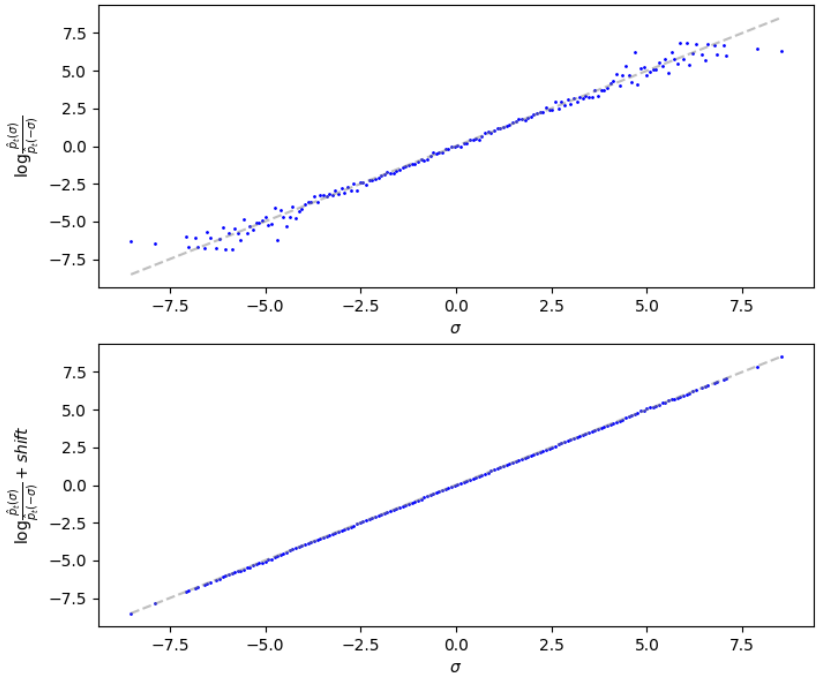

Figure 7.6: (*top panel*) From 10^5 random Gaussian data, we plot the log-ratio $\log \hat{p}_t(\sigma)/\hat{p}_t(-\sigma)$. The systematic effect at the tails discussed in Sec. 7.1.2 results in a deviation of the points from the expected slope. (*bottom panel*) The same data can be corrected by use of Eqs. (7.5) and (7.6) with the procedure explained in Sec. 7.1.3

7.1.4 Testing regions

The behavior of probability distributions at their tails affects the statistics with systematic effects, as explained in the previous Sections. Since the points closer to the origin $\sigma = 0$ are better approximating the line with unitary slope, which is expected for probability densities satisfying a FR, we can imagine to apply statistical tests to verify, for instance, a certain probability function.

This is important, since to state that we are observing a FR out of equilibrium we should also exclude the possibility that the data satisfies Gaussian distributions, a signature of the linear regime and of the central limit theorem. Including all the points obtained by taking the bin-by-bin log-ratio of forward and backward empirical probabilities, will result on tilting the estimated slope that the points follow in a way such that any statistical test on Gaussianity (for instance χ-squared tests and Kolmogorov-Smirnov's test) will lead to rejecting the Gaussian hypothesis, even in the case where data are Gaussian.

Let us define a threshold σ^{th} such that statistical tests are performed by considering only the points in the interval $[-\sigma^{\text{th}}, \sigma^{\text{th}}]$. We seek the optimal threshold which maximizes the amount of useful data, while also allowing an unbiased estimation of the slope and testing probability densities consistently. For this purpose, we employ the fact that as the tails of distributions are approached the number of empty bins increases. For instance, by taking several (100) sets of independent experiments, each with N_{sample} outcomes, we can plot the density $\rho(\hat{p}_t(\sigma))$ of non-zero bins (see Fig. 7.7) in forward realizations of the process. The corresponding density $\rho(\hat{p}_t(-\sigma))$ for the time-reversed process is obtained by symmetry respect to $\sigma = 0$. We observe that there is a region in each of those densities where no holes are present at all, and that there exist an interval in which the both forward and backward densities have no empty bins.

This interval defines a region where the points $\log \hat{p}_t(\sigma)/\hat{p}_t(-\sigma)$ are likely very close to the unitary slope and the effects due to the poor statistics at the tails of distributions can be neglected.

However, little progress has been done in this direction so far.

7.1.5 Convergence of Jarzynski equality

The last point addressed in this thesis is about the convergence of the Jarzynski estimator

$$\langle e^{-\sigma} \rangle_t = 1 \tag{7.8}$$

for the total entropy production σ. The equation above can be specialized as

$$\langle e^{-\boldsymbol{a}\cdot\boldsymbol{c}} \rangle_t = 1, \tag{7.9}$$

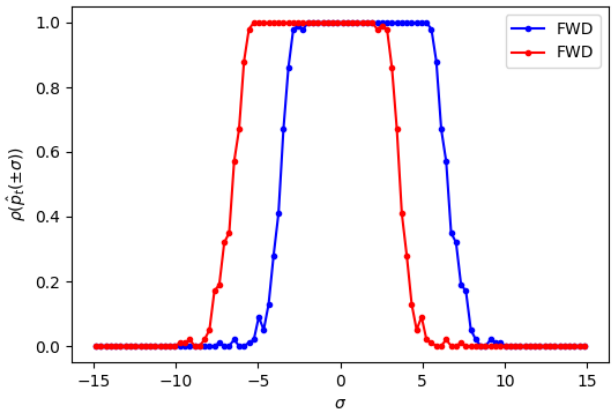

Figure 7.7: Density $\rho(\hat{p}_t(\pm\sigma))$ of non-empty bins for the forward empirical probability density $\hat{p}_t(\sigma)$ (in blue) and for the backward density $\hat{p}_t(-\sigma)$. The overlap of the flat intervals around $\rho \sim 1$ defines a region where the systematic effect due to the tails, explained in Sec. 7.1.1 can be neglected.

with $\boldsymbol{a}$ a vector of cycle affinities and $\boldsymbol{c}$ a vector of currents. The relation Eq. (7.9) holds with equality for total currents $\boldsymbol{c}$ if the set of currents is complete, in the sense explained in Sec. 2.5.1 and if the system is prepared at the stalling state [32, 55, 56]. If the latter condition is not fulfilled, the relation is still satisfied at large t, since $\boldsymbol{a}\cdot\boldsymbol{c}$ represents the cycle contribution to the total entropy production (see Sec. 2.5.1).

As anticipated at the beginning of this section, such an estimator is endowed poor convergence properties, because stochastic quantities such as entropy production and currents can only assume values in $(-\infty, +\infty)$ when evaluated up to a certain external time t. The issue is that distributions satisfying integral FRs rely on rare events which dominate the convergence of the Jarzynski estimator [60, 61], and this is reflected in the fact that the size of the sample becomes extremely large in order to reach the convergence with a reasonable error [62].

We can consider for instance an experiment where m outcomes of currents are collected from realizations of a Markov chain. To visualize the convergence of the estimator Eq. (7.9) we can plot the average value of $e^{-\boldsymbol{a}\cdot\boldsymbol{c}}$ every time a new outcome is obtained, up to m samples. An example is showed in Fig. 7.8, where the system is prepared at the stalling state, and evolves up to a time t. Here we consider only a single current c for simplicity. In fact, despite the fact that single currents in multicyclic graphs do not in general satisfy FRs, they satisfy other relations in terms of very specific auxilary dynamics [55, 56], which can be integrated away to recover the usual Jarzynski equality $\langle \exp -ac \rangle = 1$ for a single current c with effec-

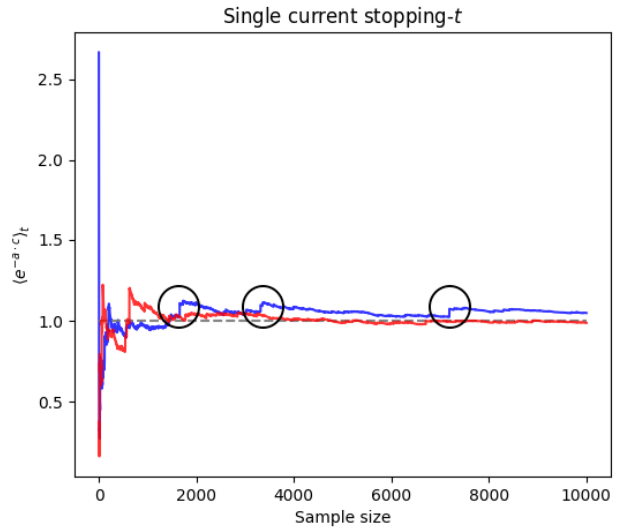

Figure 7.8: Verification of the integral FR for a single observable current evaluated at stopping-t for two different sets of data with the same number of samples. The experiment highlighted in red seems to converge very well to the expected value (horizontal dashed line). The experiment in blue, instead, deviates from the expected value because of the frequent occurrence of very rare events, highlighted by circles for visualization.

tive affinity a. Despite the convergence seems to be granted in many cases (here $m = 10^4$), there might be cases where a very rare event, say $c^* < 0$ (in the case where the affinity is positive), which occurs as the m^*-th outcome, pushes the average evaluated at $m^* - 1$ by a quantity e^{-ac^*}/m^* with a the effective affinity conjugated with c, as it is highlighted in Fig. 7.8 with circles. The blue and red lines, in fact, represent the evolution of the average with the size of the sample m for two different samples, and despite the fact that they are close to each other, the occurrence of a rare event makes the average deviate from the expected result.

The fact that the outcome space of c is unbounded when evaluated at stopping-t can result in a very large deviation from the expected average, since it is always possible to encounter a rare current outcome with opposite sign respect to its affinity which is more rare than any other encountered outcome. Everytime this occurs, the experimenter has to increase the size of the sample. However, in later measurements included in the averaged exponential, one may encounter an even rarer event which pushes the average further away.

This problematic is partially solved by changing stopping criterion, from stopping-t to stopping-n. The fact that the experiment is stopped after the

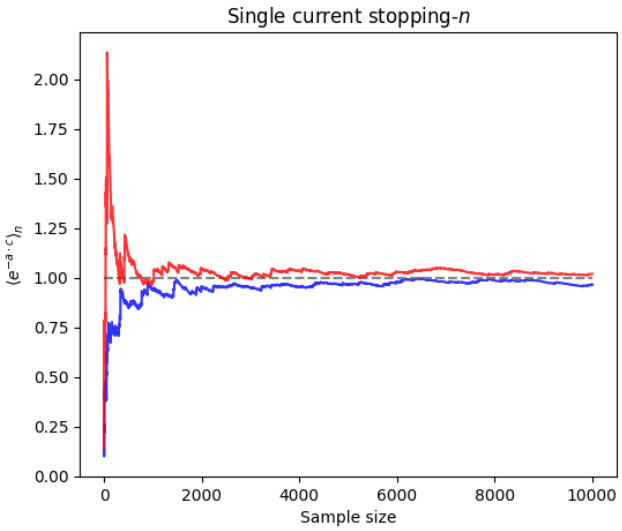

Figure 7.9: Verification of the integral FR for a single observable currents for the same setup as in the experiment represented in Fig. 7.8 but for a single observable current evaluated at stopping-n.

occurrence of a fixed number of observable transitions results in the boundedness of the outcome space of the currents. More precisely, let $c_{\min} = \min c$. For a single transition, if c is evaluated up to n observable transitions then we have that $c_{\min} = -n$. Thus, the rarest negative event $c_{\min}$ shifts the average Eq. (7.9) by at most e^{an}/m^* if it is the m^*-th outcome. As a result, the Jarzynski equality for currents evaluated at stopping-n is expected to have better convergence properties compared to the case of currents evaluated up to an external clock-time t.

The numerical experiment on a single observable current can then be repeated for the same parameters by changing the stopping criterion. Two outcomes are showed in Fig. 7.9. Despite the fact that we expect a better convergence when switching stopping criterion, however, it is evident that the noise is still very large, and the convergence very slow. In fact, the stopping-n criterion only bounds the deviation from the average when a rare event is encountered. The slow convergence does not only emerge from the unboundedness of the outcome space for the currents, but it is an intrinsic issue of averaged exponential quantities. Therefore, further work has to be done in this direction.

Chapter 8

Conclusions

In this thesis, I have addressed important points regarding the possibility of constructing a consistent thermodynamics in systems where only few observables are accessible to an experimenter. This is indeed a very common situation when dealing with microscopic systems, where most of the parameters describing the dynamics are unknown. Here we focused exclusively in the case of systems which can be described by the theory of Markov chains. In particular, we discussed different coarse-graining procedures and the problematics which arise for each of them. State space based coarse-grainings need, in fact, some assumption on the system in order to recover a markovian description, which is a requisite for the statistics of observables to satisfy fluctuation relations, strictly related with a consistent definition of the entropy production and close-to-equilibrium properties of stochastic systems.

The work done introduces new ways of treating such situations, by the introduction of a new approach based on coarse-graining transitions, and a different paradigm according to which observations are carried, everything being based on both mathematical proofs and numerical verifications. Such approach does in fact solve some issues emerging when adopting different procedures involving reduction of the state space, which typically introduce non-markovianity when no separation in the time scales is assumed, apart from very few situations. The reason is the elimination of the inter-transition times from the description, which encodes the emerging non-markovianity when the hidden part of the system contains irreversible cycles. This is done by carrying observations up to a fixed number of events, identified with the occurrence of observable transitions.

In such framework we first derived a general fluctuation relation which holds for an arbitrary number of observable currents currents, up to the number of fundamental cycles contributing to the environmental entropy production. These relations can then be specialized to recover already known results, to give consistency and robustness to our advancements. In partic-

ular, when the number of observable currents equals the number of fundamental cycles, constituting a complete set, the FR for currents Ref. [33] for cycle currents and cycle affinities emerges, where the external time variable is replaced by the total number of occurrences of visible transitions. Importantly, for all FRs is possible to find an initial probability in transition space such that the relation holds exactly at all times without the need of tracking the statistics of the occurrences at the boundaries of sequences of observable transitions.

For non-complete sets we derived exact relations which hold when from sequences of observable transitions we can extract the contribution from mixed currents, defined from sequences of transitions along different observable edges, which complement the statistics of the observable total currents and account for the correlations between them. A limit case is that of a single observable transition, where there are no mixed currents and whose associated current was known to satisfy other relations, similar to FRs, but under very specific auxiliary dynamics where the hidden part of the system is time-reversed [55, 56].

This constitutes a major advancement in the theory of coarse-grained systems, since such results are achieved without the need of performing any approximations, and under the validity of few assumptions such as irreducibility, hidden irreducibility and the distinguishability of observable transitions.

The validity of the relations derived here have important consequences. First, a set of currents whose statistics satisfy a FR automatically satisfy a fluctuation-dissipation theorem [19], thus making our theory thermodynamically consistent. The ensemble entropy production associated to such class of reduced processes is also a well defined quantity. Commenting on this, in a recent paper [29] the entropy production rate for few observable currents was proved to be splitted in a term accounting for the inter-transition times and a term accounting for sequences of transitions. The latter term was proven to lower bound the entropy production rate of a process in the case of a single observable transition. The contribution in this thesis extends this concept to an arbitrary set of observable transitions, where the exponents of FRs represents a stricter lower bound for the entropy production rate when averaged over many realizations of a process.

The description in terms of occurrences of transitions ultimately represents a natural framework where thermodynamics is established. The first result for single currents [31] was also used in the context of extremal value statistics, a particular case of first exit problems, where the interpretation of exponents of FRs in terms of martingales provides estimation of the entropy production [63] and estimation of the the affinities far from equilibrium [64].

This theory also offered perspectives for future research. In particular, an interpretation for the preferred initial probabilities in transition space, which make the FRs derived in this thesis exact at all n, is still lacking.

While for the stopping-t case there exist a physical analogue of such special initial configuration in state space, known as stalling state (despite this is true only for complete sets of currents), no physical analogue was found for the preferred probabilities in transition space, and since this would help to find operational procedures to prepare systems such that the statistics of the observable currents satisfy exact FRs, it merits further investigation.

The coarse-graining technique adopted in this work can also be identified with stochastic complementation in the space of transitions. In fact, stochastic complementation can be interpreted as a first return problem in the space in which it is applied. However, when applied in state space it provides a reduced dynamics which can not be observed in practice; the complemented states are in fact interpreted as observable states, which imply the presence of hidden states. Being able to distinguish when an observable state returns to itself after visiting the hidden part of the graph without touching any other observable state automatically implies that we are able to distinguish when the system is in some hidden state, which automatically makes it distinguishable from visible states thus creating a paradox. Even in the case where hidden states can be grouped in an unique "blurred" hidden macro-state, it is still impossible to determine whether a transition between visible states occurs through the direct channel or after visiting hidden states, unless some separation of timescales is assumed on the system. The same issue does not emerge when complementation is performed in transition space, because of the fact that observable transitions are associated to physical quantities that can be measured in the instant they occur and represent directly the exchanges with the environment.

Another consequence of the stopping-n paradigm regards the convergence of statistical estimators related to fluctuation relations, which was introduced in the last part of this thesis in a qualitative way. The improved convergence is due essentially to the fact that the outcome space of all stochastic quantities which can be extracted from the system is bounded, as a consequence of the fact that a finite number of occurrences of observable transitions are observed.

The theory presented here applies to systems which are described by successions of states punctuated by transitions. A possible interesting extension of our theory may consist in studying systems which are described in terms of populations rather than states, as for instance electronic circuits [25] and chemical reaction networks [37, 65] which can be treated in similar

ways [66] and for which a consistent thermodynamics can be established.

Acknowledgements

This thesis was made possible thanks to the guidance and support of my advisor, Dr. Matteo Polettini, who provided the fundamental ideas at the core of this work, suggested me to look at the relation between reduced processes in transition-space and stochastic complementation and provided the first version of the code in Appendix. I acknowledge my colleague, Pedro Harunari, for sharing ideas and giving valuable suggestions, which helped defining the central results in this thesis. Thanks to Prof. Massimiliano Esposito for the opportunity to work in his group, and thanks to all colleagues, current and former, with whom I shared these years at the Complex System and Statistical Mechanics unit at the University of Luxembourg.

The research was supported by the National Research Fund Luxembourg (project CORE ThermoComp C17/MS/11696700) and by the European Research Council (project NanoThermo ERC-2015-CoG Agreement No. 6815456).

Appendix A

Code used in simulations

To inspect and illustrate numerically the results in this thesis we performed numerical simulations based on the Gillespie algorithm. Our code is implemented in Python and relies on the definition of several functions and classes which are contained in the Python file `storymodel.py`, wich is imported as a module in the scripts which were used to run the simulations. The foundations of this file were provided by Matteo Polettini, and I extended its usage to the situations encountered in this thesis.

A.1 Basic functions

Before introducing the main functions which are used to simulate Markov chains and to extract the relevant measurable quantities from each single realization, we give here some important basic functions. First, we include some basic Python packages:

```
from random import uniform
from math import log, exp, sqrt
import numpy as np
import sympy
```

which contain functions and methods which are used by the functions we define.

A.1.1 Predefined rate matrix (unitary rates)

```
rates0 = [[1 for x in state] for y in state]
for x in state:
    rates0[x][x] = 0
```

Notice that in rate matrices we put equal to zero all the diagonal elements. The exit rates are in fact calculated aside.

A.1.2 Random rate matrix (from unitary distribution)

```
def randrates(dim): # generates a random rate matrix
    randrates = []
    for k in range(dim):
        size = np.random.random(dim)
        randrates.append(size.tolist())
    for  k in range(dim):
        for j in range(dim):
            if k == j:
                randrates[k][j] = 0
    for  k in (0,2):
        for j in (0,2):
            randrates[k][j] = 0
    return randrates
```

This function gives a random matrix with rates extracted from an unitary distribution between in $(0, 1)$, and requires an input `dim` corresponding to the size of the generated square matrix.

A.1.3 Matrix of exit rates

```
def diag(array):

    diag = [[0 for x in array] for y in array]

    for x in range(len(array)):

        diag[x][x] = array[x]

    return diag
```

Given a square matrix with null diagonal entries, and non-negative off-diagonal entries, returns a diagonal matrix containing the exit rates of the input rate matrix. Notice that the sum is done over the rows of the input matrix, differently from the definition of exit rate adopted in this work which is done over the columns. In some contexts (as in some examples in this Appendix), this has to be taken into account since some parts of the code are written for matrices using the latter convention, thus taking the matrix transposal is sometimes necessary. This is the case in general when we need to extract matrix elements while maintaining the same convention used throughout this work.

A.1.4 stationary state

```
def steady(rates):

    exits = [sum(rates[x]) for x in state]
    steady = []
```

```
    for x in state:
        R = np.matrix(rates)-np.diag(exits)
        R = np.delete(R, x, 0)
        R = np.delete(R, x, 1)
        steady.append(-np.linalg.det(R))

    steady = [x / sum(steady) for x in steady]

    return steady
```

Takes the rate matrix (without diagonal terms) as an input and returns the (normalized) stationary distribution for the process defined by the input rate matrix.

A.1.5 Choosing a random state

```
def x_choice(prob):

    l = len(prob)
    s = [sum(prob[0:x]) for x in range(0,l+1)]
    y = uniform(0, 1)
    for x in range(0,l):
        if y >= s[x] and y < s[x+1]:
            break
    return x
```

Given a probability vector `prob`, this function picks a state according to the given input. This function is used when updating the Markov chain as it is possible to use as an input a vector containing the transition probabilities to states connected with the current state of the chain. Notice that the Python `random` module does contain such function. However, for pedagogical purposes, we decided to import the minimal amount of predefined functions.

A.1.6 Choosing a random time

```
def t_choice(x, exits):

    return log(1 / uniform(0, 1)) / exits[x]
```

From state `x`, and given the vector of exit rates `exits`, returns a random time extracted from an exponential distribution with parameter `exits[x]`.

The functions `x_choice` and `t_choice` in Sections A.1.5 and A.1.6 represent the basic two-steps in the Gillespie algorithm to generate continuous time Markov chains.

A.2 The process

Here we give the class which is used to generate an instance of a Markov chain according to a rate matrix given in input.

```
class Process:
    def __init__(self, rates = rates0, q0 = None):

        self.rates = [x.copy() for x in rates]
        self.type = type(q0)

        if q0 is not None:

            if self.type is list:
                norm = sum(q0)
                self.q0 = [x / norm for x in q0]
            elif self.type is int:
                if q0 in state:
                    self.init = q0
                    self.q0 = [0 for x in state]
                    self.q0[q0] = 1
                else:
                    raise TypeError("Only states in " + str(
                                                    state) + "
                                                    allowed")

        else:

            self.q0 = steady(self.rates)
            self.type = list

        self.exits = [sum(self.rates[x]) for x in state]
        self.chain = [[self.rates[x][y] / self.exits[x] for y
                                        in state] for x in
                                        state]
        self.generator = [[self.rates[x][y] for y in state] for
                                         x in state]
        for x in state:
            self.generator[x][x] = - self.exits[x]


        # insert methods here
```

If no initial probability `q0` is specified, the process is assumed to start from its stationary state.

A.2.1 Methods for Process class

stationary state

```
  # to be put inside Process class (care of indentation)

    def steady(self):
```

```
        return steady(self.rates)
```

Returns the stationary state associated with the process.

Tilted generator

```
# to be put inside Process class (care of indentation)

  def tilted(self,q ,transitions = [(0, 1)], weights = [1]):
      tilted = [x.copy() for x in p.generator]

      for i in range(len(transitions)):

          da = transitions[i][0]
          ad = transitions[i][1]
          tilted[ad][da] *= exp(q) * weights[i]

      return tilted
```

Returns the tilted generator along edge `(0,1)` if no other edge is specified.

Scaled Cumulant Generating Function

```
# to be put inside Process class (care of indentation)

  def scgf(self, q, transitions = [(0, 1)] , weights = [1]):

      qq = sympy.Symbol('qq')
      tilted = [x.copy() for x in self.generator]

      for i in range(len(transitions)):

          da = transitions[i][0]
          ad = transitions[i][1]
          tilted[ad][da] *= sympy.exp(qq) * weights[i]

      m = sympy.Matrix(tilted)

      for x in state:
          dominant = m.eigenvals(multiple = list)[x]
          n = float(sympy.re(dominant.subs({qq:0}).evalf()))
          if chop(n) == 0:
              break
```

Returns the scaled cumulant generating function for the current along `(0,1)` if no other edge is specified.

A.3 Fully observable processes

In this section, we give classes and functions which can be used to extract informations from single realizations of a process where all transitions and

states are assumed to be observable. In the next Section we give the same classes and functions readapted to the case where only some transitions are observable.

A.3.1 The path function

The path function is a function which given a process defined by the class above returns the time series of visited states and the permanence times for each visited state. This is the main function from which we extract the relevant informations we are interested in.

```
def path(n_or_t, p = Process()):

    '''Accepts both an integer number of steps or a real-valued
                                    final time for stopping.
                                   '''

    states = []
    times = []
    x = x_choice(p.start) if p.type is list else p.init

    if type(n_or_t) is int:
        states.append(x)
        for k in range(n_or_t):
            t = t_choice(x, p.exits)
            times.append(t)
            x = x_choice(p.chain[x])
            states.append(x)

    elif type(n_or_t) is float:

        t_tot = 0

        while t_tot < n_or_t:
            t = t_choice(x, p.exits)
            states.append(x)
            times.append(t)
            x = x_choice(p.chain[x])
            t_tot += t

        times[-1] += n_or_t - t_tot
    return states, times
```

This function accepts both integers and float numbers. In the first case it generates a process which is arrested after a number of transitions which corresponds to the input. In the latter, a process up to a certain input external time is generated

A.3.2 Observing a process

The following class takes a process as input and a number `n_or_t` which can be an integer or a float number (see `path` function above)

```
class Observe:

    def __init__(self, n_or_t, p = Process()):

        self.path = path(n_or_t, p)
        self.pathsingle = pathsingle(n_or_t,p)
        self.pathmul = pathmul(n_or_t,p)
        self.states = self.path[0]
        self.times = self.path[1]
        self.statessingle = self.pathsingle[0]
        self.timessingle = self.pathsingle[1]
        self.statesmul = self.pathmul[0]
        self.timesmul = self.pathmul[1]
        self.steps = len(self.states)
        self.stepssingle = len(self.statessingle)
        self.stepsmul = len(self.statesmul)
        self.duration = sum(self.times)
```

The functions `pathsingle` and `pathmul` are alternative path functions, which are introduced later in Section A.5 in the context of partially observable processes.

A.3.3 Methods for Observe class

Permanence times

```
  # to be put inside Observe class (care of indentation)
    def souj(self):

        souj = [0 for x in state]

        for k in range(self.steps):
            souj[self.states[k]] += self.times[k]

        return souj
```

Returns the permanence time in each state visited by the chain.

Total time

```
  # to be put inside Observe class (care of indentation)
    def get_total_time(self):
        totaltime = sum(self.timesbound)
        return totaltime
```

Returns the total external time in which the chain occur. In the case where `n_or_t` is a float, this will equal the input time. If `n_or_t` is an integer, it returns the time the process takes to perform `n_or_t` transitions.

Fluxes

```
# to be put inside Observe class (care of indentation)
  def fluxes(self, transitions = None):

      fluxes = {(x,y):0 for x in state for y in state if x!=y
                                                    }
      for k in range(self.steps - 1):
          fluxes[(self.states[k], self.states[k + 1])] += 1

      return fluxes
```

Returns a dictionary where the keys represent the transitions performed during a single realization of the process, and the values representing how many times that specific transition occurred.

Total currents

```
# to be put inside Observe class (care of indentation)
  def currents(self, transitions = None):

      if transitions == None:
          transitions = [(x, y) for x in state for y in state
                                              if x < y]

      sym_trans = transitions.copy()
      for k in transitions:
          sym_trans.append((k[1], k[0]))

      f = self.fluxes(sym_trans)

      c = {}
      for k in transitions:
          c[k] = f[(k[0], k[1])] - f[(k[1], k[0])]

      return c
```

Returns a dictionary where the keys represent the transitions performed during a single realizations, and the values representing the total current along the same edge. Notice that the edges are now oriented and thus if `(x,y)` appears in the dictionary, the reversed `(y,x)` does not show up.

Empirical rates

```
# to be put inside Observe class (care of indentation)
  def emprates(self):

      fluxes = self.fluxes()
      souj = self.souj()

      rates = [[0 for x in state] for y in state]
```

```
        for k in fluxes:
            rates[k[0]][k[1]] = fluxes[k] / souj[k[0]]

        return rates
```

Returns the empirical rates calculated from the empirical fluxes.

Environmental entropy production

```
  # to be put inside Observe class (care of indentation)
    def entropyproduction(self,rates):

        fluxes = self.fluxes()
        ep = 0

        for k in fluxes:
            if (k[1], k[0]) in fluxes:
              ep += log(rates[k[0]][k[1]] / rates[k[1]][k[0]])
                                              * fluxes[k]
            else:
              return None

        return ep
```

Returns the environmental entropy production in a single realization, only due to the occurring transitions, and evaluated via the true rates if the input `rates` is the original rate matrix (with zero diagonal entries).

Total entropy production

```
  # to be put inside Observe class (care of indentation)
    def totalepr(self,rates,q0 = steady(self.rates)):
        fluxes = self.fluxes()
        ep = 0

        for k in fluxes:
            if (k[1], k[0]) in fluxes:
              ep += np.log(rates[k[0]][k[1]]    / rates[k[1]][k[
                                              0]]) * fluxes[k]
            else:
              return None

        return ep + np.log(q0[self.states[0]]/q0[self.states[-1
                                          ]])
```

Returns the total entropy production in a process. Notice that this expression does not take into account the fact that the true probability distribution changes between initial and final time. Thus, this should be only used when the initial probability is the stationary distribution, since it takes a single probability distribution as input.

A.4 Examples

In this section we give an example on the use of the module `storymodel` and on how to extract relevant data. We proceed by executing lines of Python code directly inside the Python terminal, `>>>` indicating the inputs. First, we import `storymodel`

```
Python 3.6.9 (default, Mar 10 2023, 16:46:00)
[GCC 8.4.0] on linux
Type "help", "copyright", "credits" or "license" for more information.
```

We define a matrix containing the rates in the off-diagonal elements, define the **time** variable and the number of transitions (inside the Python environment).

```
>>> from storymodel import Process, Observe, x_choice, t_choice, path
>>> t = 10.   # float number
>>> n = 15   # integer number
>>> rates=[[0,3,1,1],[2,0,1,1],[1,1,0,1],[2,2,1,0]]
```

A single realization of the process is defined by the assignment

```
>>> p=Process(rates)
```

which is automatically initialized at its stationary distribution.

A.4.1 Single realizations

After all the steps above are done, we proceed on observing the process up to the given time.

```
>>> o=Observe(t,p)
```

From the abovedefined object `o` we can extract for instance the fluxes

```
>>> o.fluxes()
{(0, 1): 7, (0, 2): 1, (0, 3): 1, (1, 0): 5, (1, 2): 7, (1, 3): 2, (2, 0): 2, (2,
↪  1): 5, (2, 3): 3, (3, 0): 2, (3, 1): 2, (3, 2): 3}
```

the total currents

```
>>> o.currents()
{(0, 1): 2, (0, 2): -1, (0, 3): -1, (1, 2): 2, (1, 3): 0, (2, 3): 0}
```

the environmental entropy production

```
>>> o.entropyproduction(rates)
1.5040773967762735
```

and the total entropy production

```
>>> o.totalepr(rates,p.steady())
1.0986122886681093
```

The same process can be observed up to a fixed number of transitions. This is done by modifying the time argument when calling an istance of the Observe class:

```
>>> o=Observe(n,p)
```

We can now evaluate the same quantities before but in the case where observation is stopped after `n` transitions

```
>>> o.fluxes()
{(0, 1): 4, (0, 2): 1, (0, 3): 1, (1, 0): 3, (1, 2): 1, (1, 3): 1, (2, 0): 1, (2,
↪  1): 0, (2, 3): 1, (3, 0): 1, (3, 1): 1, (3, 2): 0}
>>>
>>> o.currents()
{(0, 1): 1, (0, 2): 0, (0, 3): 0, (1, 2): 1, (1, 3): 0, (2, 3): 1}
>>>
>>> o.entropyproduction(rates)
0.40546510810816416
>>>
>>> o.totalepr(rates,p.steady())
0.8109302162163292
```

A.4.2 Multiple realizations

It is possible to create different istances of a process and the respective observations by calling the two classes inside loops. For instance, we can generate `1000` such realization and extract information from each of them. In this example we generate the histogram of the total entropy production for `1000` realizations.

```
>>> from storymodel import Process, Observe, x_choice, t_choice, path
>>> t=10.
>>> rates=[[0,3,1,1],[2,0,1,1],[1,1,0,1],[2,2,1,0]]
>>>
>>> epr=[]  # define empty list
>>> k=0     # initialize counter
>>> p=Process(rates)
>>>
>>> while k<1000:
...     o=Observe(t,p)
...     epr.append(o.totalepr(rates,p.steady()))
...     k+=1
...
```

So far we have created an array of total entropy production outcomes, each of them associated to a single realization of the process. If we wish, for instance, to plot the histogram of the obtained data we proceed as follows

```
>>> import matplotlib.pyplot as plt
>>> plt.xlabel('EPR')
>>> plt.ylabel('frequency')
>>> plt.hist(epr,bins='auto')
(array([  2.,   4.,  17.,  16.,  35.,  42.,  50.,  88.,  97.,  63., 120.,
       115.,  80.,  83.,  75.,  35.,  40.,  10.,  12.,   8.,   2.,   6.]),
array([-2.89037176, -2.52238307, -2.15439438, -1.78640569, -1.41841701,
       -1.05042832, -0.68243963, -0.31445094,  0.05353774,  0.42152643,
        0.78951512,  1.15750381,  1.52549249,  1.89348118,  2.26146987,
```

```
        2.62945856,  2.99744724,  3.36543593,  3.73342462,  4.10141331,
        4.469402  ,  4.83739068,  5.20537937]), <a list of 22 Patch objects>)
>>> plt.show()
```

The histogram is showed in Fig. A.1.

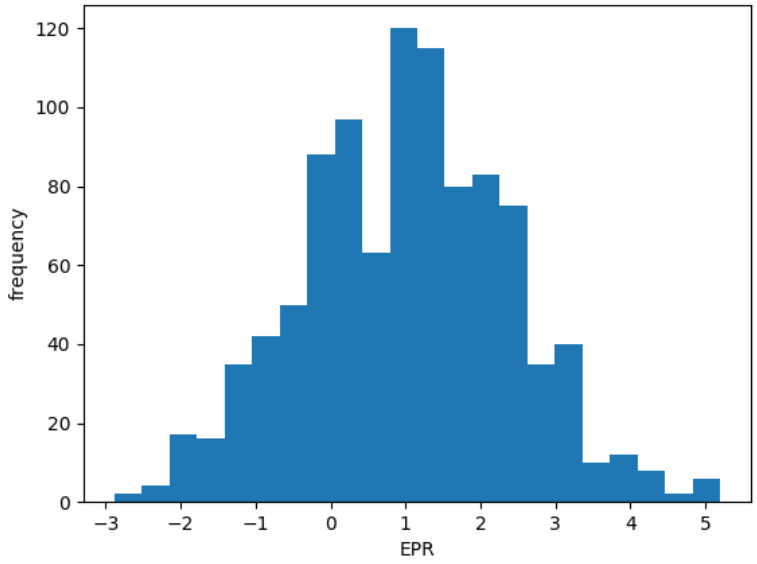

Figure A.1: Plot obtained as the outcome of the example in Sec. A.4.2.

A.5 Partially observable processes

The functions given in the previous sections are limited to the case where the process is assumed to be fully known. In this thesis, we focused our attention to the opposite case, which is when only few observable transitions are accessible. The codes above remain valid in this case when the observations are carried up to a fixed total time. If we are interested, for instance, on a single current, we may generate trajectories and extract the current along the chosen edge by simply calling the `currents` method for the class `Observe`, and from the resulting dictionary select the key containing the source and target states of the observed transition.

However, we are interested in working on processes which are stopped after the occurrence of a fixed number of transitions. This means that it is necessary to modify the `path` function so that it is stopped according to this criterion instead of after a fixed number of transitions occurring in the full

graph (remember we can choose this option by using an integer time when calling the `path` function).

Therefore, we simply proceed by defining a couple of extra functions and methods to be included in the `Observe` class.

A.5.1 Modified path functions

The following functions takes as input an integer number `n` representing the total number of observable transitions and a process `p` as an istance of a `Process` class.

```
def pathsingle(n, p = Process(),to_observe = (0,1)):

    '''n is an integer number'''

    states = []
    times = []
    x = x_choice(p.start) if p.type is list else p.init

    if type(n) is int:
        states.append(x)
        counter = 0
        while counter < n:
            t = t_choice(x, p.exits)
            times.append(t)
            x = x_choice(p.chain[x])
            states.append(x)
            if len(states) >= 2:
                if (states[-1],states[-2]) == to_observe:
                    counter += 1
                elif (states[-1],states[-2]) == tuple(reversed(
                                                    to_observe)):
                    counter +=1
    return states, times
```

This function provides a list of visited states (in chronological order) of the full process, and the respective permanence times, and stops only after `n` observable transitions occur. If no pair of states is specified in input, the function consider the transition between the tuple of states `(0,1)` as the observable one.

Analogously we can define a path function stopping after `n` observable transitions along two edges:

```
def pathmul(n_or_t, p = Process(),to_observe = (0,1),
                                to_observe2 = (2,3)):

    '''n is an integer number'''

    states = []
    times = []
    x = x_choice(p.start) if p.type is list else p.init

    if type(n_or_t) is int:
```

```
        states.append(x)
        counter = 0
        while counter < n_or_t:
            t = t_choice(x, p.exits)
            times.append(t)
            x = x_choice(p.chain[x])
            states.append(x)
            if len(states) >= 2:
                if (states[-1],states[-2]) == to_observe:
                    counter += 1
                elif (states[-1],states[-2]) == tuple(reversed(
                                                    to_observe)):
                    counter += 1
                if (states[-1],states[-2]) == to_observe2:
                    counter += 1
                elif (states[-1],states[-2]) == tuple(reversed(
                                                    to_observe2)):
                    counter += 1
    return states, times
```

By default, the transitions between the pairs `(0,1)` and `(2,3)` are counted.

A.5.2 Additional methods

According to the new functions introduced above, we can define the methods of the `Observe` class which only accounts for quantities evaluated along visible transitions.

Fluxes along a single edge

```
  # to be put inside Observe class (care of indentation)
    def fluxessingle(self,to_observe = (0,1)):
        fluxes = {(x,y):0 for x in to_observe for y in
                                        to_observe if x!=y}
        for k in range(self.stepssingle - 1):
            if (self.statessingle[k] == to_observe[0] and self.
                                            statessingle[k+1] =
                                            = to_observe[1]) or
                                             (self.statessingle
                                            [k] == to_observe[1
                                            ] and self.
                                            statessingle[k+1] =
                                            = to_observe[0]):
                fluxes[(self.statessingle[k], self.statessingle
                                                [k + 1])] += 1
        return fluxes
```

Fluxes along two edges

```
  # to be put inside Observe class (care of indentation)
    def fluxesmul(self, to_observe = (0,1),to_observe2 = (2,3))
                                        :
        fluxes = {(x,y):0 for x in to_observe for y in
                                          to_observe if x!=y}
        fluxes2 = {(x,y):0 for x in to_observe2 for y in
                                          to_observe2 if x!=y}
        for k in range(self.stepsmul - 1):
            if (self.statesmul[k] == 0 and self.statesmul[k+1]
                                            == 1) or (self.
                                            statesmul[k] == 1
                                            and self.statesmul[
                                            k+1] == 0):
                fluxes[(self.statesmul[k], self.statesmul[k + 1
                                                ])] += 1
            elif (self.statesmul[k] == 2 and self.statesmul[k+1
                                            ] == 3) or (self.
                                            statesmul[k] == 3
                                            and self.statesmul[
                                            k+1] == 2):
                fluxes2[(self.statesmul[k], self.statesmul[k +
                                                1])] += 1
        return fluxes, fluxes2
```

Notice that the definition of the methods above is not strictly necessary. In fact, the same outputs can be obtained from trajectories generated with the functions `pathsingle` and `pathmul`, via the use of the already defined method `fluxes`, by selecting the key in the ouput dictionary which correspond to the observable edges. However, the method `fluxes` evaluates all the fluxes, and the new defined methods `fluxessingle` and `fluxesmul` only consider the observable edges, thus decreasing the computational time when dealing with partially observable chains. The same argument holds for the methods introduced below, which give the observable currents as outcome.

Single observable current

```
  # to be put inside Observe class (care of indentation)
    def singlecurrent(self,to_observe=(0,1)):
        fluxes = self.fluxessingle(to_observe)
        return fluxes[(to_observe)] - fluxes[tuple(reversed(
                                          to_observe))]
```

Returns the total current along the observable edge. Default positive direction is `0->1`.

Two observable currents

```
  # to be put inside Observe class (care of indentation)
    def twocurrents(self,to_observe1=(0,1),to_observe2=(2,3)):
```

```
        fluxes = self.fluxesmul(to_observe1,to_observe2)
        fluxes1=fluxes[0]
        fluxes2=fluxes[1]
        c1=fluxes1[(to_observe1)] - fluxes1[tuple(reversed(
                                        to_observe1))]
        c2=fluxes2[(to_observe2)] - fluxes2[tuple(reversed(
                                        to_observe2))]
        return c1,c2
```

Returns two currents `c1` and `c2` along two different observable edges. Default positive directions are `0->1` and `2->3` respectively.

A.5.3 Examples with two observable currents

As before, we first import the modules we need, the number of observable transitions, the rate matrix and the process:

```
>>> from storymodel import Process, Observe, x_choice, t_choice, path
>>> from storymodel import pathsingle, pathmul
>>> n=15
>>> rates=[[0,3,1,1],[2,0,1,1],[1,1,0,1],[2,2,1,0]]
>>> p=Process(rates)
```

With two observable currents we have to use the method `twocurrents` in the `Observe` class. Then

```
>>> for k in range(1000):
...     o=Observe(n,p)
...     curr=o.twocurrents()
...     c1.append(curr[0])
...     c2.append(curr[1])
```

creates two vectors `c1` and `c2` of currents along different edges. Since the currents assume only integer values, the bins are defined as following

```
>>> import matplotlib.pyplot as plt
>>> extr1 = np.max([np.abs(np.min(c1)),np.abs(np.max(c1))])
>>> extr2 = np.max([np.abs(np.min(c2)),np.abs(np.max(c2))])
>>> bins1 = np.linspace(-extr1-0.5, extr1+0.5, 2*extr1 + 2)
>>> bins2 = np.linspace(-extr2-0.5, extr2+0.5, 2*extr2 + 2)
```

and the histogram of the currents can be plotted as

```
>>> fig, axs = plt.subplots(2,figsize = (5,6))
>>> axs[0].set_xlabel('current 1')
Text(0.5, 0, 'current 1')
>>> axs[1].set_xlabel('current 2')
Text(0.5, 0, 'current 2')
>>> axs[0].set_ylabel('frequency')
Text(0, 0.5, 'frequency')
>>> axs[1].set_ylabel('frequency')
Text(0, 0.5, 'frequency')
>>> axs[0].hist(c1,bins=bins1)
(array([  0.,   2.,   2.,   6.,  33.,  82., 155., 199., 199., 153., 101.,
        46.,  18.,   3.,   1.]), array([-7.5, -6.5, -5.5, -4.5, -3.5, -2.5, -1.5,
        ↪  -0.5,  0.5,  1.5,  2.5,
        3.5,  4.5,  5.5,  6.5,  7.5]), <a list of 15 Patch objects>)
```

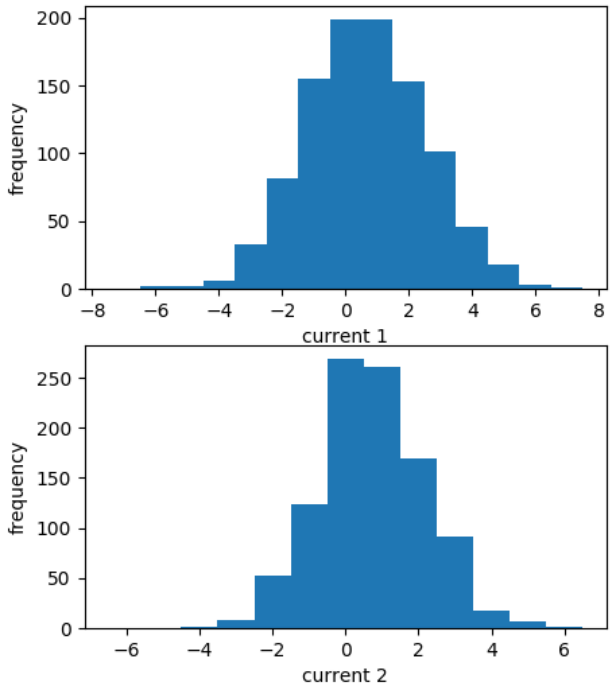

Figure A.2: Histogram of the currents for the example in Sec. A.5.3

```
>>> axs[1].hist(c2,bins=bins2)
(array([  0.,   0.,   1.,   8.,  52., 124., 269., 261., 169.,  91.,  17.,
         7.,   1.]), array([-6.5, -5.5, -4.5, -3.5, -2.5, -1.5, -0.5,  0.5,  1.5,
         ↪  2.5,  3.5,
        4.5,  5.5,  6.5]), <a list of 13 Patch objects>)
>>> plt.show()
```

The histograms are showed in Fig. A.2

A.5.4 Generating the reduced Markov chain

The process at stopping-n, as discussed in this thesis, can be directly generated in numerical simulations by defining a discrete time Markov chain in the space of observable transitions, via a stochastic matrix called trans-transition matrix, which is derived from the original process in state space via Eq. (3.17). Since in this thesis the focus is on currents in transition space, we use a custom function which generates a sequence of observable transitions. In addition, generating sequences of observable transitions directly via the trans-transition matrix is convenient from the point of view of computational speed, since we can avoid to generate random exponential

permanence times unlike the case of continuous-time processes.

For the case of a single observable transition in both directions

```
def markovchainsingle(ntrans,p1,P):
    k = 0
    x = x_choice(p1)
    traj=[x]
    while k < ntrans-1:
        if x == 0:
            xs = x_choice([P[0][0],P[1][0]])
        if x == 1:
            xs = x_choice([P[0][1],P[1][1]])
        traj.append(xs)
        x = np.copy(xs)
        k += 1
    return traj
```

with `ntrans` the lenght (i.e. number of observable transitions) of the generated trajectory, `p1` the initial probability vector in transition space, and `P` the trans-transition matrix, which is a 2×2 matrix.

The observable current is then evaluated, given a trajectory `traj` in transition space (by convention `0` is $\uparrow$ and `1` is $\downarrow$) by the function

```
def current(traj):
    up = 0
    down = 0
    for k in range(len(traj)):
        if traj[k] == 0:
            up += 1
        else:
            down += 1
    return up - down
```

For two observable transitions $\{\uparrow_1, \downarrow_1, \uparrow_2, \downarrow_2$ along different edges (`0` is $\uparrow_1$, `1` is $\downarrow_1$, `2` is $\uparrow_2$, `4` is $\downarrow_2$), the sequence of observable transitions is generated by the function

```
def markovchainmul(ntrans,p1,P):
    k = 0
    x = x_choice(p1)
    traj=[x]
    while k < ntrans-1:
        if x == 0:
            xs = x_choice([P[0][0],P[1][0],P[2][0],P[3][0]])
        if x == 1:
            xs = x_choice([P[0][1],P[1][1],P[2][1],P[3][1]])
        if x == 2:
            xs = x_choice([P[0][2],P[1][2],P[2][2],P[3][2]])
        if x == 3:
            xs = x_choice([P[0][3],P[1][3],P[2][3],P[3][3]])

        traj.append(xs)
        x = np.copy(xs)
        k += 1
    return traj
```

The total currents `c1` and `c2` along the respective observable edges are obtained via the function

```
def totalcurrents(traj):
    up1 = 0
    down1 = 0
    up2 = 0
    down2 = 0
    for k in range(len(traj)):
        if traj[k] == 0:
            up1 += 1
        elif traj[k] == 1:
            down1 += 1
        elif traj[k] == 2:
            up2 += 1
        elif traj[k] == 3:
            down2 += 1
    return up1 - down1, up2 - down2
```

and the mixed currents

```
def mixedcurrents(traj):
    n_up1up2 = 0
    n_up2up1 = 0
    n_up1down2 = 0
    n_up2down1 = 0
    n_down1up2 = 0
    n_down1down2 = 0
    n_down2up1 = 0
    n_down2down1 = 0
    for k in range(len(traj)-1):
        if (traj[k+1] == 0) and (traj[k] == 2):
            n_up1up2 += 1
        elif (traj[k+1] == 0) and (traj[k] == 3):
            n_up1down2 += 1
        elif (traj[k+1] == 1) and (traj[k] == 2):
            n_down1up2 += 1
        elif (traj[k+1] == 1) and (traj[k] == 3):
            n_down1down2 += 1
        elif (traj[k+1] == 2) and (traj[k] == 0):
            n_up2up1 += 1
        elif (traj[k+1] == 2) and (traj[k] == 1):
            n_up2down1 += 1
        elif (traj[k+1] == 3) and (traj[k] == 0):
            n_down2up1 += 1
        elif (traj[k+1] == 3) and (traj[k] == 1):
            n_down2down1 += 1
    return n_up1up2 - n_down2down1, n_up1down2 - n_up2down1,
                                    n_down1up2 - n_down2up1,
                                    n_down1down2 - n_up2up1
```

The reason why the total currents and the mixed currents are evaluated separately is because in the case of complete sets of currents there is no need to evaluate the mixed currents, as proved in Section 5.6.

A.5.5 Example with a single current in transition space

We give an example of a process in the space of observable transitions $\{\uparrow, \downarrow\}$, i.e. a single observable transition in both directions. The rate matrix is the same as the one used in previous examples

```
>>> from storymodel import x_choice
>>> from storymodel import markovchainsingle, current
>>> import numpy as np
>>> ntrans = 15
>>> rates=[[0,3,1,1],[2,0,1,1],[1,1,0,1],[2,2,1,0]]
```

To evaluate the trans-transition matrix for a single observable transition in both directions, we proceed as follow

```
>>> exits = [sum(x) for x in np.transpose(rates)]
>>> stalling = np.array(rates)-np.diag(exits)
>>> stalling[1,0] = 0
>>>
>>> stalling[0,1] = 0
>>> invstall = np.linalg.inv(stalling)
>>> P = [[-rates[0][1]*invstall[1,0],
↪  -rates[0][1]*invstall[1,1]],[-rates[1][0]*invstall[0,0],
↪  -rates[1][0]*invstall[0,1]]]
```

Now we generate `1000` trajectories in the observable transition space, prepared from the initial state `p1 = [0.5,0.5]`

```
>>> p1 = [0.5,0.5]
>>> curr=[]
>>> for k in range(1000):
...     MC = markovchainsingle(ntrans,p1,P)
...     curr.append(current(MC))
...
```

and thus, as usual, we plot as

```
>>> import matplotlib.pyplot as plt
>>> extr = np.max([np.abs(np.min(curr)),np.abs(np.max(curr))])
>>> bins = np.linspace(-extr-0.5, extr+0.5, 2*extr + 2)
>>> plt.xlabel('current')
>>> plt.ylabel('frequency')
>>> plt.hist(curr,bins = bins)
(array([  0.,   0.,   0.,   0.,   1.,   0.,  13.,   0.,  80.,   0., 226.,
         0., 341.,   0., 240.,   0.,  79.,   0.,  14.,   0.,   5.,   0.,
         1.]), array([-11.5, -10.5,  -9.5,  -8.5,  -7.5,  -6.5,  -5.5,  -4.5,
        ↪  -3.5,
        -2.5,  -1.5,  -0.5,   0.5,   1.5,   2.5,   3.5,   4.5,   5.5,
         6.5,   7.5,   8.5,   9.5,  10.5,  11.5]), <a list of 23 Patch objects>)
>>> plt.show()
```

The histogram is showed in Fig. A.3

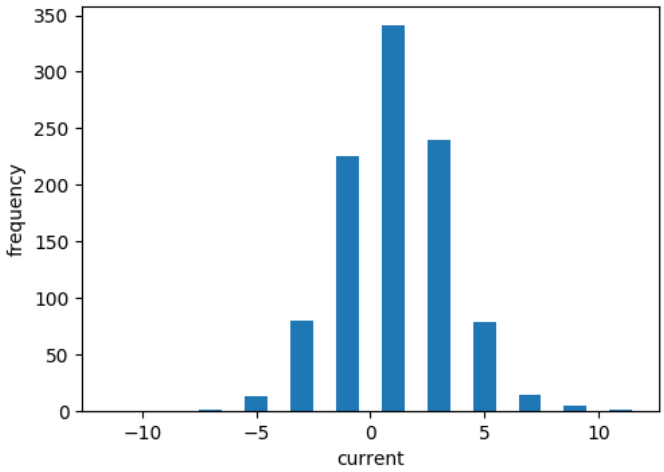

Figure A.3: Histogram of the currents for the example in Sec. A.5.5

Bibliography

[1] Sadi Carnot. *Réflexions sur la puissance motrice du feu*, volume 26. Vrin, 1979.

[2] Miriam R Wilson, Jordi Solà, Armando Carlone, Stephen M Goldup, Nathalie Lebrasseur, and David A Leigh. An autonomous chemically fuelled small-molecule motor. *Nature*, 534(7606):235–240, 2016.

[3] Shuntaro Amano, Stephen DP Fielden, and David A Leigh. A catalysis-driven artificial molecular pump. *Nature*, 594(7864):529–534, 2021.

[4] Alessandro Sorrenti, Jorge Leira-Iglesias, Akihiro Sato, and Thomas M Hermans. Non-equilibrium steady states in supramolecular polymerization. *Nature communications*, 8(1):15899, 2017.

[5] Sergey N Semenov, Lewis J Kraft, Alar Ainla, Mengxia Zhao, Mostafa Baghbanzadeh, Victoria E Campbell, Kyungtae Kang, Jerome M Fox, and George M Whitesides. Autocatalytic, bistable, oscillatory networks of biologically relevant organic reactions. *Nature*, 537(7622):656–660, 2016.

[6] Jasper P Fried, Xinya Bian, Jacob L Swett, Ivan I Kravchenko, G Andrew D Briggs, and Jan A Mol. Large amplitude charge noise and random telegraph fluctuations in room-temperature graphene single-electron transistors. *Nanoscale*, 12(2):871–876, 2020.

[7] J Jomaah and F Balestra. Low-frequency noise in advanced cmos/soi devices. *IEE Proceedings-Circuits, Devices and Systems*, 151(2):111–117, 2004.

[8] Linda Geppert. Quantum transistors: toward nanoelectronics. *IEEE Spectrum*, 37(9):46–51, 2000.

[9] Udo Seifert. Stochastic thermodynamics, fluctuation theorems and molecular machines. *Reports on progress in physics*, 75(12):126001, 2012.

[10] Ken Sekimoto. Stochastic energetics, 2010.

[11] C. Van den Broeck and M. Esposito. Ensemble and trajectory thermodynamics: A brief introduction. *Physica A: Statistical Mechanics and its Applications*, 418:6–16, 2015. Proceedings of the 13th International Summer School on Fundamental Problems in Statistical Physics.

[12] Gavin E Crooks. Entropy production fluctuation theorem and the nonequilibrium work relation for free energy differences. *Physical Review E*, 60(3):2721, 1999.

[13] Giovanni Gallavotti and Ezechiel Godert David Cohen. Dynamical ensembles in nonequilibrium statistical mechanics. *Physical review letters*, 74(14):2694, 1995.

[14] Giovanni Gallavotti and Ezechiel Godert David Cohen. Dynamical ensembles in stationary states. *Journal of Statistical Physics*, 80:931–970, 1995.

[15] Giovanni Gallavotti. Breakdown and regeneration of time reversal symmetry in nonequilibrium statistical mechanics. *Physica D: Nonlinear Phenomena*, 112(1-2):250–257, 1998.

[16] Jorge Kurchan. Fluctuation theorem for stochastic dynamics. *Journal of Physics A: Mathematical and General*, 31(16):3719, 1998.

[17] R Van Zon and EGD Cohen. Extension of the fluctuation theorem. *Physical Review Letters*, 91(11):110601, 2003.

[18] Alexandre Lazarescu, Tommaso Cossetto, Gianmaria Falasco, and Massimiliano Esposito. Large deviations and dynamical phase transitions in stochastic chemical networks. *The Journal of Chemical Physics*, 151(6), 2019.

[19] David Andrieux and Pierre Gaspard. A fluctuation theorem for currents and non-linear response coefficients. *Journal of Statistical Mechanics: Theory and Experiment*, 2007(02):P02006–P02006, feb 2007.

[20] Giovanni Gallavotti. Extension of onsager's reciprocity to large fields and the chaotic hypothesis. *Physical Review Letters*, 77(21):4334, 1996.

[21] Roop Mallik, Brian C Carter, Stephanie A Lex, Stephen J King, and Steven P Gross. Cytoplasmic dynein functions as a gear in response to load. *Nature*, 427(6975):649–652, 2004.

[22] Masayoshi Nishiyama, Hideo Higuchi, and Toshio Yanagida. Chemomechanical coupling of the forward and backward steps of single kinesin molecules. *Nature Cell Biology*, 4(10):790–797, 2002.

[23] Stefano Bo and Antonio Celani. Multiple-scale stochastic processes: Decimation, averaging and beyond. *Physics Reports*, 670:1–59, feb 2017.

[24] Massimiliano Esposito. Stochastic thermodynamics under coarse graining. *Physical Review E*, 85(4), apr 2012.

[25] Nahuel Freitas, Jean-Charles Delvenne, and Massimiliano Esposito. Stochastic thermodynamics of nonlinear electronic circuits: A realistic framework for computing around k t. *Physical Review X*, 11(3):031064, 2021.

[26] Jiayin Gu and Pierre Gaspard. Stochastic approach and fluctuation theorem for charge transport in diodes. *Physical Review E*, 97(5):052138, 2018.

[27] Jiayin Gu and Pierre Gaspard. Microreversibility, fluctuations, and nonlinear transport in transistors. *Physical Review E*, 99(1):012137, 2019.

[28] Massimiliano Esposito, Upendra Harbola, and Shaul Mukamel. Fluctuation theorem for counting statistics in electron transport through quantum junctions. *Physical Review B*, 75(15):155316, 2007.

[29] Pedro E. Harunari, Annwesha Dutta, Matteo Polettini, and Édgar Roldán. What to learn from a few visible transitions' statistics? *Phys. Rev. X*, 12:041026, Dec 2022.

[30] Jann van der Meer, Benjamin Ertel, and Udo Seifert. Thermodynamic inference in partially accessible markov networks: A unifying perspective from transition-based waiting time distributions. *Phys. Rev. X*, 12:031025, Aug 2022.

[31] Pedro E. Harunari, Alberto Garilli, and Matteo Polettini. The beat of a current, 2022.

[32] Matteo Polettini and Massimiliano Esposito. Transient fluctuation theorems for the currents and initial equilibrium ensembles. *Journal of Statistical Mechanics: Theory and Experiment*, 2014(10):P10033, oct 2014.

[33] David Andrieux and Pierre Gaspard. Fluctuation theorem for currents and schnakenberg network theory. *Journal of statistical physics*, 127:107–131, 2007.

[34] Carl D. Meyer. Stochastic complementation, uncoupling markov chains, and the theory of nearly reducible systems. *SIAM Review*, 31(2):240–272, 1989.

[35] Matteo Polettini and Alberto Garilli. Sustaining a temperature difference. *SciPost Phys.*, 9:030, 2020.

[36] Kotaro Suzumura. Perron-frobenius theorem on non-negative square matrices: An elementary proof. *Hitotsubashi Journal of Economics*, pages 137–141, 1983.

[37] Tim Schmiedl and Udo Seifert. Stochastic thermodynamics of chemical reaction networks. *The Journal of chemical physics*, 126(4), 2007.

[38] Massimiliano Esposito and Christian Van den Broeck. Three faces of the second law. i. master equation formulation. *Physical Review E*, 82(1), jul 2010.

[39] Luca Peliti and Simone Pigolotti. *Stochastic Thermodynamics: An Introduction*. Princeton University Press, 2021.

[40] Markus F Weber and Erwin Frey. Master equations and the theory of stochastic path integrals. *Reports on Progress in Physics*, 80(4):046601, 2017.

[41] J. Schnakenberg. Network theory of microscopic and macroscopic behavior of master equation systems. *Rev. Mod. Phys.*, 48:571–585, Oct 1976.

[42] Matteo Polettini. Cycle/cocycle oblique projections on oriented graphs. *Letters in Mathematical Physics*, 105:89–107, 2015.

[43] Christos H Skiadas and Charilaos Skiadas. Exploring life expectancy limits: First exit time modeling, parameter analysis and forecasts. In *Chaos theory: Modeling, simulation and applications*, pages 357–368. World Scientific, 2011.

[44] Jian-Xun Zhang, Dang-Bo Du, Xiao-Sheng Si, Yang Liu, and Chang-Hua Hu. Prognostics based on stochastic degradation process: The last exit time perspective. *IEEE Transactions on Reliability*, 70(3):1158–1176, 2021.

[45] Wei Dai, Anirvan M Sengupta, and Ronald M Levy. First passage times, lifetimes, and relaxation times of unfolded proteins. *Physical review letters*, 115(4):048101, 2015.

[46] Linkan Bian and Nagi Gebraeel. Computing and updating the first-passage time distribution for randomly evolving degradation signals. *IIE Transactions*, 44(11):974–987, 2012.

[47] Babak MS Arani, Stephen R Carpenter, Leo Lahti, Egbert H Van Nes, and Marten Scheffer. Exit time as a measure of ecological resilience. *Science*, 372(6547):eaay4895, 2021.

[48] Ken Sekimoto. Derivation of the first passage time distribution for markovian process on discrete network. *arXiv preprint arXiv:2110.02216*, 2021.

[49] James R Norris. *Markov chains*. Number 2. Cambridge university press, 1998.

[50] Ronald D Vale, Thomas S Reese, and Michael P Sheetz. Identification of a novel force-generating protein, kinesin, involved in microtubule-based motility. *Cell*, 42(1):39–50, 1985.

[51] Matteo Polettini and Massimiliano Esposito. Irreversible thermodynamics of open chemical networks. i. emergent cycles and broken conservation laws. *The Journal of chemical physics*, 141(2), 2014.

[52] Philipp Strasberg, Gernot Schaller, Tobias Brandes, and Massimiliano Esposito. Quantum and information thermodynamics: A unifying framework based on repeated interactions. *Phys. Rev. X*, 7:021003, Apr 2017.

[53] Andre C Barato and Udo Seifert. Stochastic thermodynamics with information reservoirs. *Physical Review E*, 90(4):042150, 2014.

[54] Hugo Touchette. The large deviation approach to statistical mechanics. *Physics Reports*, 478(1-3):1–69, 2009.

[55] Matteo Polettini and Massimiliano Esposito. Effective thermodynamics for a marginal observer. *Phys. Rev. Lett.*, 119:240601, Dec 2017.

[56] Matteo Polettini and Massimiliano Esposito. Effective fluctuation and response theory. *Journal of Statistical Physics*, 176(1):94–168, apr 2019.

[57] Kutluyil Doğançay and Vikram Krishnamurthy. On fast aggregation of markov chain functionals using stochastic complementation. *Signal Processing*, 74(3):223–237, 1999.

[58] R Bruce Mattingly. A revised stochastic complementation algorithm for nearly completely decomposable markov chains. *ORSA Journal on Computing*, 7(2):117–124, 1995.

[59] E Seneta. Complementation in stochastic matrices and the gth algorithm. *SIAM journal on matrix analysis and applications*, 19(2):556–563, 1998.

[60] Gavin E Crooks and Christopher Jarzynski. On the work distribution for the adiabatic compression of a dilute classical gas. *arXiv preprint cond-mat/0603116*, 2006.

[61] Christopher Jarzynski. Rare events and the convergence of exponentially averaged work values. *Physical Review E*, 73(4):046105, 2006.

[62] Nicole Yunger Halpern and Christopher Jarzynski. Number of trials required to estimate a free-energy difference, using fluctuation relations. *Physical Review E*, 93(5):052144, 2016.

[63] Izaak Neri and Matteo Polettini. Extreme value statistics of edge currents in markov jump processes and their use for entropy production estimation. *SciPost Physics*, 14(5):131, 2023.

[64] Matteo Polettini and Izaak Neri. Phenomenological boltzmann formula for currents. *arXiv preprint arXiv:2208.02888*, 2022.

[65] Riccardo Rao and Massimiliano Esposito. Nonequilibrium thermodynamics of chemical reaction networks: Wisdom from stochastic thermodynamics. *Physical Review X*, 6(4):041064, 2016.

[66] Francesco Avanzini, Nahuel Freitas, and Massimiliano Esposito. Circuit theory for chemical reaction networks. *Physical Review X*, 13(2):021041, 2023.

[67] Adrián A Budini, Robert M Turner, and Juan P Garrahan. Fluctuating observation time ensembles in the thermodynamics of trajectories. *Journal of Statistical Mechanics: Theory and Experiment*, 2014(3):P03012, mar 2014.

[68] Christian Van den Broeck et al. Stochastic thermodynamics: A brief introduction. *Phys. Complex Colloids*, 184:155–193, 2013.

[69] Frédéric Douarche, Sergio Ciliberto, Artyom Petrosyan, and Ivan Rabbiosi. An experimental test of the jarzynski equality in a mechanical experiment. *Europhysics Letters*, 70(5):593, 2005.

[70] A Mossa, M Manosas, N Forns, J M Huguet, and F Ritort. Dynamic force spectroscopy of DNA hairpins: I. force kinetics and free energy landscapes. *Journal of Statistical Mechanics: Theory and Experiment*, 2009(02):P02060, feb 2009.

[71] Jan Liphardt, Sophie Dumont, Steven B. Smith, Ignacio Tinoco, and Carlos Bustamante. Equilibrium information from nonequilibrium measurements in an experimental test of jarzynski's equality. *Science*, 296(5574):1832–1835, 2002.

[72] O-P Saira, Y Yoon, T Tanttu, Mikko Möttönen, DV Averin, and Jukka P Pekola. Test of the jarzynski and crooks fluctuation relations in an electronic system. *Physical review letters*, 109(18):180601, 2012.

[73] R Labbé, J-F Pinton, and S Fauve. Power fluctuations in turbulent swirling flows. *Journal de Physique II*, 6(7):1099–1110, 1996.

[74] Sergio Ciliberto, Nicolas Garnier, S Hernandez, Cédrick Lacpatia, J-F Pinton, and G Ruiz Chavarria. Experimental test of the gallavotti–cohen fluctuation theorem in turbulent flows. *Physica A: Statistical Mechanics and its Applications*, 340(1-3):240–250, 2004.

[75] Patrick P Potts and Peter Samuelsson. Thermodynamic uncertainty relations including measurement and feedback. *Physical Review E*, 100(5):052137, 2019.

[76] Jordan M Horowitz and Todd R Gingrich. Thermodynamic uncertainty relations constrain non-equilibrium fluctuations. *Nature Physics*, 16(1):15–20, 2020.

[77] Ryo Suzuki, Hong-Ren Jiang, and Masaki Sano. Validity of fluctuation theorem on self-propelling particles. *arXiv preprint arXiv:1104.5607*, 2011.

[78] Todd R. Gingrich, Jordan M. Horowitz, Nikolay Perunov, and Jeremy L. England. Dissipation bounds all steady-state current fluctuations. *Physical Review Letters*, 116(12), mar 2016.

[79] Andre C. Barato and Udo Seifert. Thermodynamic uncertainty relation for biomolecular processes. *Physical Review Letters*, 114(15), apr 2015.

[80] Denis J Evans, Ezechiel Godert David Cohen, and Gary P Morriss. Probability of second law violations in shearing steady states. *Physical review letters*, 71(15):2401, 1993.

[81] Denis J Evans and Debra J Searles. Equilibrium microstates which generate second law violating steady states. *Physical Review E*, 50(2):1645, 1994.

[82] Alberto Garilli, Pedro E. Harunari, and Matteo Polettini. Fluctuation relations for a few observable currents at their own beat, 2023.

[83] Hannes Risken. *Fokker-planck equation*. Springer, 1996.

[84] Ken Sekimoto. Langevin equation and thermodynamics. *Progress of Theoretical Physics Supplement*, 130:17–27, 1998.

[85] C Van den Broeck. Stochastic thermodynamics. In *Selforganization by Nonlinear Irreversible Processes: Proceedings of the Third International Conference Kühlungsborn, GDR, March 18–22, 1985*, pages 57–61. Springer, 1986.

[86] GA Pavliotis and AM Stuart. An introduction to multiscale methods. *Lecture Notes*, 2006.

[87] Grigoris Pavliotis and Andrew Stuart. *Multiscale methods: averaging and homogenization*. Springer Science & Business Media, 2008.

[88] Gregory Bulnes Cuetara, Massimiliano Esposito, and Pierre Gaspard. Fluctuation theorems for capacitively coupled electronic currents. *Physical Review B*, 84(16):165114, 2011.

[89] Andrew Pohorille, Christopher Jarzynski, and Christophe Chipot. Good practices in free-energy calculations. *The Journal of Physical Chemistry B*, 114(32):10235–10253, 2010.

[90] Nicole Yunger Halpern, Andrew JP Garner, Oscar CO Dahlsten, and Vlatko Vedral. Introducing one-shot work into fluctuation relations. *New Journal of Physics*, 17(9):095003, 2015.

[91] Francesco Coghi, Lorenzo Buffoni, and Stefano Gherardini. Convergence of the integral fluctuation theorem estimator for nonequilibrium markov systems. *Journal of Statistical Mechanics: Theory and Experiment*, 2023(6):063201, 2023.

[92] Francesco Avanzini, Massimo Bilancioni, Vasco Cavina, Sara Dal Cengio, Massimiliano Esposito, Gianmaria Falasco, Danilo Forastiere, Nahuel Freitas, Alberto Garilli, Pedro E. Harunari, Vivien Lecomte, Alexandre Lazarescu, Shesha G. Marehalli Srinivas, Charles Moslonka, Izaak Neri, Emanuele Penocchio, William D. Piñeros, Matteo Polettini, Adarsh Raghu, Paul Raux, Ken Sekimoto, and Ariane Soret. Methods and conversations in (post)modern thermodynamics, 2023.